

~~CLASSIFICATION CANCELLED~~
CONFIDENTIAL
SECURITY INFORMATION

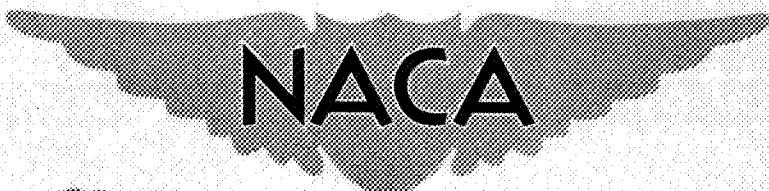
Status: **INACTIVE**

REC'D AUG 14 1952
12 24 " " 18 "

Copy **1**
RM SA52R04

NACA RM SA52R04

Source of Acquisition
CASI Acquired



~~CLASSIFICATION CANCELLED~~

RESEARCH MEMORANDUM

for the

United States Air Force

WIND-TUNNEL INVESTIGATION OF THE LOW-SPEED STATIC LONGITUDINAL
CHARACTERISTICS OF THE REPUBLIC RF-84F AIRPLANE

By Lynn W. Hunton, Roy N. Griffin, Jr.,
and Harry A. James

Ames Aeronautical Laboratory
Moffett Field, Calif.

~~CLASSIFICATION CANCELLED~~

~~J. W. Crowley~~ 1/14/55

~~off~~ NACA change # 2925

Status: **INACTIVE**

This material contains information affecting the National Defense of the United States within the meaning of the espionage laws, Title 18, U.S.C., Secs. 793 and 794, the transmission or revelation of which in any manner to unauthorized person is prohibited by law.

NATIONAL ADVISORY COMMITTEE FOR AERONAUTICS

WASHINGTON

Aug. 4, 1952

FILE COPY

To be returned to
the files of the National
Advisory Committee
for Aeronautics
Washington, D.C.

~~CLASSIFICATION CANCELLED~~
CONFIDENTIAL
SECURITY INFORMATION

147

~~CONFIDENTIAL~~
~~SECURITY INFORMATION~~
~~CANCELLED~~

~~CONFIDENTIAL~~
~~CANCELLED~~

NATIONAL ADVISORY COMMITTEE FOR AERONAUTICS

RESEARCH MEMORANDUM

for the

United States Air Force

WIND-TUNNEL INVESTIGATION OF THE LOW-SPEED STATIC LONGITUDINAL
CHARACTERISTICS OF THE REPUBLIC RF-84F AIRPLANEBy Lynn W. Hunton, Roy N. Griffin, Jr.,
and Harry A. James

SUMMARY

Tests in the Ames 40- by 80-foot wind tunnel of the static longitudinal characteristics of the Republic RF-84F were made to determine both the origin and a suitable remedy for a pitch-up tendency of the airplane encountered at moderate lift coefficients.

The results indicated that the pitch-up at moderate lift coefficients was caused by an abrupt change in downwash at the tail which in turn was traceable presumably to flow conditions associated with the inlet-to-wing leading-edge discontinuity. Attempts to eliminate this pitch-up characteristic with various fairings and stall-control devices were not wholly successful. The investigation revealed, however, that significant gains in the performance of the airplane could be achieved in the upper lift range. Three different configurations consisting of a partial-span modified leading edge combined with one or with two fences or a leading-edge extension each delayed the onset of separation to higher lift coefficients and provided large improvements in the stability of the airplane in the upper lift range.

INTRODUCTION

The Republic RF-84F is a high-performance swept-wing aircraft designed for photo reconnaissance and features wing-root inlets in place of the standard nose inlet. Evaluation tests in flight revealed the airplane to possess buffeting and pitch-up tendencies at moderate lift coefficients. This tendency persisted throughout the subcritical Mach number range, consequently seriously affecting the maneuvering qualities of the airplane as well as the landing characteristics.

~~CONFIDENTIAL~~
~~SECURITY INFORMATION~~
~~CANCELLED~~

CONFIDENTIAL
SECURITY INFORMATION

At the request of the Air Research and Development Command, an investigation was undertaken in the Ames 40- by 80-foot wind tunnel to determine the origin and a suitable remedy for the pitch-up phenomena of the airplane. The advanced stage of design and the production schedules already set up for the airplane necessarily narrowed the field of acceptable modifications to those of a simple nature. The "fixes" to the airplane investigated and reported upon herein included fairings in the vicinity of the inlet, wing leading-edge modifications, fences, spoilers, vortex generators, and leading- and trailing-edge extensions.

The airplane used for the wind-tunnel investigation was the advanced F-84F (prototype number 345) fighter bomber which is identical to the RF-84F (prototype number 828) with the exception of the fuselage nose and vertical-tail size. For most of the tests the nose of the F-84F was altered to the RF-84F nose shape. Results are also presented herein of tests made to evaluate any differences in the longitudinal characteristics of the two airplanes associated with the difference in fuselage nose.

NOTATION

Coefficients and Symbols

C_D	drag coefficient
C_L	lift coefficient
C_m	pitching-moment coefficient based on a c.g. at 0.21 \bar{c} and 0.30 feet below fuselage center line
ΔC_{m_t}	increment of pitching-moment coefficient contributed by horizontal tail
b	wing span
\bar{c}	mean aerodynamic chord of wing
\bar{c}_t	mean aerodynamic chord of horizontal tail
c	wing chord
c'	wing chord normal to wing quarter-chord line
i_t	tail incidence angle referred to fuselage center line
R	Reynolds number based on \bar{c}

V	free-stream velocity
$\frac{V_i}{V}$	inlet velocity ratio
α	angle of attack of fuselage center line
α_u	uncorrected angle of attack
η	fraction of semispan

Airplane Configurations

Following are the basic airplane (all control surfaces neutral) and detail configuration notations. The total airplane configuration will be described herein by combining the appropriate detail items with the particular basic airplane configuration used for the test.

A ₁	F-84F airplane
A ₂	simulated RF-84F airplane
A ₄	F-84F airplane with a low horizontal tail and a stub vertical tail
CE	leading-edge extension
F	fence
G	fairings in vicinity of inlet
I	inlet closure plug fairing
LE	leading-edge radius modification
N	blunted and cambered leading-edge modification
S	slats extended
SB	inlet side-edge fairing
Sp	leading-edge spoiler
T	horizontal tail and upper vertical-tail assembly
TE	trailing-edge extension
V	vortex generator

- δ_e elevator deflected
- δ_f trailing-edge plain flaps deflected 40° unless specified otherwise

DESCRIPTION OF THE AIRPLANE

Dimensions of the Republic RF-84F prototype photo-reconnaissance airplane (No. 828) are given in table I and in the three-view sketch of figure 1. The airplane actually tested was the F-84F prototype fighter bomber (No. 345) which is identical to the RF-84F with the exception of the fuselage nose shape and the vertical tail size. The former difference is noted in figure 1. For the wind-tunnel investigation, simulation of the RF-84F was effected by modifying the fuselage nose of the F-84F to duplicate that of the RF-84F. In view of the interest in only the longitudinal characteristics of the airplane, the difference in vertical-tail size was ignored. Photographs of the test installations of the simulated RF-84F and the F-84F airplanes in the wind tunnel are shown in figure 2.

The jet engine was removed from the airplane and replaced by a duct insert to gain the maximum efficiency of the air induction system. All cooling air ports were sealed and all control surfaces were locked in neutral. The main landing gear was replaced by fittings for attachment to the wind-tunnel support struts.

Dimensions of the various fence and leading-edge configurations tested are given in figures 3 and 4, respectively. Details of all other configurations tested are given with the data on each figure. The configurations tested are designated by the method described in the section Notation.

TESTS AND CORRECTIONS

Measurements of the lift, drag, and pitching moment of the airplane were made through a range of angle of attack from -2° to 22° . All tests were made with the airplane at zero sideslip and with the control surfaces and horizontal tail undeflected except where noted otherwise. For the basic airplane in the clean condition, tests were made at values of airspeed and Reynolds number as follows:

<u>Airspeed</u> (mph)	<u>Reynolds number</u>
45	4.0×10^6
100	9.2×10^6
126	11.6×10^6
167	15.4×10^6

For the airplane with flaps or with flaps and slats deflected, tests were made at Reynolds numbers of 9.2×10^6 and 11.6×10^6 . The latter figure is the approximate Reynolds number for the airplane in landing, based on a wing loading of 50 pounds per square foot and sea-level conditions. Exploratory tests of the numerous stall-control devices on the airplane were for the most part conducted at the lower Reynolds number of 9.2×10^6 to reduce the buffeting loads on the tail.

Tests of the effectiveness of the elevator and of the variable-incidence horizontal tail were made at a Reynolds number of 11.6×10^6 . Lift, drag, and pitching-moment data were measured through a range of angles of attack for fixed deflection angles of the elevator of 0° , -10° , -20° , and -25° and incidences of the tail of 4° , 0° , and -8° .

In table II all the configurations tested are listed and the figures of the report are indexed.

The data presented herein have been corrected for airplane-strut interference and tare effects and for air-stream inclination. Tunnel-wall corrections that were applied to the drag coefficient, angle of attack, and pitching-moment data were as follows:

$$\Delta\alpha = 0.717 C_L$$

$$\Delta C_D = 0.0125 C_L^2$$

$$\Delta C_m = 0.00945 C_L$$

RESULTS AND DISCUSSION

Objective of Wind-Tunnel Investigation

Preliminary evaluation tests of the airplane in flight revealed buffet and pitch-up to occur at moderate lift coefficients, these characteristics being observed both in the clean and landing conditions. Of these two conditions, the one considered the more serious was the clean configuration where buffeting and pitch-up were found to occur in accelerated maneuvers at all subcritical Mach numbers, thus seriously affecting the maneuvering capabilities of the airplane. The principal attention of this investigation, therefore, was directed toward improving the stability and stalling behavior of the clean airplane. The characteristics of the airplane in the landing condition, while important, were considered secondary and, consequently, were investigated only in the cases involving configurations which appeared promising from the standpoint of the clean airplane characteristics.

CONFIDENTIAL
SECURITY INFORMATION

Inlet-Flow Characteristics

The inlet-flow velocity characteristics as a function of angle of attack are given in figure 5 for the airplane with the jet engine removed. Free flow through the air induction system at a test airspeed of 126 mph resulted in a maximum inlet velocity ratio of 0.8.

Basic Longitudinal Characteristics

The basic longitudinal characteristics of the simulated RF-84F and the F-84F airplanes (configurations A_2 and A_1 as noted under Notation) are given in figure 6. Included in these results are the tail-off characteristics of the F-84F. It is evident from these data that virtually no difference in longitudinal characteristics exists between the RF-84F and F-84F airplanes. Consequently, for purposes of this investigation either configuration may serve as the base airplane and no distinction between the two will be made in the remainder of the discussion. In figure 7 the effect of a variation in Reynolds number on the basic longitudinal characteristics of the airplane is shown for airplane configurations clean, slats extended, flaps deflected, and slats and flaps deflected.

Isolation of Causes for Pitching Behavior

The data of figures 6(a) and 7(a) for the clean airplane indicate that a loss in stability occurs at a lift coefficient of about 0.55. This value of C_L correlates reasonably well with the flight-test reports mentioned earlier in connection with observed buffet and pitch-up in flight. The wind-tunnel data further indicate that following the loss in stability the airplane exhibited a pitch-down tendency at a C_L of about 0.75. This abrupt increase in stability, shown for the airplane either with or without tail, was attributed to flow separation at the wing tips. A similar effect of tip stall on the wing pitching moments was demonstrated in reference 1 for a wing of similar plan form and airfoil section.

When tip stall is delayed to higher C_L , such as with extension of the slat (fig. 6(b)), the pitch-up tendency originating at a C_L of 0.55 becomes progressively worse with increase in C_L . The pitching moments of the airplane with slats extended but with tail removed show no such unstable tendency. Thus, it would appear that the pitch-up problem was associated principally with a change in flow conditions at the tail. Evidence further substantiating this reasoning may be seen in

figure 8 wherein are presented results of brief tests of a horizontal tail in a low position. Again with slats extended to exclude tip stall from the problem it is evident that lowering of the tail virtually eliminated the pitch-up tendency.

Investigation of Modifications

Devices for improving the basic flow conditions on the wing.- One of the first steps undertaken by the contractor to improve the pitch-up characteristics of the airplane was an investigation in flight of various fence configurations designed to improve the stalling behavior of the wing. The most promising of these flight fence configurations was tested in the wind tunnel, the results being given in figure 9. While the fences provided some improvement by reducing the severity of the pitch-up at $C_{L_{max}}$ it appears from the data that little delay in initial flow separation at the tip was effected.

One means of delaying flow separation of the laminar or leading-edge type is the use of an increased leading-edge radius together with forward camber. The effectiveness of this method is demonstrated in references 2 and 3. The leading-edge modification of reference 1, found to provide significant gains in wing $C_{L_{max}}$ with virtually no deleterious effects at high Mach number, was tried on the leading edge of the wing. Results of tests of several different span coverages with this leading-edge modification are given in figure 10. For each of the coverages separation was delayed in varying amounts, the full-span modification increasing the C_L for separation from a value of about 0.7 to 0.88.

The effect of the addition of a 0.5-chord wrap-around fence at the inboard end of the modified leading edges of various span coverages is shown in figure 11. For all the configurations, a loss in stability can be seen to begin at a C_L of about 0.6 and continue to a C_L of 0.8 to 0.9 where the stability suddenly increases. Observations of tufts on the wing indicated that this abrupt stable tendency in each case correlated closely with occurrence of flow separation on the inboard side of the fence. On the basis of these force data the configuration designated N_3F_9 with a 0.35 semispan modified leading edge and fence was investigated further at several Reynolds numbers, with flaps and slats, and with tail removed. These results are given in figure 12. The principal improvement in the characteristics of the airplane afforded by this configuration is in the clean condition where it can be seen that the value of $C_{L_{max}}$ has been increased from 1.0 to 1.2 and there is considerable positive stability in approaching $C_{L_{max}}$. The landing characteristics of the airplane were virtually unchanged by this modification.

CONFIDENTIAL
SECURITY INFORMATION

Devices directed at altering the flow conditions to achieve a favorable change in downwash characteristics.— The partial-span leading-edge modification and fence combination (N_3F_9), although it improved the general stalling behavior of the wing in the high lift range, in no way altered the loss in stability occurring at a C_L of about 0.55. It was mentioned previously that this reduction in stability was traceable to a reduction in tail effectiveness which in turn was believed to stem from a change in flow behind the wing as a result of the inlet-to-wing leading-edge discontinuity. Hence, several modifications intended to distribute spanwise some of the vorticity concentrated at the side of the inlet were tried. A redistribution spanwise of this vorticity, it was felt, might effect a favorable change in the downwash pattern. Results of tests of three such fairing modifications are given in figure 13. The effect generally of these modifications was to reduce slightly the destabilizing effect of the inlet, but this gain was largely offset by a sizable loss in static margin as a result of the addition of area ahead of the wing center of pressure. Results of tests of other treatments of the side of the inlet, but not included herein, such as blunting or sharpening, indicated little or no change. Tests of an end plate at the edge of the inlet and extending back over the wing showed a significant improvement in the stability characteristics but, again, at a cost of a large reduction in static margin.

Since it appeared that no simple refairing of the side of the inlet would alter the flow conditions sufficiently to provide the desired changes in stability, efforts were directed toward investigating various devices which might conceivably alter the stall pattern on the wing and hence the downwash flow conditions such as to gain the necessary improvement in stability. Various fences in the region of the inlet were tried in combination with the partial-span blunt leading edge and fence (N_3F_9). These results are given in figure 14. Of the five fences tested, the one designated F_5 and located on the edge of the inlet was found to provide the most stability, although none of the fence configurations tested gave any indication of alleviating the initial pitch-up tendency beginning at a C_L of 0.55. In figure 15 additional data for the F_5 configuration are given for the airplane in the clean condition for various Reynolds numbers and for the airplane with flaps and slats deflected and with the tail removed. With flaps alone or with flaps and slats deflected the stability near $C_{L_{max}}$ is greatly improved by the inboard fence, the improvement being somewhat greater than for the clean condition.

To determine the effect of modifications to the wing leading edge in the vicinity of the inlet on the stability and/or $C_{L_{max}}$ of the airplane with these two fences and partial-span blunt leading edge ($N_3F_9F_5$), tests were made of two constant leading-edge radius modifications of 1/2 inch and 1 inch and with the basic outboard blunt nose extended to the inboard

CONFIDENTIAL
SECURITY INFORMATION

end of the slat (N_1) and into the inlet (N_2). These results are given in figure 16 for the airplane clean and with flaps deflected. The results indicate that no advantages are to be gained over the original leading-edge radius from any of the modifications tested.

Vortex generators in recent investigations, such as reference 4, have been shown to be effective as a means of intermixing high-energy air with the boundary layer and thereby producing significant changes in the stalling behavior of swept wings. In figure 17 data are shown for four different configurations of vortex generators. For each of the configurations the individual generators consisted of 0.062-inch-thick flat metal plates and were oriented parallel to the free stream (see fig. 17) with the expectation that the vortex from the side of the inlet would provide the necessary angularity in flow for the proper functioning of the generators. From the data it is evident that three of the configurations involving V_1 were effective while the one involving V_2 was not. However, all configurations tested introduced a considerable increase in general shaking and buffeting of the airplane at stall and hence were not investigated further.

Figure 18 shows the results of tests of two spoilers on the wing in combination with various fences. The spoilers, extending spanwise 12- and 4-percent semispan, consisted of a sharp angle attached symmetrically to the wing leading edge (see fig. 18). It is evident from the data that stall of inboard sections with attendant changes in downwash provided significant increases in stability in the upper lift range. Again, however, the stability was gained at a cost of a considerable increase in buffeting and a loss of 0.1 in $C_{L_{max}}$.

Small-scale tests have shown that the stability of swept wings in some cases can be improved by various chord extensions, these being of two types, leading-edge extensions to outboard regions of the wing and trailing-edge extensions to inboard regions of the wing. Two spans of leading-edge extensions, 10- and 15-percent semispan, and one trailing-edge extension were tested and the results given in figures 19 and 20, respectively. For the airplane in the clean condition the 15-percent-semispan leading-edge extension showed a significant improvement in stability; whereas the trailing-edge extension caused no perceptible change in the characteristics of the airplane. With flaps extended the leading-edge extensions provided virtually no improvement in the stability of the airplane.

Flap, Tail, and Elevator Deflection Results

In figures 21, 22, and 23 are given the longitudinal force and moment characteristics of the airplane with several different flap angles, tail incidences, and elevator deflections, respectively.

CONFIDENTIAL
SECURITY INFORMATION

CONCLUDING REMARKS

As stated earlier, the purpose of this investigation was to explore means of relieving the pitch-up characteristics of the airplane, these means being restricted to those of a simple modification which could be added to the airplane without involving any changes to the basic airplane structure. The loss in stability occurring at moderate lift coefficients, on the basis of the basic airplane data tail-on and tail-off and on tests of a tail in a low position, was demonstrated to be caused by an abrupt loss in tail effectiveness which presumably was traceable to flow conditions associated with the inlet. Attempts to alter the flow characteristics in the vicinity of the side of the inlet in such a manner as to provide some improvement in stability were unsuccessful. Efforts in another direction, attempts to modify the stalling characteristics of the wing, produced three promising configurations: (1) the partial-span modified leading edge with one fence (N_3F_9); (2) the same configuration plus the addition of the inboard fence ($N_3F_9F_5$); and (3) the 15-percent-semispan leading-edge extension. Of the three configurations, the second is considered the optimum since it improved the stability characteristics of the airplane both in the clean and landing condition. In figure 24 are given tail-effectiveness data for the airplane with each of these three fix configurations plus that for the original airplane. It is clear from these results that none of the configurations effected any significant change in the downwash and hence tail effectiveness, thus indicating that the improvements in airplane stability obtained with these fixes were accomplished by increases in the basic stability of the wing. This latter fact accounts for the lack of any improvement in stability afforded by these fixes in the moderate lift range from C_L of 0.55 to 0.70 for which lift range no flow separation was present on the wing.

On the basis of these wind-tunnel results, two of these promising fix configurations involving the blunt nose and fences have been evaluated in flight. The first, with only one fence (N_3F_9), was reported to have greatly improved the clean airplane characteristics by reducing not only the pitch-up tendency but the aileron buffet as well. The landing characteristics were unimproved by this configuration, thus showing good correlation with the wind-tunnel data reported herein. For the second configuration involving the blunt nose and two fences ($N_3F_9F_5$), the picture was quite different. Flight-test reports confirmed the improvements in stability indicated by the wind-tunnel tests but rated this configuration unacceptable due to a condition of severe buffet of the aileron. The ailerons during the wind-tunnel tests were rigidly clamped in neutral which eliminated all evidence of such a buffet condition. In view of the afore-mentioned development, it is readily apparent that the achievement of satisfactory stability of the airplane constitutes only a partial solution to the problem, and that some quantitative measure of buffeting must

be considered in wind-tunnel tests if such investigations are to be an important link in the development of aircraft.

Ames Aeronautical Laboratory
National Advisory Committee for Aeronautics
Moffett Field, Calif.

REFERENCES

1. Kolbe, Carl D., and Boltz, Frederick W.: The Forces and Pressure Distribution at Subsonic Speeds on a Plane Wing Having 45° of Sweepback, an Aspect Ratio of 3, and a Taper Ratio of 0.5. NACA RM A51G31, 1951.
2. Demele, Fred A., and Sutton, Fred B.: The Effects of Increasing the Leading-Edge Radius and Adding Forward Camber on the Aerodynamic Characteristics of a Wing With 35° of Sweepback. NACA RM A50K28a, 1951.
3. Maki, Ralph L.: Full-Scale Wind-Tunnel Investigation of the Effects of Wing Modifications and Horizontal-Tail Location on the Low-Speed Static Longitudinal Characteristics of a 35° Swept-Wing Airplane. NACA RM A52B05, 1952.
4. Weiberg, James A., and McCullough, George B.: Wind-Tunnel Investigation at Low Speed of a Twisted and Cambered Wing Swept Back 63° With Vortex Generators and Fences. NACA RM A52A17, 1952.

TABLE I.- GEOMETRIC DATA ON THE REPUBLIC RF-84F AIRPLANE

Wing ¹	
Area, square feet	325
Span, feet	33.52
Aspect ratio	3.45
Taper ratio	0.58
Cathedral, degrees	3°30'
Mean aerodynamic chord, feet	10.04
Sweepback of 0.25-chord line, degrees	40
Geometric twist, degrees	0
Incidence, degrees	1°30'
Airfoil section normal to 0.25-chord line	NACA 64A010
Trailing-edge flap	
Type	Plain-hinged at lower surface
Span, feet	6.62
Area, square feet	30.2
Hinge line, percent c'	75
Deflection, degrees	40
Leading-edge slat	
Type	Drooped-slotted
Span, feet	8.0
Area, square feet	22.8
Chord, percent c	16.55
Forward extension, percent c'	8.4
Downward extension, percent c'	7.24

¹Inlet area of 18.32 square feet not included in dimensions.

TABLE I.- CONCLUDED

Horizontal tail	
Area, square feet	55.8
Span, feet	14.17
Aspect ratio	3.59
Taper ratio	1.0
Dihedral, degrees	0
Sweepback, degrees	40
Incidence, degrees	4 up 9 down
Airfoil section normal to leading edge	NACA 64A009
0.25 \bar{c} to 0.25 \bar{c}_t , feet	19.6
Elevator	
Type	Trailing-edge flap - internally balanced
Chord (constant), feet	1.2
Area, square feet	14.9
Hinge line, percent chord	70
Angular travel, degrees	12 down 27 up
Alternate horizontal tail (low tail tested in wind tunnel)	
Area, square feet	37.8
Span, feet	14.34
Aspect ratio	5.53
Taper ratio	0.38
Dihedral, degrees	10
Sweepback, degrees	35
Incidence, degrees	0
Airfoil section parallel to center line	NACA 0010-64
0.25 \bar{c} to 0.25 \bar{c}_t , feet	19.0

TABLE II.- INDEX OF DATA PRESENTED

Subject	Figure No.	Configuration	$R \times 10^{-6}$	Data presented
Inlet flow	5	A_1	11.6	V_i/V vs α
Basic airplane	6(a)	A_1, A_1-T, A_2	11.6	C_D, α, C_m vs C_L
	6(b)	A_1S, A_1S-T, A_2S	11.6	
	6(c)	$A_1\delta_f, A_2\delta_f$	9.2	
	6(d)	$A_1\delta_fS, A_1\delta_fS-T, A_2\delta_fS$	9.2	
Reynolds number	7(a)	A_2	4.0, 9.2, 11.6, 15.4	C_D, α, C_m vs C_L
	7(b)	A_2S	9.2, 11.6	
	7(c)	$A_2\delta_f$	9.2, 11.6	
	7(d)	$A_2\delta_fS$	4.0, 9.2, 11.6	
Low tail	8	$A_4, A_4S, A_4\delta_fS$	9.2	C_D, α, C_m vs C_L
Flight fences	9	$A_1 + F_3F_4$ $A_1\delta_fS + F_3F_4$	9.2	C_D, α, C_m vs C_L
Blunted and cambered leading edge (N)	10	$A_1 + N_2$ $A_2 + N_1$ $A_2 + N_3$	9.2	C_D, α, C_m vs C_L
N + fences (F)	11	$A_2 + N_1F_7a$ $A_2 + N_4F_{11}$ $A_2 + N_3F_9$ $A_2 + N_5F_{12}$	9.2	C_D, α, C_m vs C_L
Optimum N plus one fence (N_3F_9)	12(a)	$A_2 + N_3F_9$	9.2, 11.6, 15.4	C_D, α, C_m vs C_L
		$A_1 + N_3F_9-T$	11.6	
	12(b)	$A_2\delta_f + N_3F_9$ $A_2\delta_fS + N_3F_9$ $A_1\delta_f + N_3F_9-T$ $A_1\delta_fS + N_3F_9-T$	11.6	C_D, α, C_m vs C_L
Inlet fairings	13(a)	$A_2 + N_3F_9 + G_4$ $A_2 + N_3F_9 + G_4 + SB$ $A_2 + N_3F_9 + G_5$	9.2	C_D, α, C_m vs C_L
	13(b)	$A_2 + N_1 + G_2$ $A_2 + N_1 + G_2 + I$	9.2	C_D, α, C_m vs C_L

TABLE II.- CONTINUED

Subject	Figure No.	Configuration	R × 10 ⁻⁶	Data presented
Inboard fences with N ₃ F ₉	14	A ₂ +N ₃ F ₉ +F ₁₀ A ₂ +N ₃ F ₉ +F ₅ A ₂ +N ₃ F ₉ +F ₆ A ₂ +N ₃ F ₉ +F ₃ A ₂ +N ₃ F ₉ +F ₇	9.2	C _D , α, C _m vs C _L
Optimum N plus two fences (N ₃ F ₉ F ₅)	15(a)	A ₂ +N ₃ F ₉ F ₅	9.2, 11.6 15.4	C _D , α, C _m vs C _L
		A ₁ +N ₃ F ₉ F ₅ -T	11.6	
	15(b)	A ₂ δ _f +N ₃ F ₉ F ₅ A ₂ δ _f S+N ₃ F ₉ F ₅ A ₁ δ _f +N ₃ F ₉ F ₅ -T A ₁ δ _f S+N ₃ F ₉ F ₅ -T	11.6	C _D , α, C _m vs C _L
		Inboard leading-edge modification with N ₃ F ₉ F ₅	16(a)	A ₂ +F ₉ F ₅ +N ₃ LE ₁ A ₂ +F ₉ F ₅ +N ₃ LE ₂ A ₂ +F ₉ F ₅ +N ₂ A ₂ +F ₉ F ₅ +N ₁
16(b)	A ₂ δ _f +F ₉ F ₅ +N ₃ LE ₂ A ₂ δ _f +F ₉ F ₅ +N ₂ A ₂ δ _f +F ₉ F ₅ +N ₁			11.6
Vortex generators	17	A ₂ +N ₃ F ₉ +V _{1a} A ₂ +N ₃ F ₉ +V _{1b} A ₂ +N ₃ F ₉ +V _{1c} A ₂ +N ₃ F ₉ +V ₂	9.2	C _D , α, C _m vs C _L
Inboard spoilers	18(a)	A ₁ +N ₁ +Sp ₁ A ₁ +N ₁ +F ₁ Sp ₁ A ₁ +F ₁ Sp ₁ A ₂ +N ₃ F ₉ +F ₃ Sp ₂	9.2	C _D , α, C _m vs C _L
	18(b)	A ₁ δ _f S+F ₁ Sp ₁ A ₂ δ _f +N ₃ F ₉ +F ₃ Sp ₂	9.2	C _D , α, C _m vs C _L
Leading-edge extensions	19(a)	A ₁ +CE ₁	9.2	C _D , α, C _m vs C _L
		A ₁ +CE ₂ A ₁ +CE ₂ -T	11.6	
	19(b)	A ₁ δ _f +CE ₁	9.2	C _D , α, C _m vs C _L
		A ₁ δ _f +CE ₂ A ₁ δ _f +CE ₂ -T	11.6	

TABLE II.- CONCLUDED

Subject	Figure No.	Configuration	$R \times 10^{-6}$	Data presented
Trailing-edge extension	20	A_2+TE A_2S+TE	9.2	C_D, α, C_m vs C_L
Flap effectiveness	21	$A_2+N_3F_9+\delta_f 35^\circ$ $A_2+N_3F_9+\delta_f 40^\circ$ $A_2+N_3F_9+\delta_f 45^\circ$ $A_2+N_3F_9+\delta_f 50^\circ$	9.2	C_D, α, C_m vs C_L
Tail incidence	22	$A_2+N_3F_9F_5+i_t 4^\circ$ $A_2+N_3F_9F_5+i_t 0^\circ$ $A_2+N_3F_9F_5+i_t -8^\circ$	11.6	C_D, α, C_m vs C_L
Elevator effectiveness	23(a)	$A_2+N_3F_9F_5+\delta_e 0^\circ$ $A_2+N_3F_9F_5+\delta_e -20.5^\circ$	11.6	C_D, α, C_m vs C_L
	23(b)	$A_2\delta_f+N_3F_9F_5+\delta_e 0^\circ$ $A_2\delta_f+N_3F_9F_5+\delta_e -10^\circ$ $A_2\delta_f+N_3F_9F_5+\delta_e -20^\circ$ $A_2\delta_f+N_3F_9F_5+\delta_e -25^\circ$	11.6	C_D, α, C_m vs C_L
Tail effectiveness	24	A_1 $A_2+N_3F_9$ $A_2+N_3F_9F_5$ A_1+CE_2	11.6	ΔC_{m_t} vs α_u

FIGURE LEGENDS

- Figure 1.- Three view sketch of the Republic RF-84F airplane.
- Figure 2.- View of the airplane mounted in the wind tunnel. (a) Simulated RF-84F. Configuration $A_2+N_3F_3F_5$.
- Figure 2.- Concluded. (b) F-84F. Configuration A_1-T .
- Figure 3.- Dimensions of fences.
- Figure 4.- Dimensions of the modified leading edge.
- Figure 5.- Inlet flow characteristics with engine removed. $V = 126$ mph.
- Figure 6.- Longitudinal aerodynamic characteristics of the RF-84F and F-84F airplanes. (a) Clean.
- Figure 6.- Continued. (b) Slats extended.
- Figure 6.- Continued. (c) Flaps deflected.
- Figure 6.- Concluded. (d) Flaps and slats extended.
- Figure 7.- Longitudinal aerodynamic characteristics of the test airplane at several Reynolds numbers. (a) Clean.
- Figure 7.- Continued. (a) Concluded, clean.
- Figure 7.- Continued. (b) Slats extended.
- Figure 7.- Continued. (c) Flaps extended.
- Figure 7.- Concluded. (d) Flaps and slats extended.
- Figure 8.- Effectiveness of a low horizontal tail on the characteristics of the airplane. $R = 9.2 \times 10^6$. (a) C_L vs C_D , α
- Figure 8.- Concluded. (b) C_L vs C_m .
- Figure 9.- Effects of flight test fences on the characteristics of the airplane. $R = 9.2 \times 10^6$.
- Figure 10.- Effects of a modified leading edge of various partial spans on the characteristics of the airplane. $R = 9.2 \times 10^6$.
- Figure 11.- Effects of a modified leading edge of various partial spans combined with a fence on the characteristics of the airplane. $R = 9.2 \times 10^6$. (a) C_L vs C_D , α .

- Figure 11.- Concluded. (b) C_L vs C_m .
- Figure 12.- Effects of a 0.35 span modified leading edge and a fence (N_3F_9) on the characteristics of the airplane with and without the horizontal tail. (a) Clean.
- Figure 12.- Continued. (b) Flaps and slats extended, $R = 11.6 \times 10^6$.
- Figure 12.- Concluded. (b) Concluded, flaps and slats extended, $R = 11.6 \times 10^6$.
- Figure 13.- Effects of fairings in the vicinity of the inlet on the characteristics of the airplane. (a) Fairings, G_4 , G_5 , and SB. $R = 9.2 \times 10^6$.
- Figure 13.- Concluded. (b) Fairings G_1 , G_2 and I. $R = 9.2 \times 10^6$.
- Figure 14.- Effects of various inboard fences on the characteristics of the airplane with configuration N_3F_9 . $R = 9.2 \times 10^6$. (a) C_L vs C_D , α .
- Figure 14.- Concluded. (b) C_L vs C_m .
- Figure 15.- Effects of a 0.35 span modified leading edge and two fences ($N_3F_9F_5$) on the characteristics of the airplane with and without the horizontal tail. (a) Clean.
- Figure 15.- Continued. (b) Flaps and slats deflected, $R = 11.6 \times 10^6$.
- Figure 15.- Concluded. (b) Concluded, flaps and slats deflected, $R = 11.6 \times 10^6$.
- Figure 16.- Effects of changes of the leading-edge radius of inboard sections on the characteristics of the airplane with configuration $N_3F_9F_5$. (a) Clean.
- Figure 16.- Continued. (a) Concluded, clean.
- Figure 16.- Concluded. (b) Flaps extended, $R = 11.6 \times 10^6$.
- Figure 17.- Effects of vortex generators on the characteristics of the airplane with configuration N_3F_9 . $R = 9.2 \times 10^6$.
(a) C_L vs C_D , α .
- Figure 17.- Concluded. (b) C_L vs C_m .

Figure 18.- Effects of sharp leading-edge spoilers on the characteristics of the airplane. (a) Clean. $R = 9.2 \times 10^6$.

Figure 18.- Continued. (a) Concluded, clean. $R = 9.2 \times 10^6$.

Figure 18.- Concluded. (b) Flaps and slats deflected. $R = 9.2 \times 10^6$.

Figure 19.- Effects of leading-edge extensions on the characteristics of the airplane with and without the horizontal tail. (a) Clean.

Figure 19.- Continued. (b) Flaps deflected.

Figure 19.- Concluded. (b) Concluded, flaps deflected.

Figure 20.- Effects of a trailing-edge extension on the characteristics of the airplane with and without slats extended. $R = 9.2 \times 10^6$.

Figure 21.- Effects of flap deflection angle on the characteristics of the airplane with configuration N_3F_9 . $R = 9.2 \times 10^6$.
(a) C_L vs C_D , α .

Figure 21.- Concluded. (b) C_L vs C_m .

Figure 22.- Effects of horizontal-tail incidence angle on the characteristics of the airplane with configuration $N_3F_9F_5$. $R = 11.6 \times 10^6$.

Figure 23.- Effects of elevator deflection angle on the characteristics of the airplane with configuration $N_3F_9F_5$.
(a) Clean, $R = 11.6 \times 10^6$.

Figure 23.- Continued. (b) Flaps deflected. $R = 11.6 \times 10^6$.

Figure 23.- Concluded. (b) Concluded, Flaps deflected. $R = 11.6 \times 10^6$.

Figure 24.- Comparison of the increments of pitching-moment coefficient contributed by the horizontal tail for the airplane with several of the more promising modifications.

DAVID ...

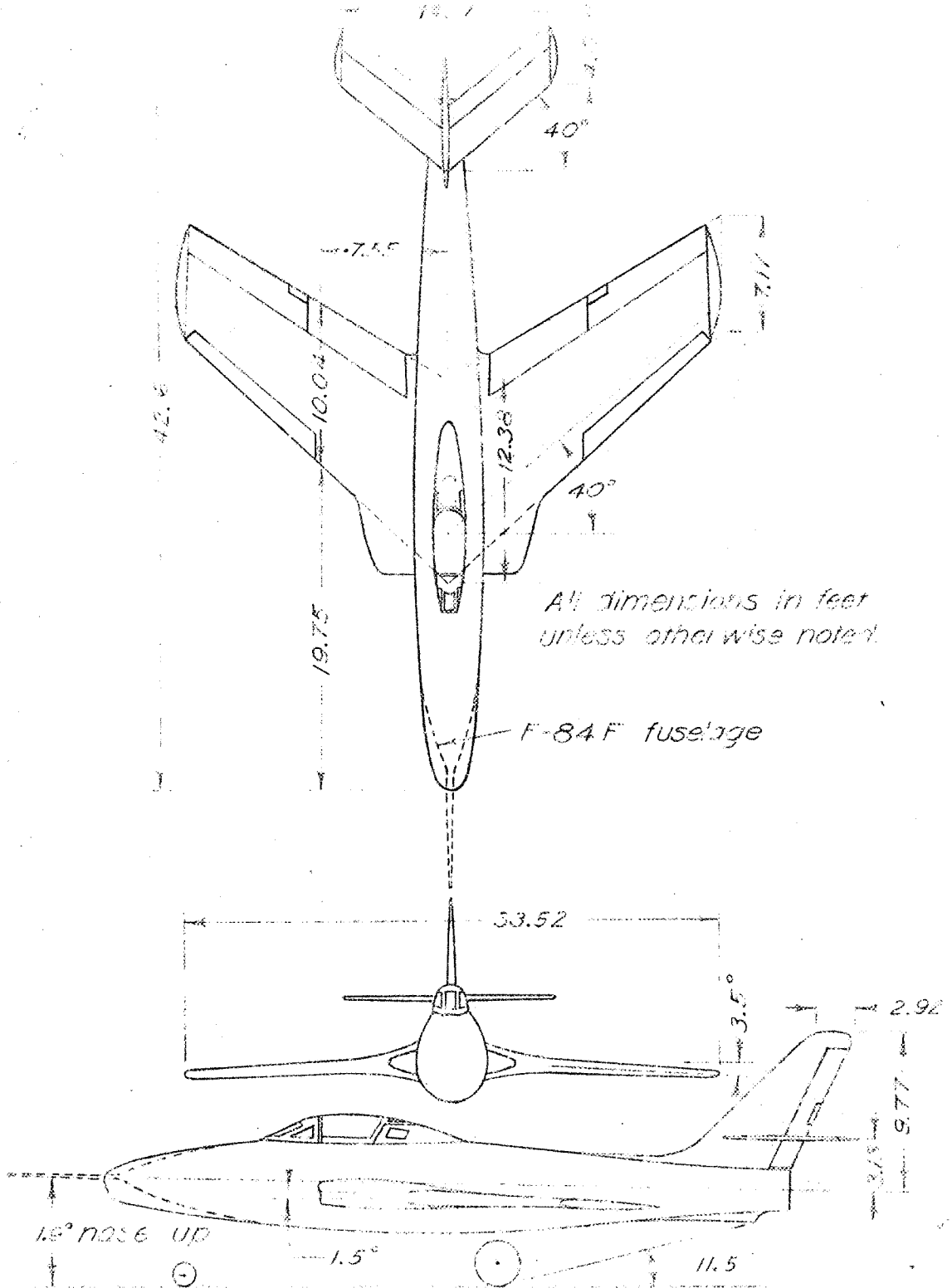
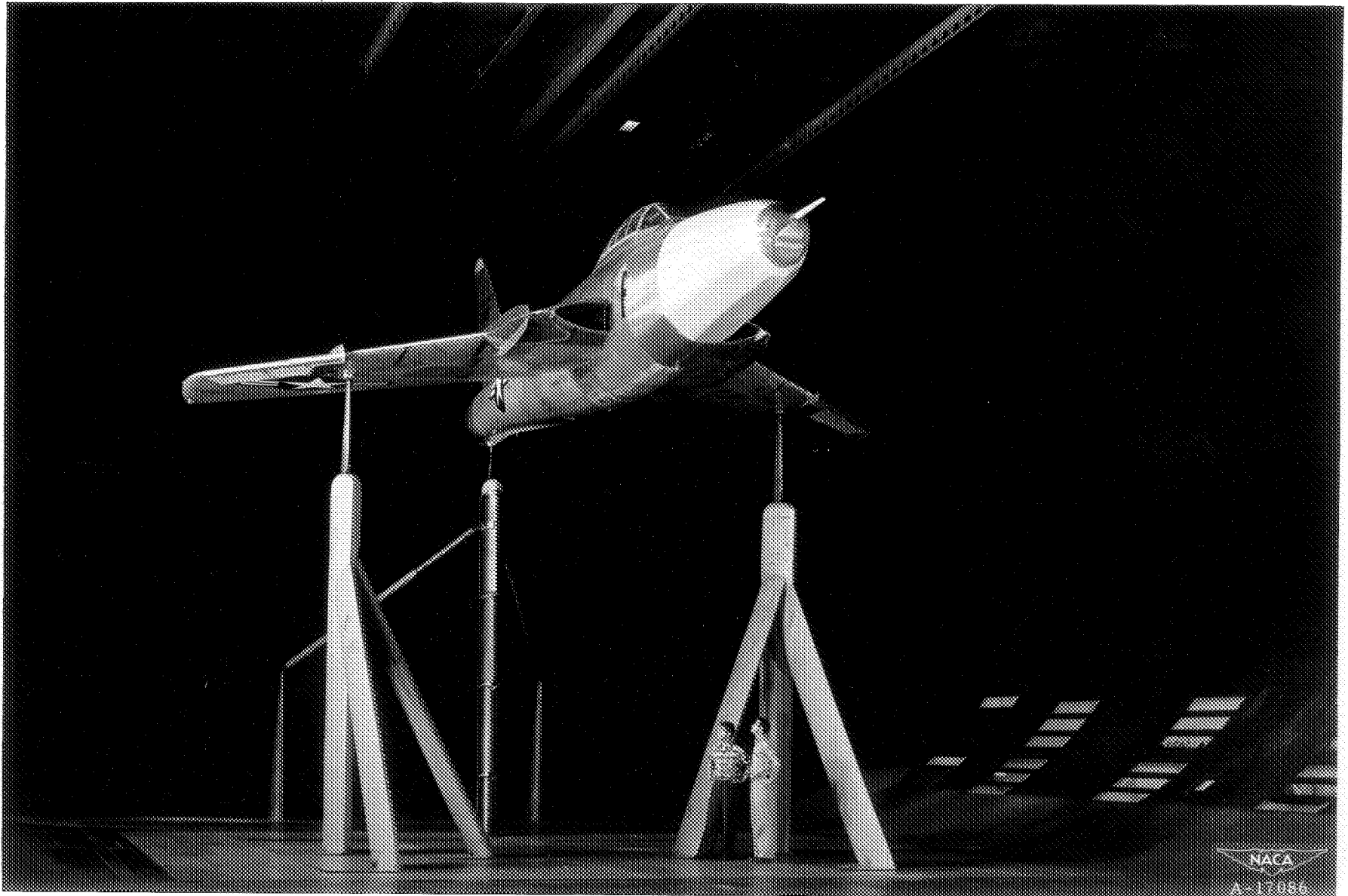


Figure 1.- Three view sketch of the Republic RF-84F airplane.



(a) Simulated RF-84F. Configuration $A_2+N_3F_9F_5$.

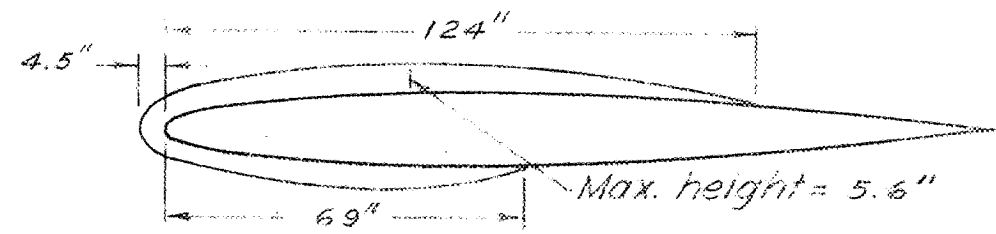
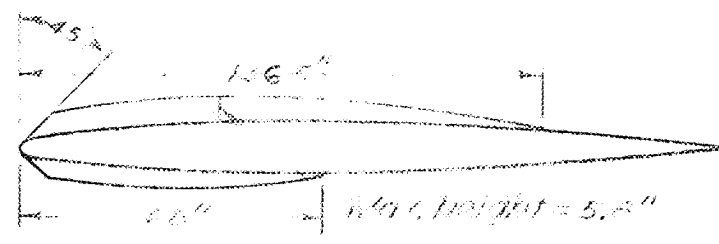
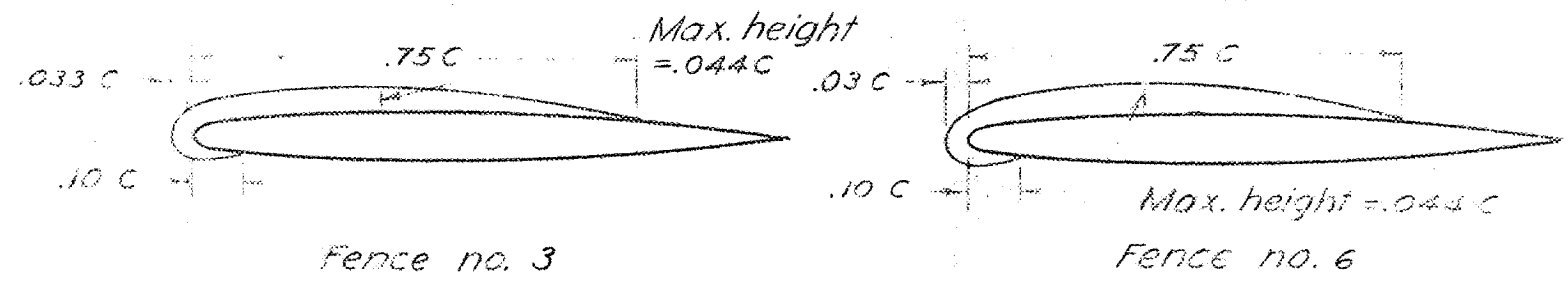
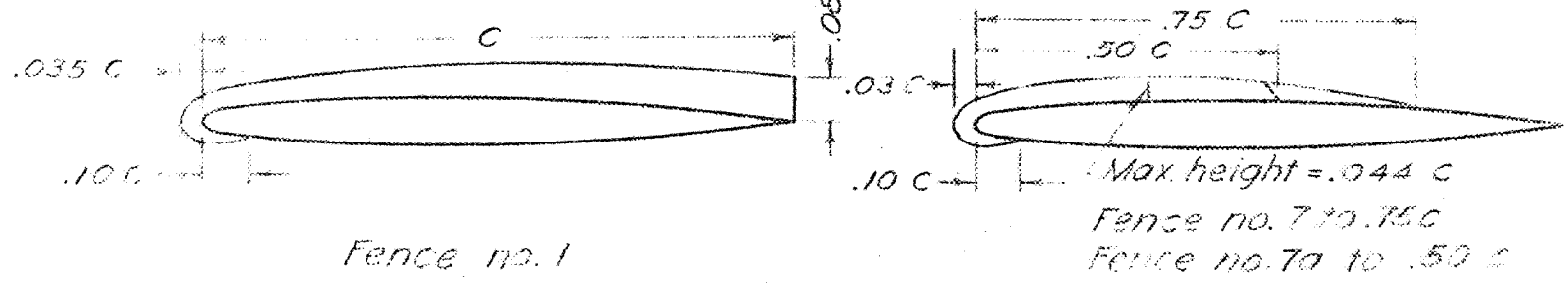
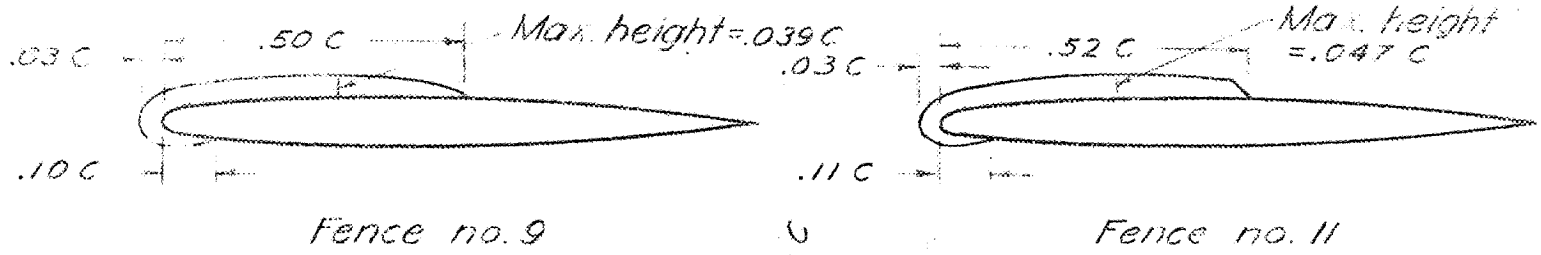
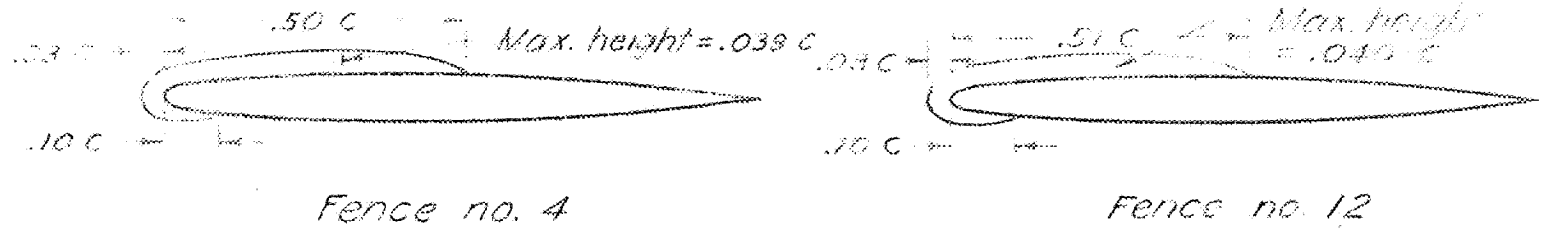
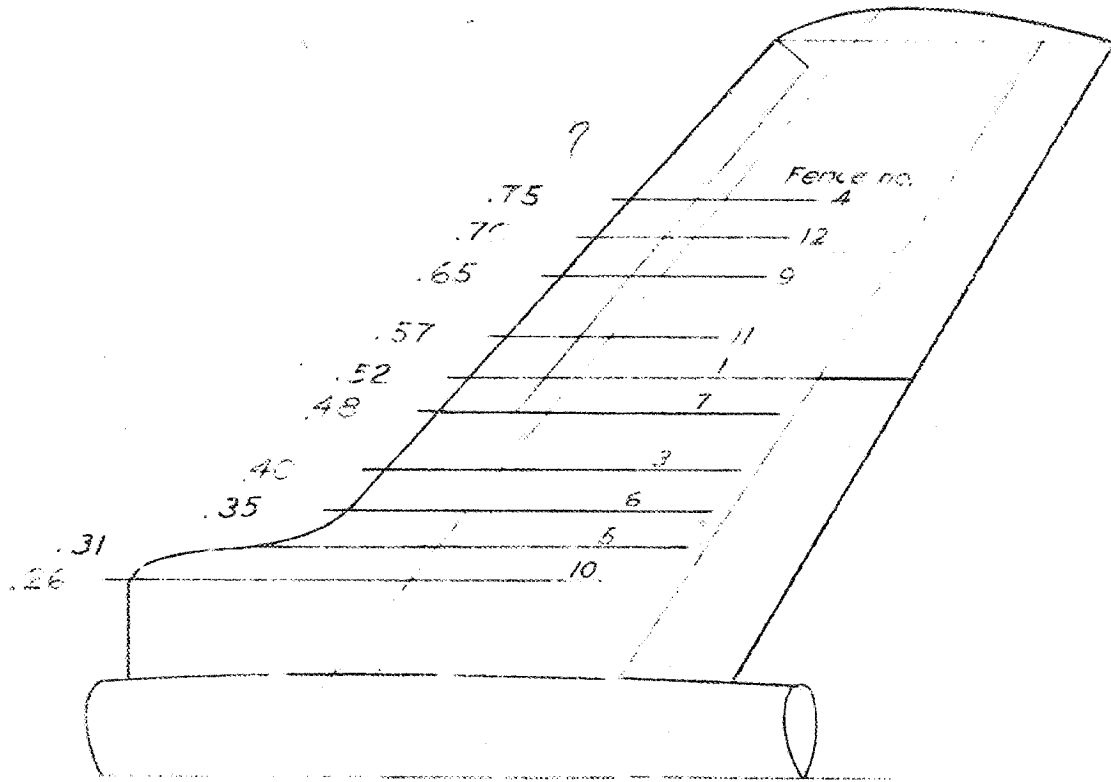
Figure 2.-- View of the airplane mounted in the wind tunnel.



(b) F-84F. Configuration A₁-T.

Figure 2.- Concluded.

CONFIDENTIAL
SECURITY INFORMATION

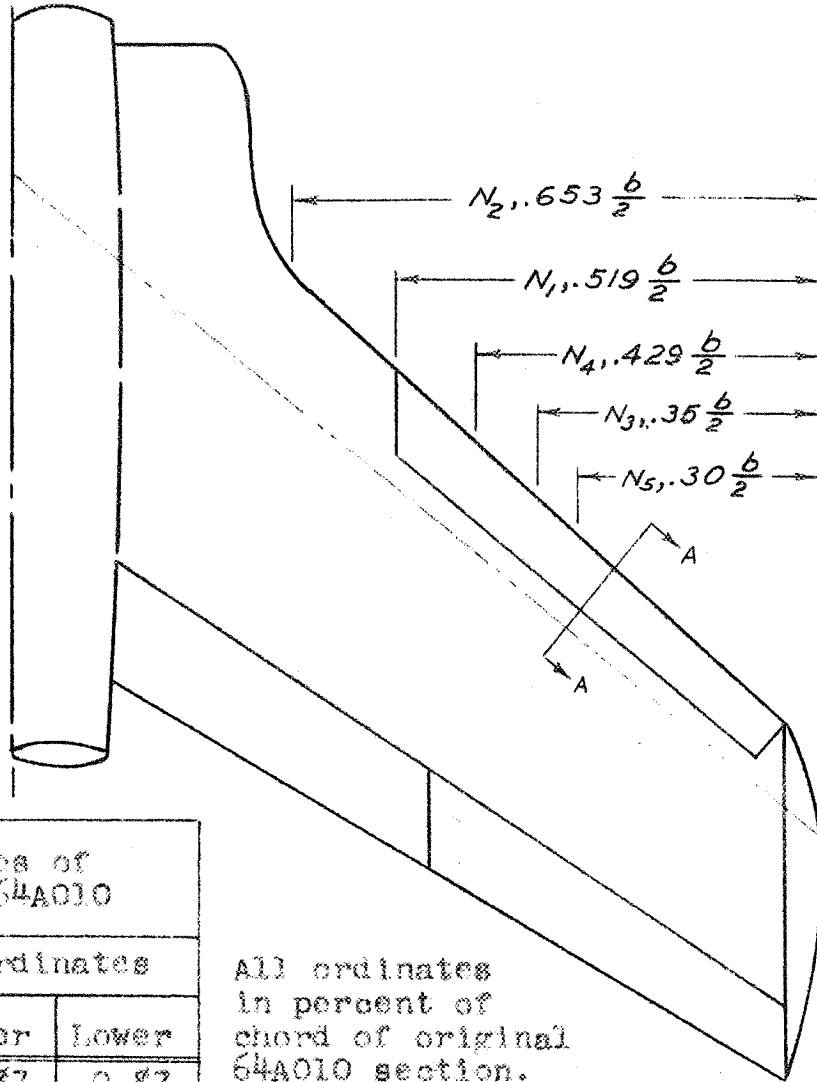


Fence no. 5

Fence no. 10

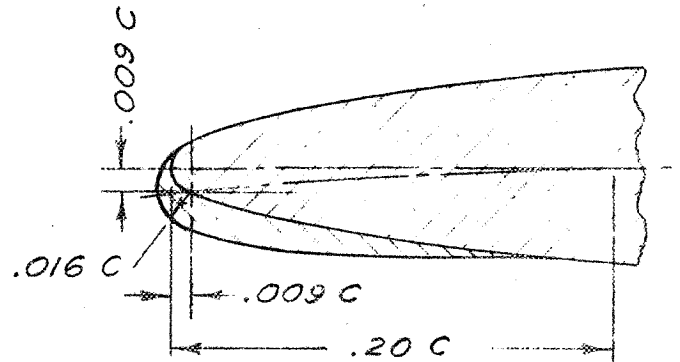
CONFIDENTIAL
SECURITY INFORMATION

Figure 3.- Dimensions of fences



Coordinates of modified 64A010		
Station	Ordinates	
	Upper	Lower
-0.72	-0.87	-0.87
-0.71	-0.75	-1.02
-0.50	-0.09	-1.69
-0.25	0.23	-2.03
0	0.46	-2.25
0.50	0.82	-2.54
0.75	0.97	-2.67
1.25	↑	-2.88
2.50		-3.25
5.00	Same	-3.58
7.50	as	-3.72
10.00	64A010	-3.81
15.00	↓	-3.96
L.E.R. = 1.600		

All ordinates in percent of chord of original 64A010 section.



Section A-A

Ordinates same as 64A010 aft of .15c

Figure 4.- Dimensions of the modified leading edge.

CONFIDENTIAL
SECURITY INFORMATION



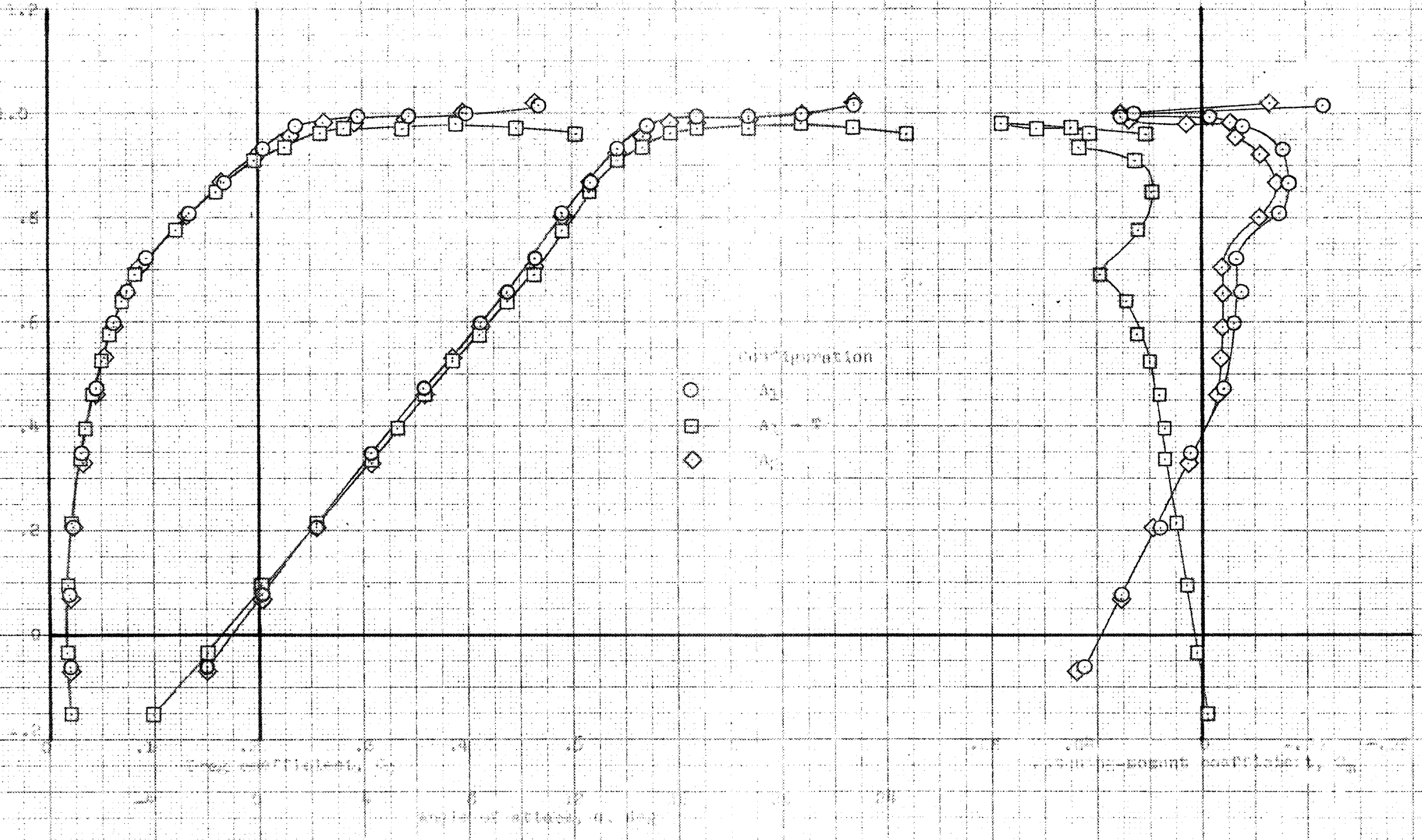
WACA RM 5A528H

Figure 5. Inlet flow characteristics with engine removed. $V = 126$ mph

CONFIDENTIAL
SECURITY INFORMATION

CONFIDENTIAL

SECURITY INFORMATION



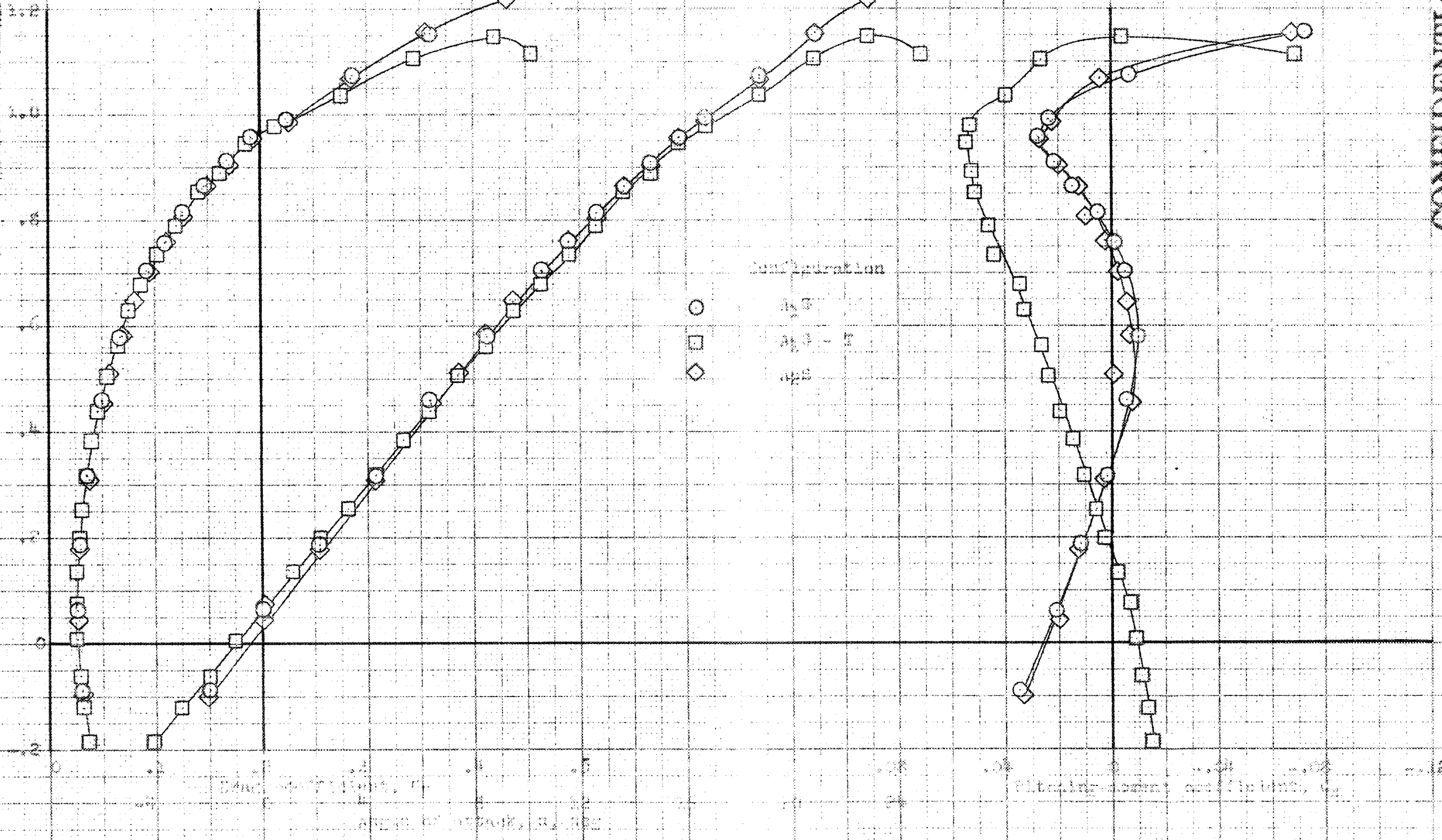
(a) Clear.

Figure 1. Theoretical characteristics of the system. CONFIDENTIAL SECURITY INFORMATION

DATA ON CARTRIDGE

CONFIDENTIAL
SECURITY INFORMATION

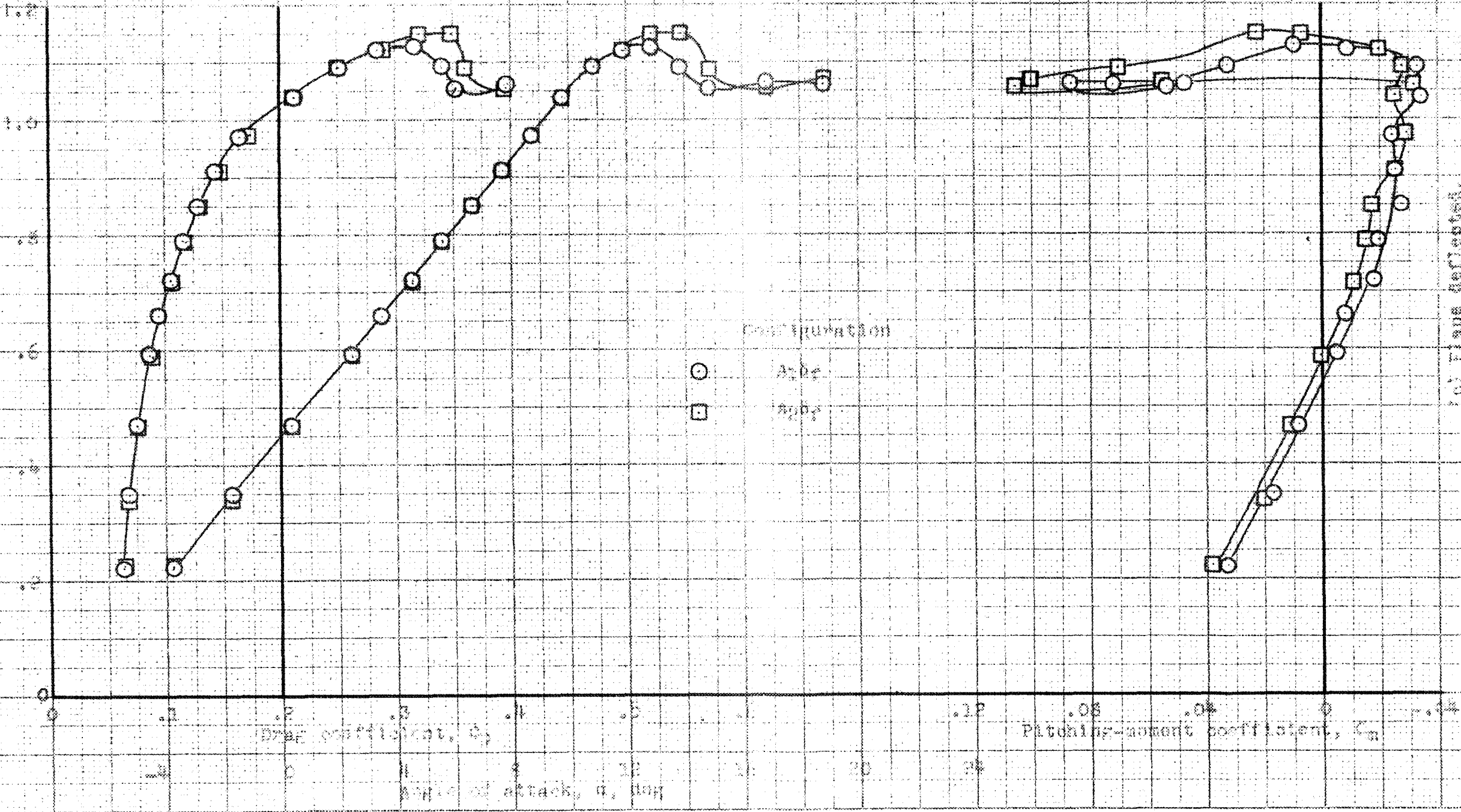
FORM 10-62 (REV. 10-6-64)



CONFIDENTIAL
SECURITY INFORMATION

(b) Data extended
Figure 1 - Continued

CONFIDENTIAL
SECURITY INFORMATION

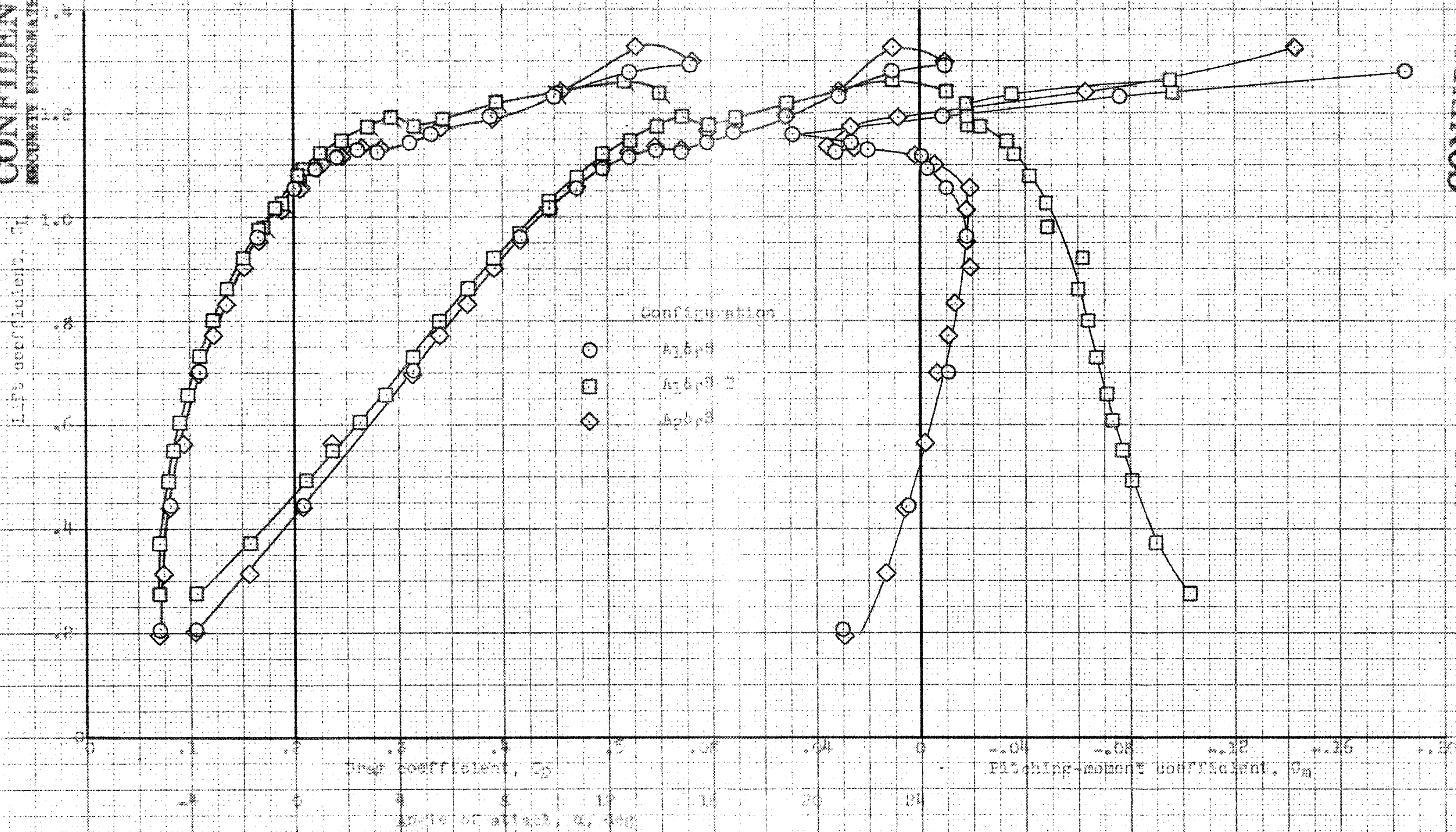


(a) Flaps reflected.

(b) Flaps deflected.

CONFIDENTIAL
SECURITY INFORMATION

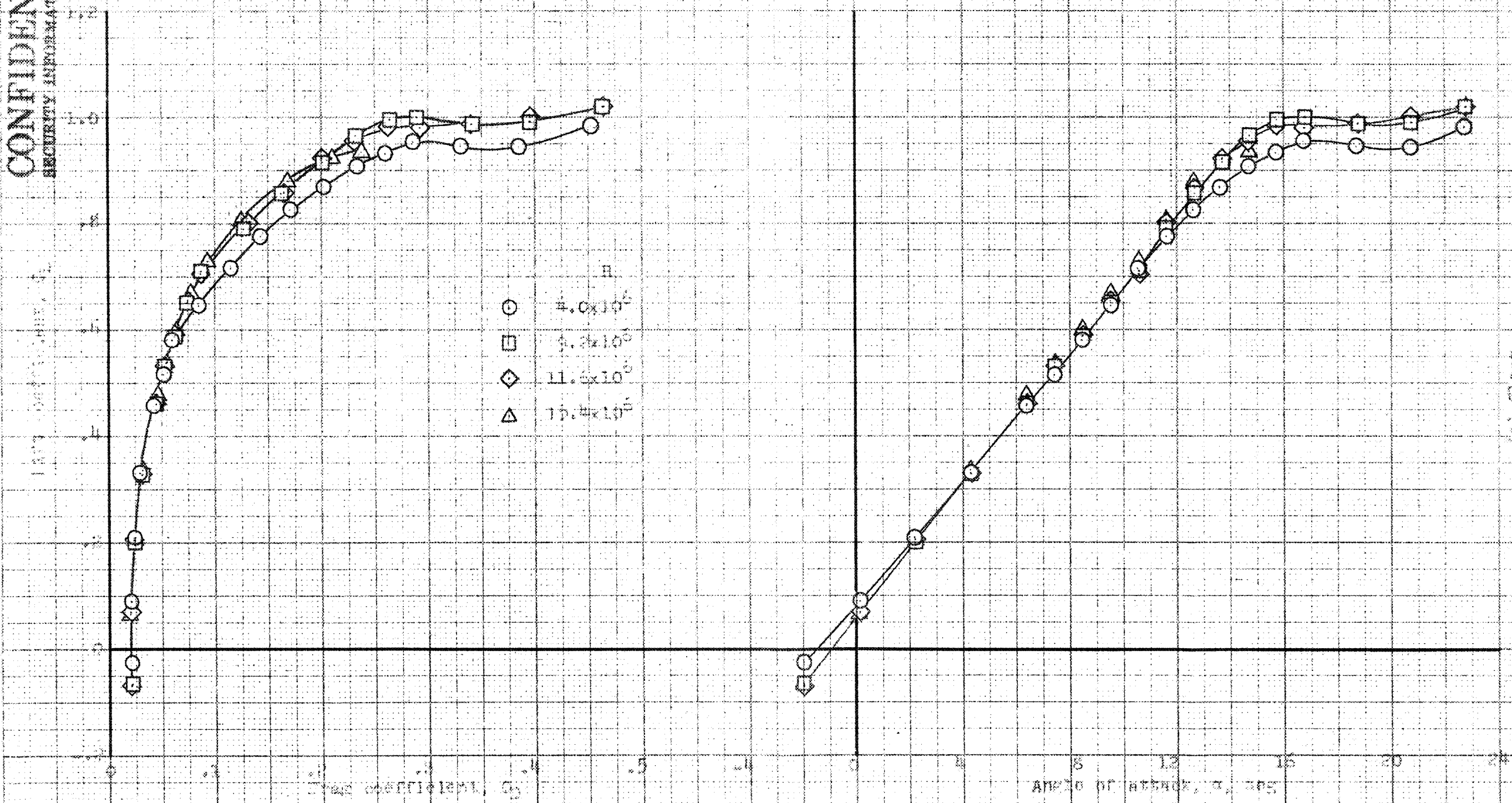
CONFIDENTIAL
SECURITY INFORMATION



CONFIDENTIAL
SECURITY INFORMATION

(a) Plans and slots extended.
Figure 6... Concluded.

FORM NO. 1052HD4

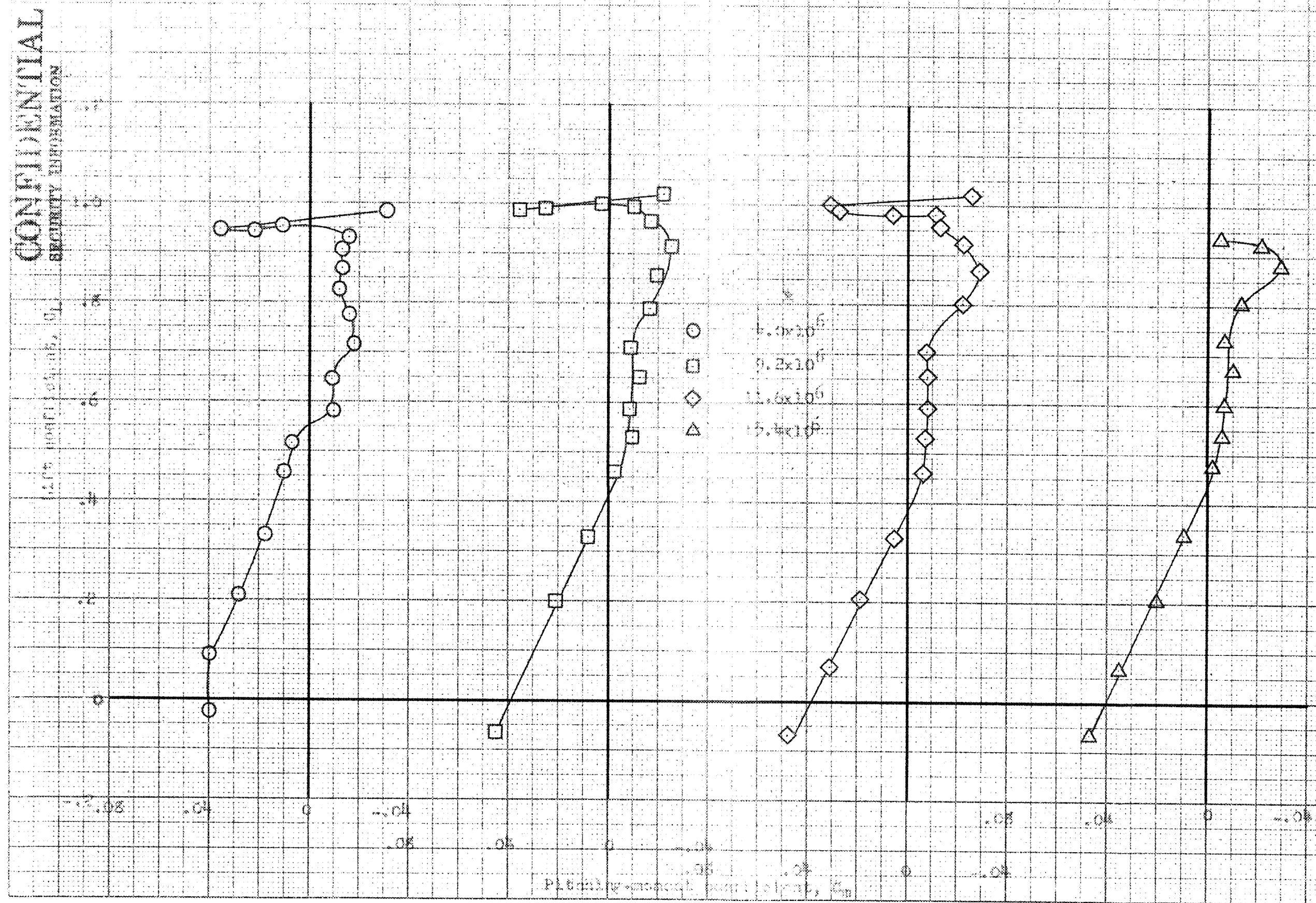


(a) Clean.

Figure 7. - Identical lift characteristics of the B-29 bomber at several Reynolds numbers.

CONFIDENTIAL
SECURITY INFORMATION

DATA ON CAPTURE



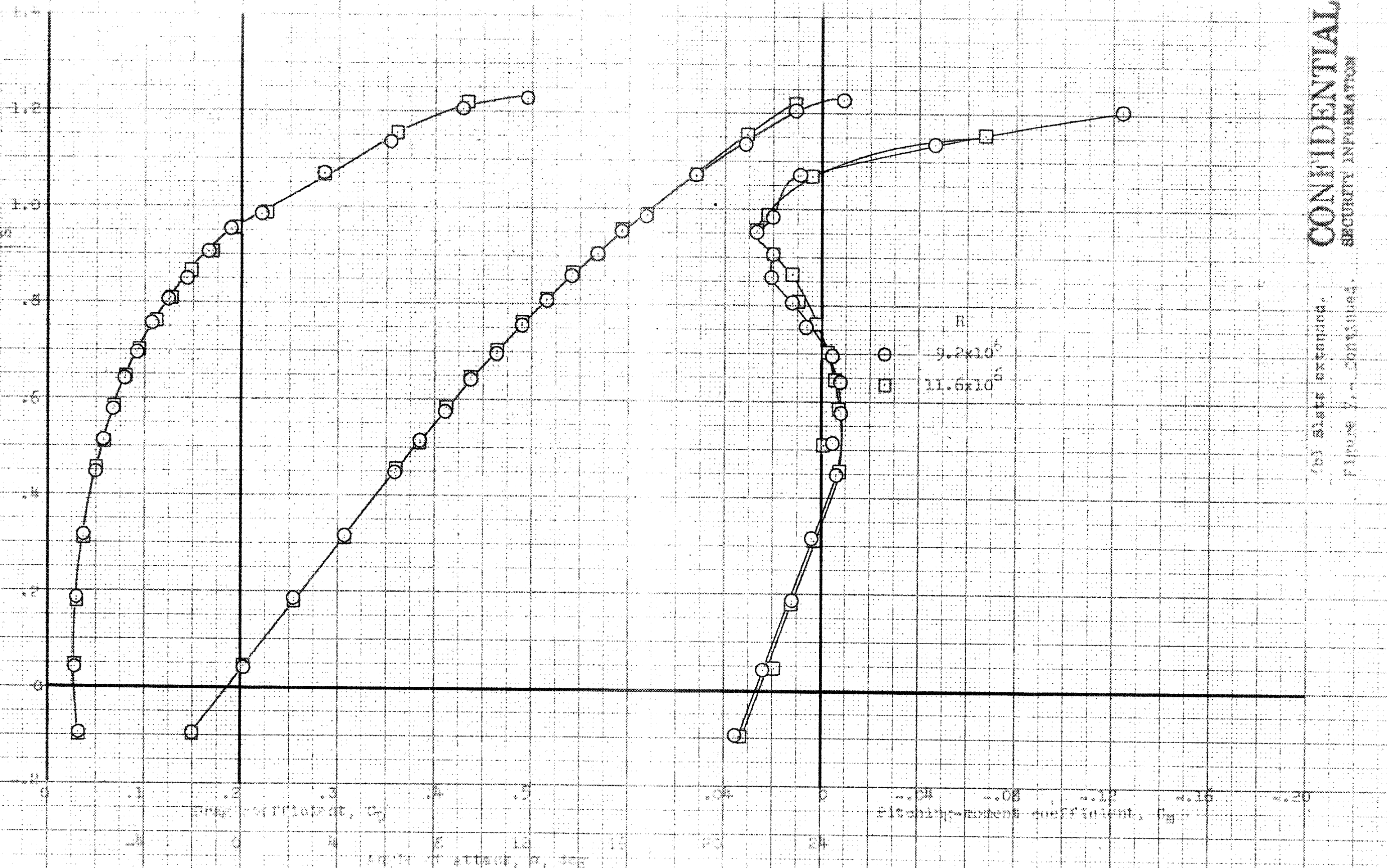
(a) Continued, please.

Figure 7, continued.

CONFIDENTIAL
SECURITY INFORMATION

CONFIDENTIAL
SECURITY INFORMATION

Figure 7.10 (continued)



CONFIDENTIAL
SECURITY INFORMATION

(b) Data extended.
Figure 7.10 (continued)

CONFIDENTIAL
SECURITY INFORMATION

CONFIDENTIAL
SECURITY INFORMATION

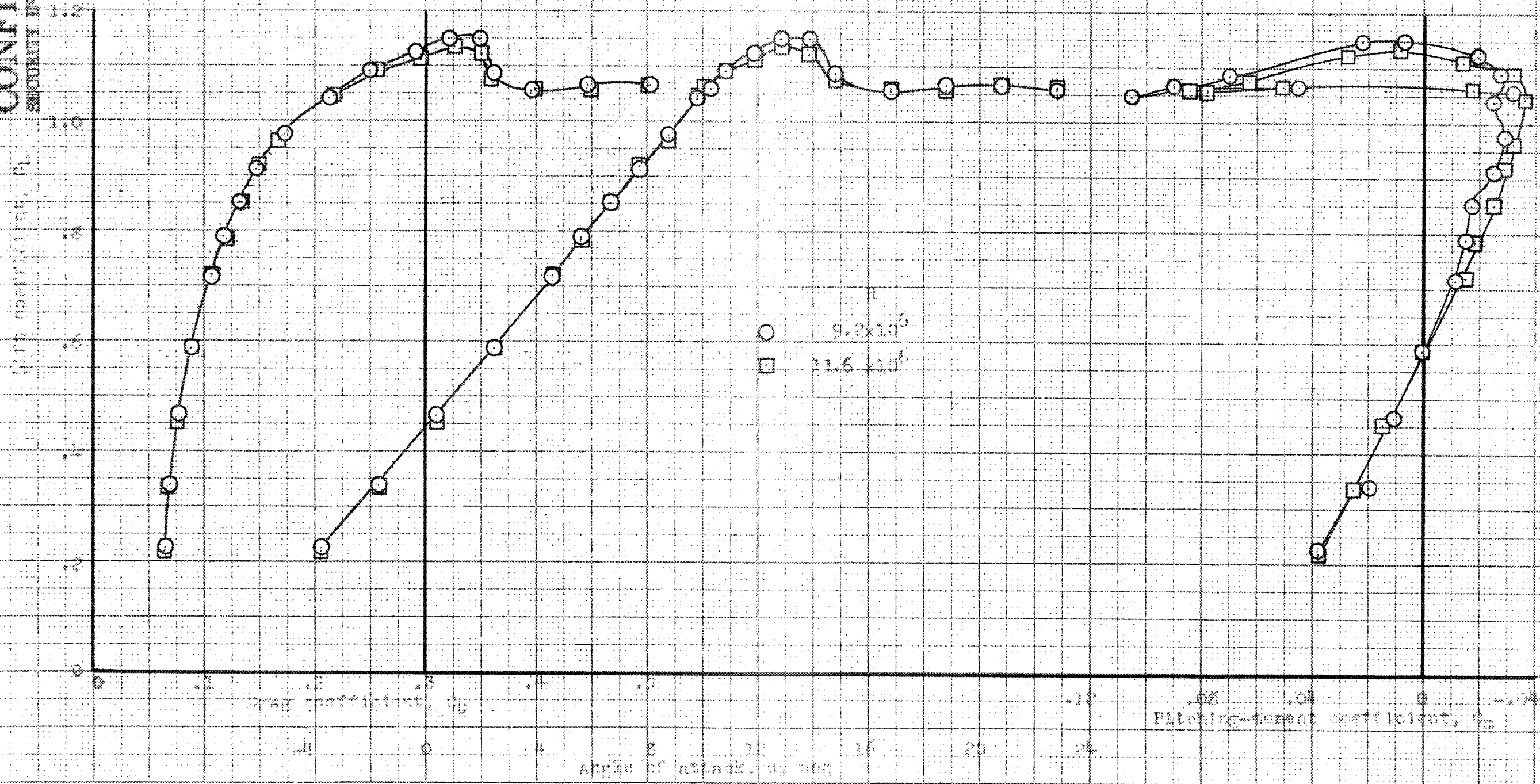
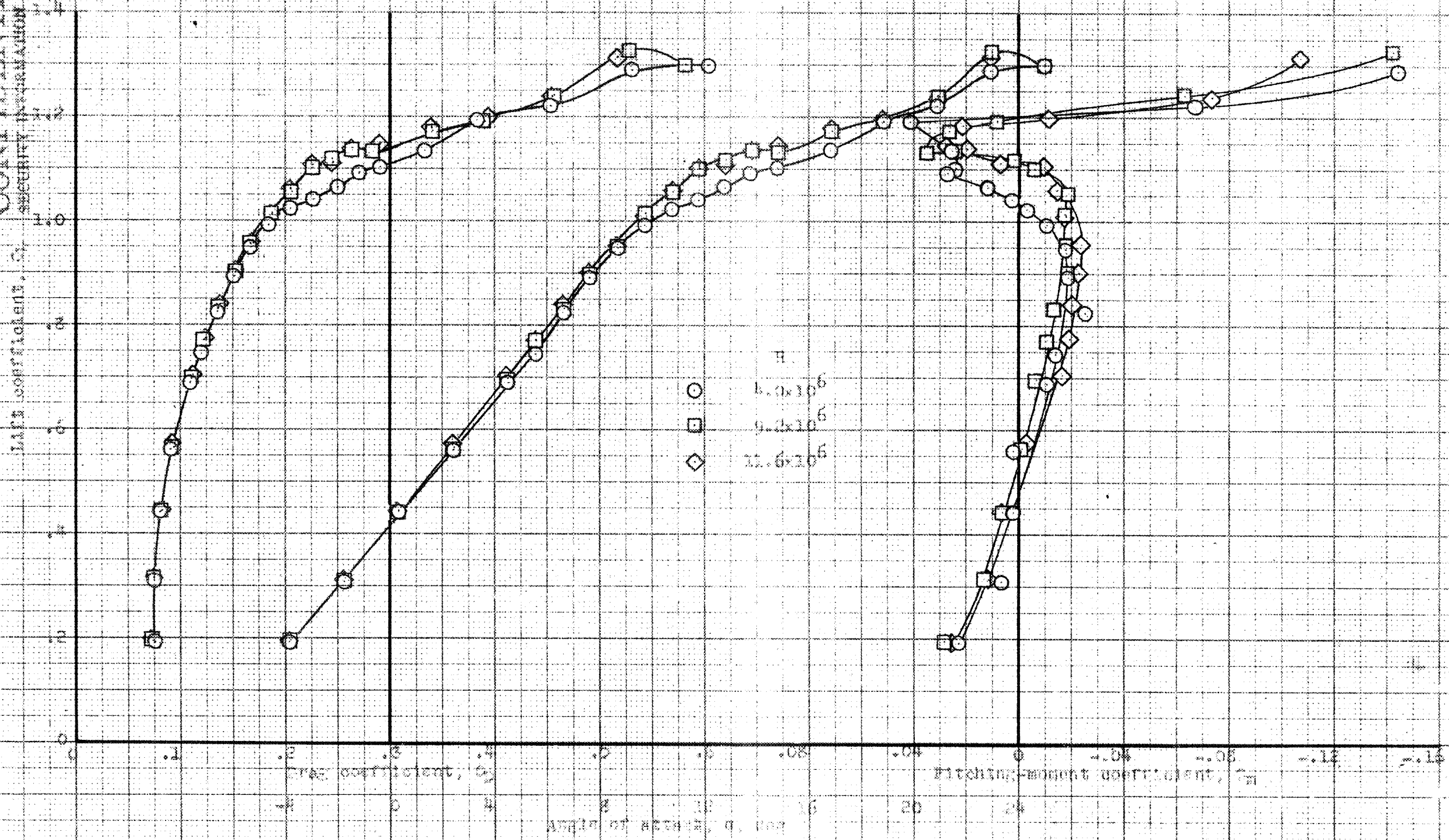


Figure 7. - Continued.

CONFIDENTIAL

DATA ON HANDBOOK



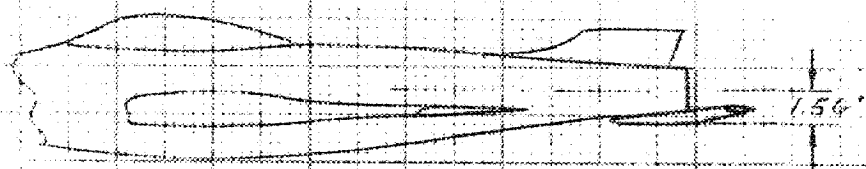
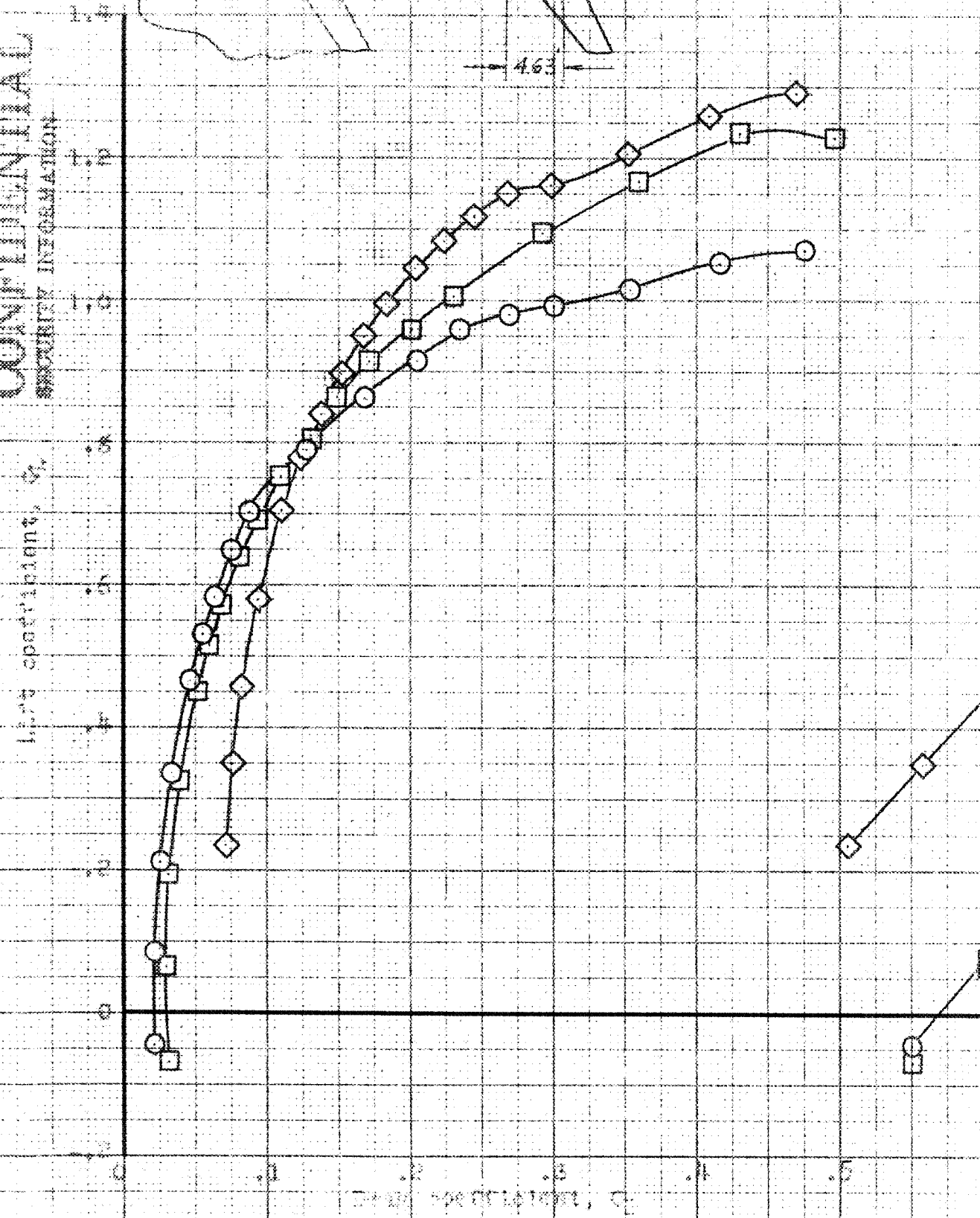
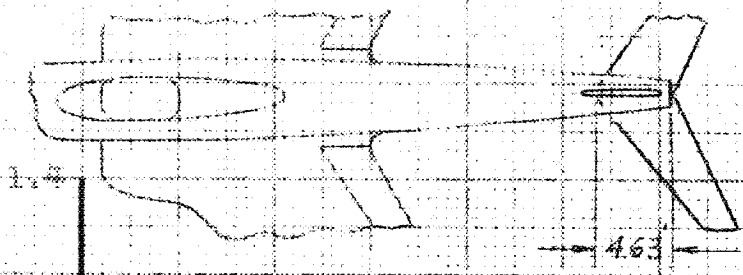
(d) Plans and data extended.

Figure 7-- Concluded.

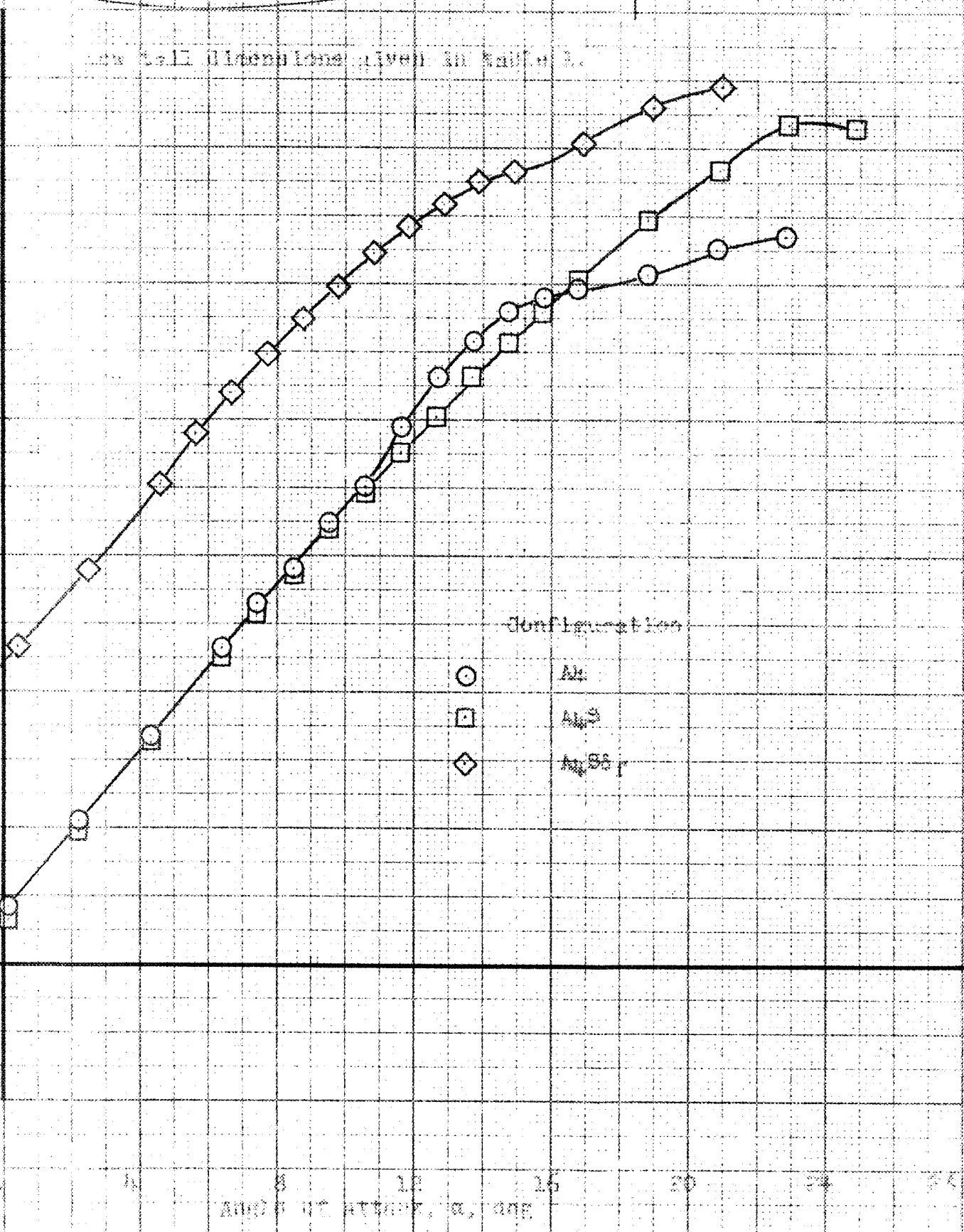
CONFIDENTIAL

SECURITY INFORMATION

CONFIDENTIAL
SECURITY INFORMATION



low tail dimensions given in Table 1.



Configuration
 \circ $M_{\infty} = 0.8$
 \square $M_{\infty} = 0.9$
 \diamond $M_{\infty} = 0.95$

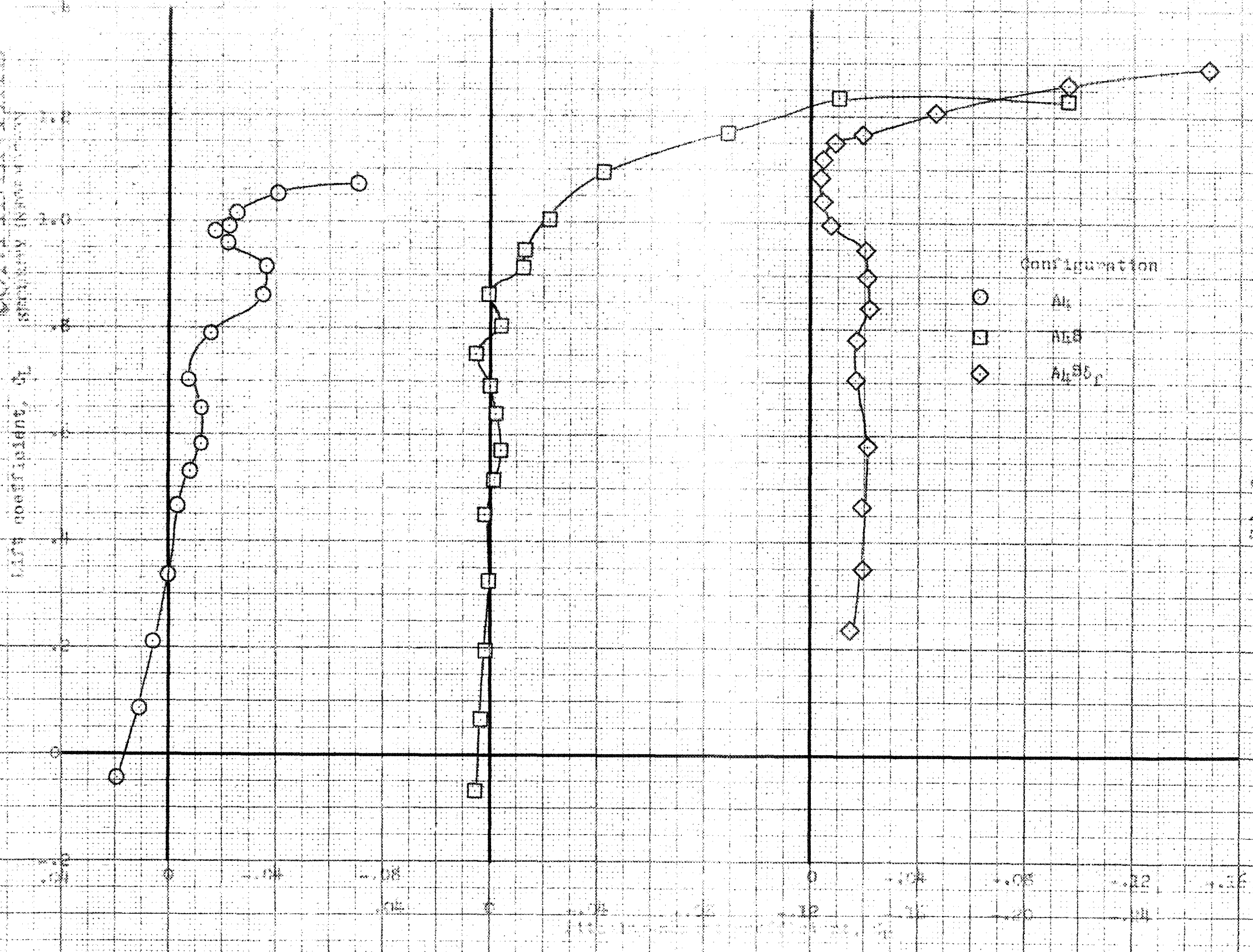
(a) C_L vs C_D , α

Figure 8. Effectiveness of a low horizontal tail on characteristics of the airplane. $M_{\infty} = 0.8$ to 0.95 .

CONFIDENTIAL
SECURITY INFORMATION

CONFIDENTIAL

DATA DELETED



(b) C_L vs. α
Figure 5 - Continued

CONFIDENTIAL
SECURITY INFORMATION

CONFIDENTIAL

3004 NI 002104

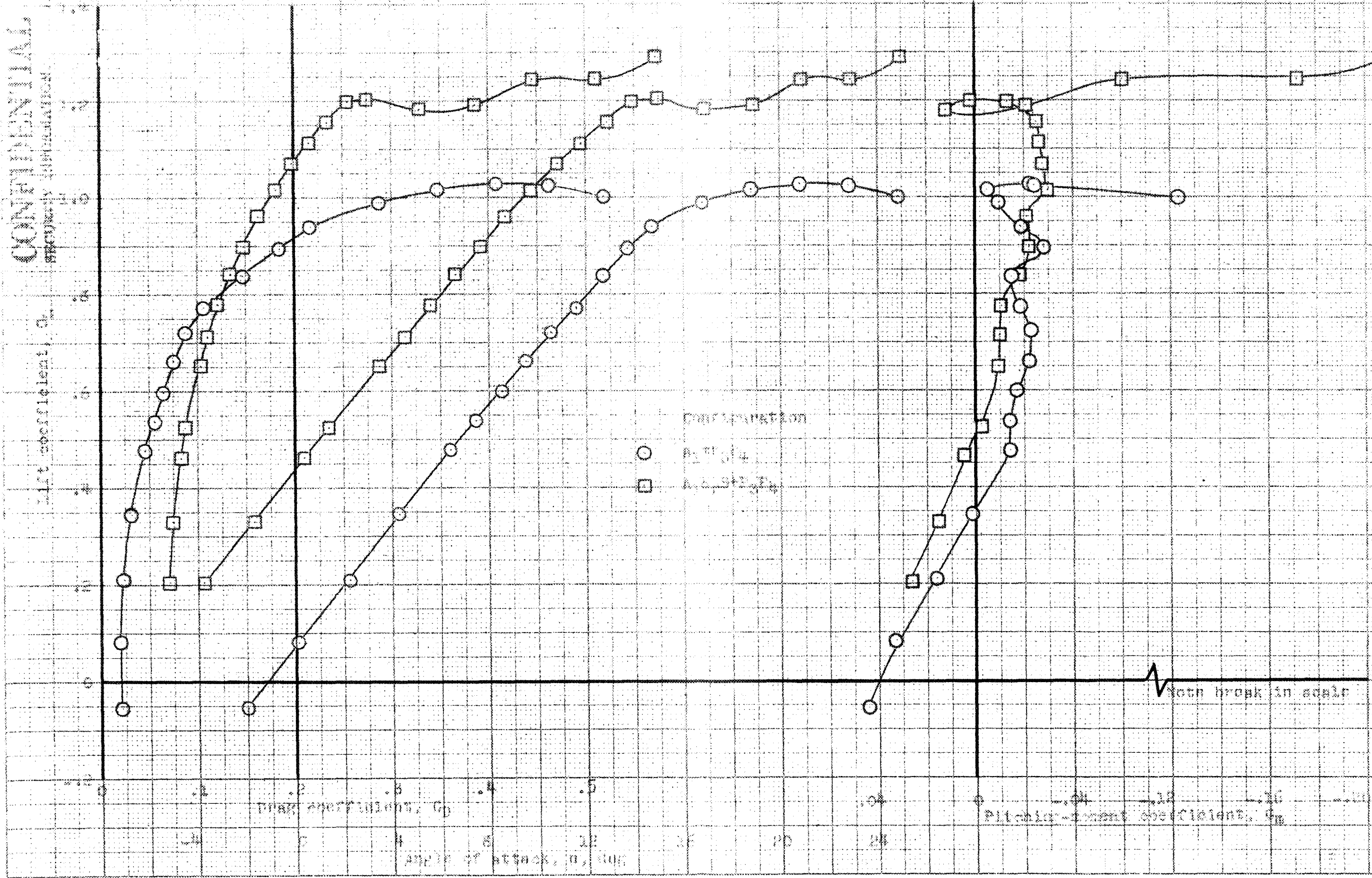


Figure 9. - Effects of flight test fence on the aerodynamic characteristics of the airplane. $M = 0.4$.

CONFIDENTIAL

SECURITY INFORMATION

CONFIDENTIAL

CONFIDENTIAL

CONFIDENTIAL

CONFIDENTIAL

CONFIDENTIAL

CONFIDENTIAL

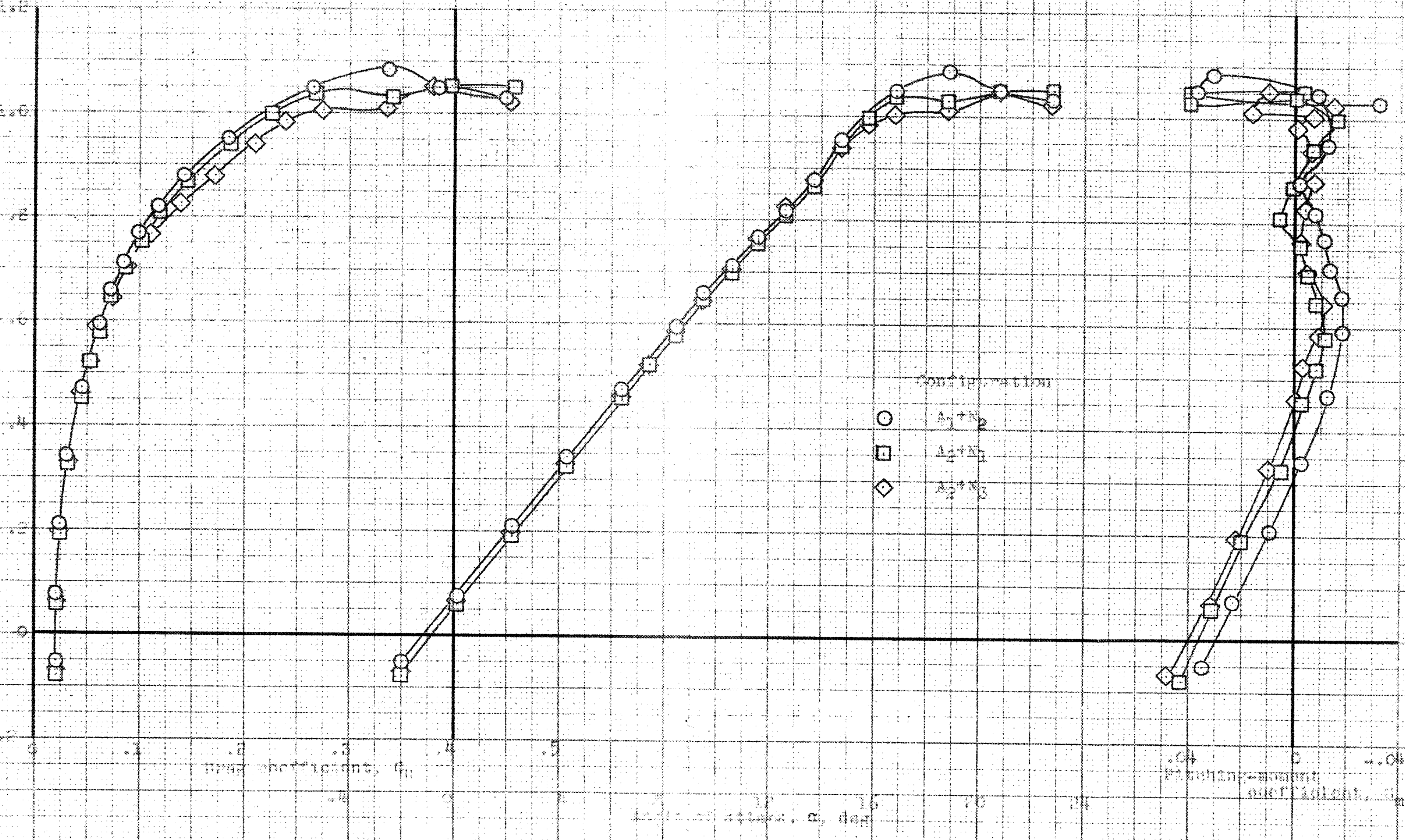


Figure 10. Effects of a modified leading edge of various percent spans on the deradialization of the material.

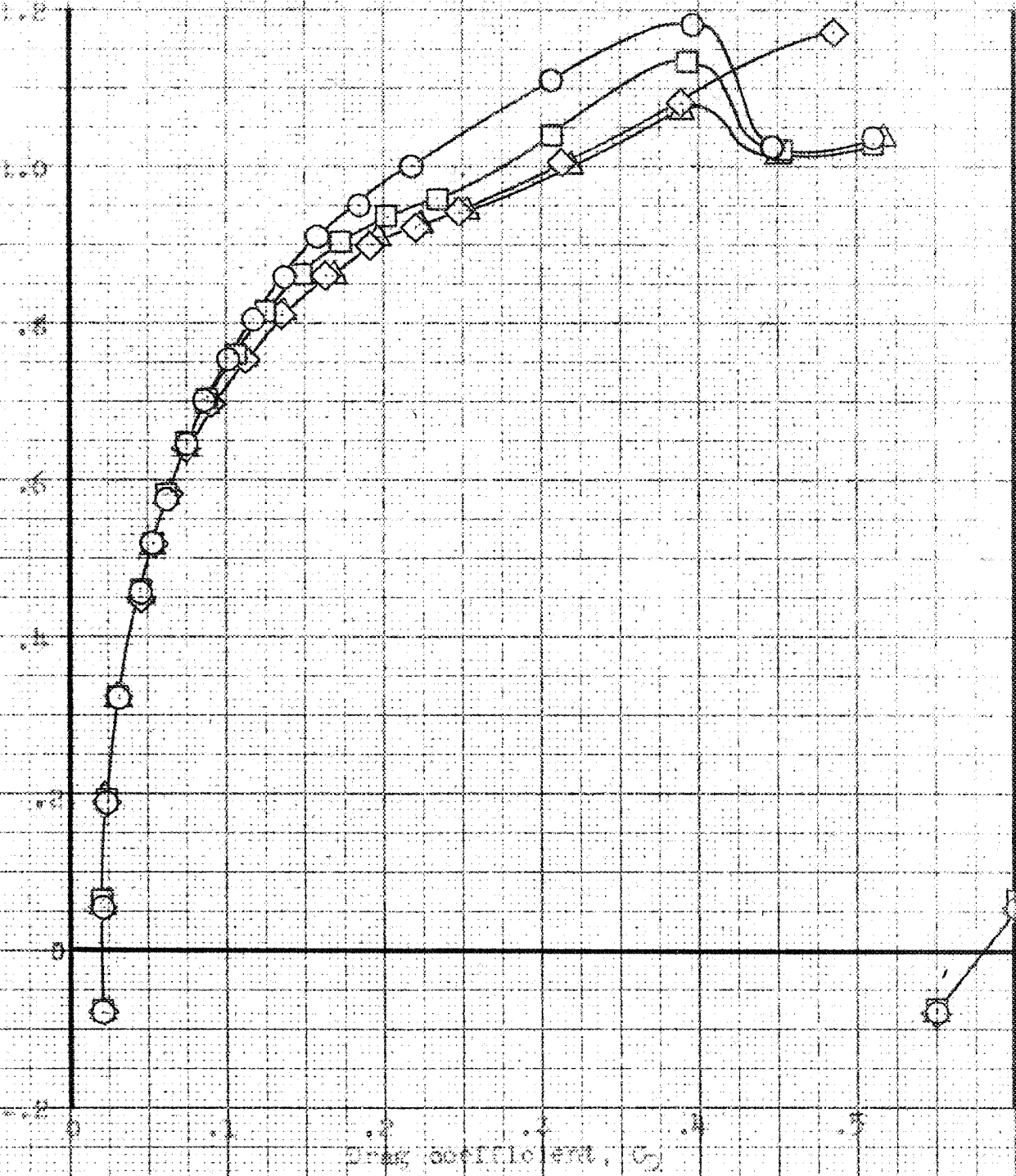
CONFIDENTIAL

CONFIDENTIAL

CONFIDENTIAL

WPA 00 04, 28.6

Lift coefficient, C_L



Angle of attack, α , deg

- Configuration
- $A_2 + N_1 P_7 a$
 - $A_2 + N_4 P_{11}$
 - ◇ $A_2 + N_3 P_9$
 - △ $A_2 + N_5 P_{12}$

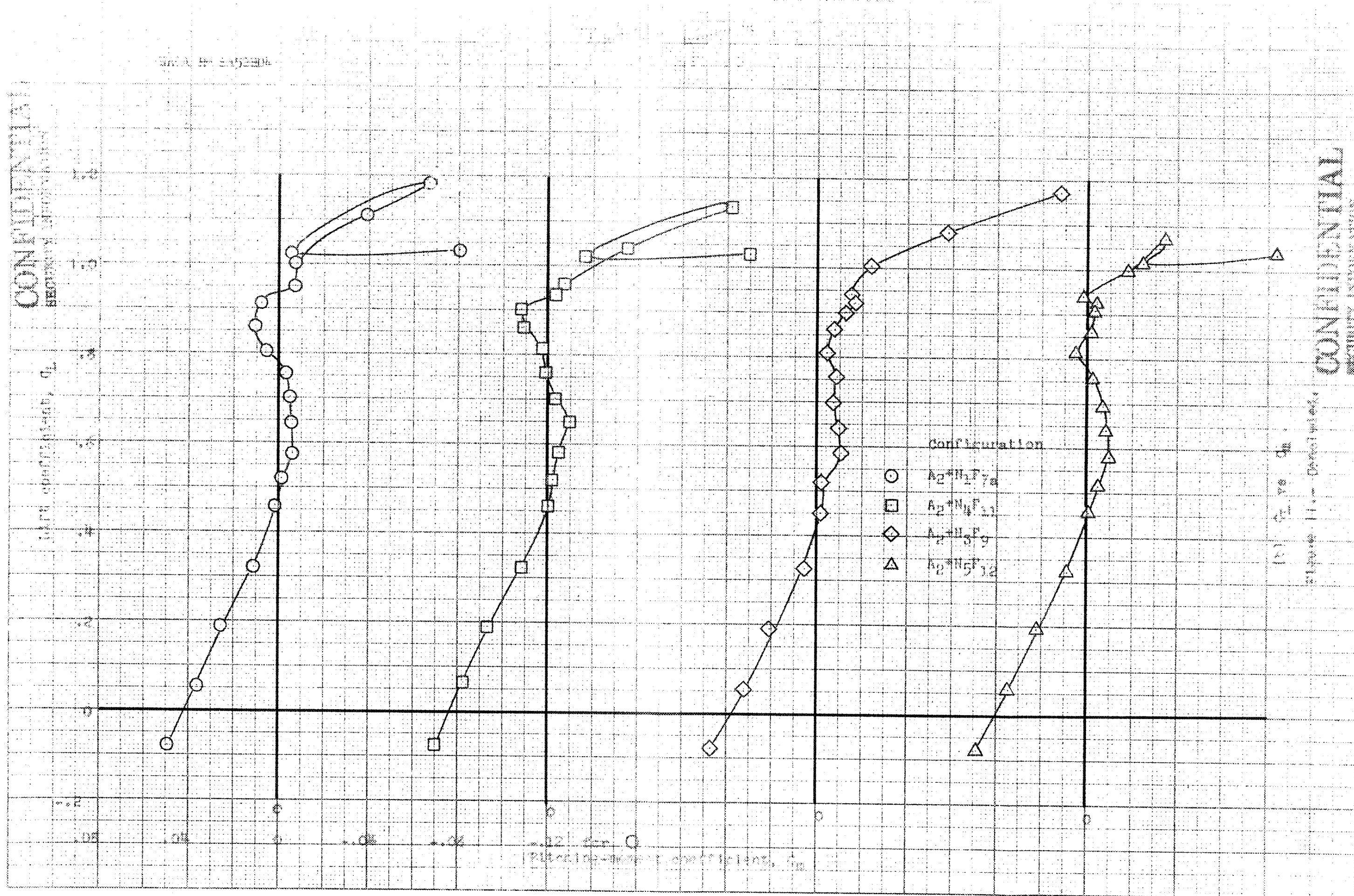
WPA 00 04, 28.6

Figure 11. Effects of a modified leading edge of various partial spans combined with a fence of the characteristics of the airplane. (WPA 00 04, 28.6)

CONFIDENTIAL

CONFIDENTIAL

SECURITY INFORMATION



CONFIDENTIAL

SECURITY INFORMATION

Figure 11 - Continued

CONFIDENTIAL
SECURITY INFORMATION

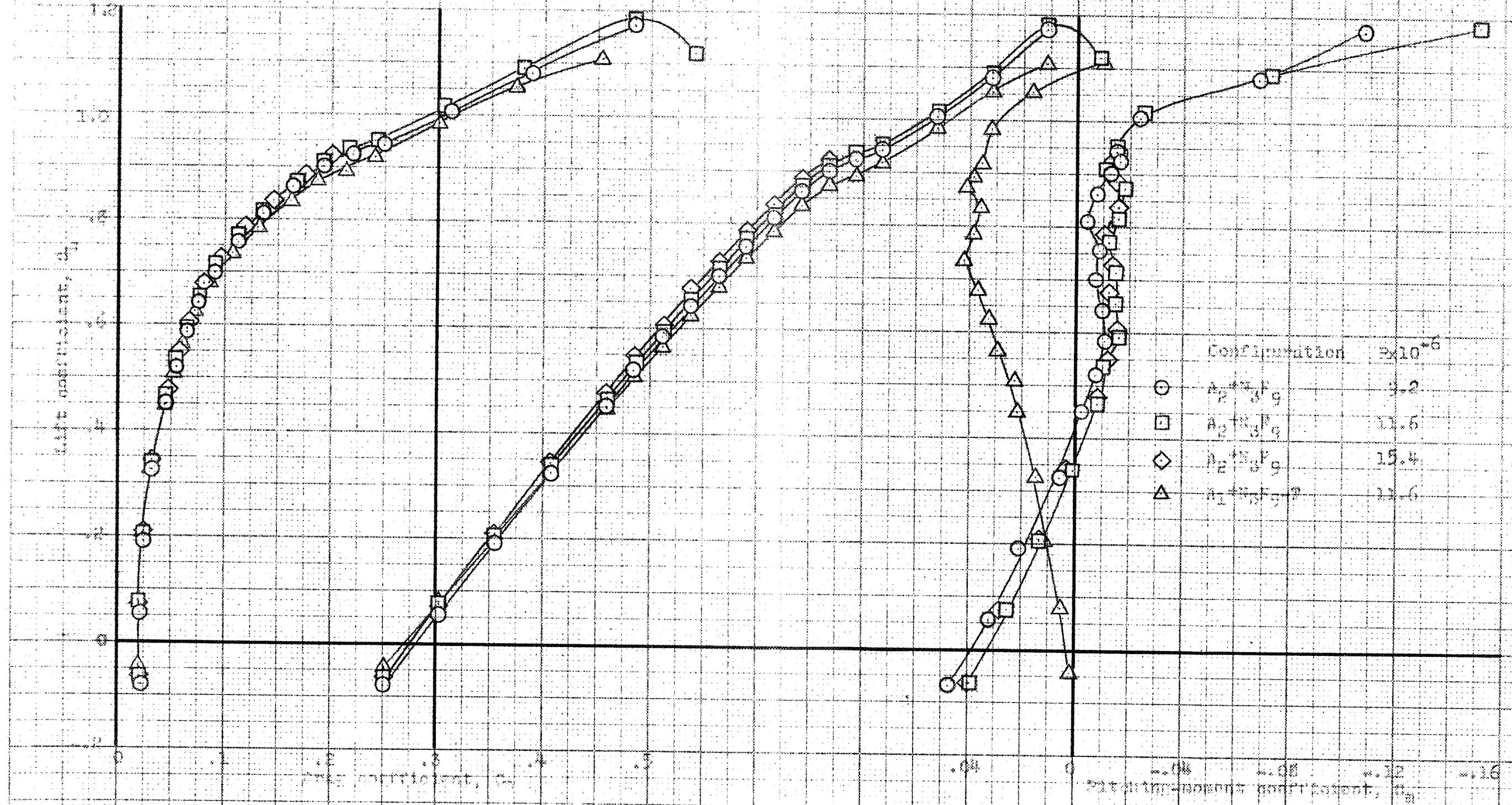
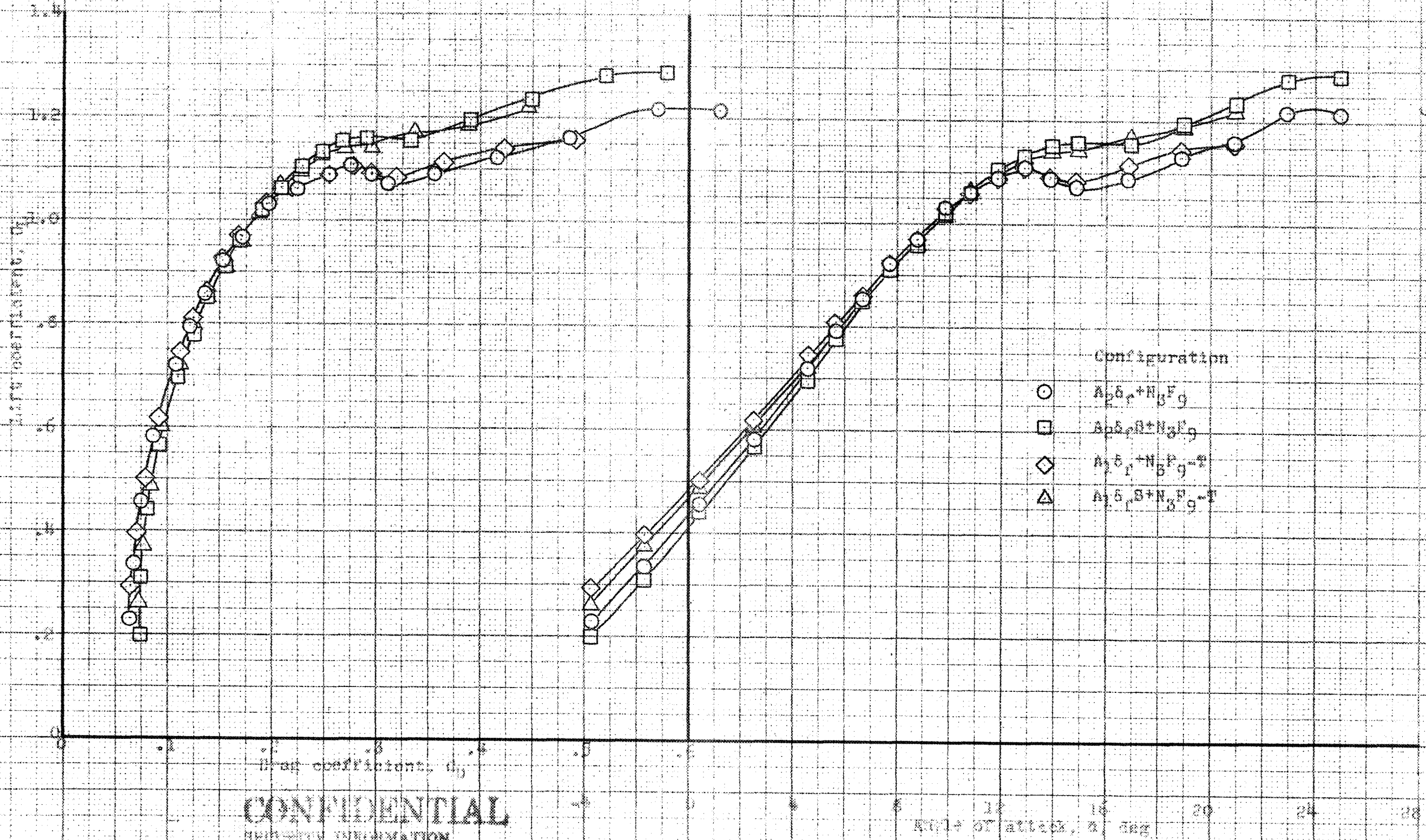


Figure 12. Effects of a 0.55 span modified leading edge and a 10% $V_{L/D}$ on the characteristics of the airplane with and without the controlled tail.

CONFIDENTIAL
SECURITY INFORMATION

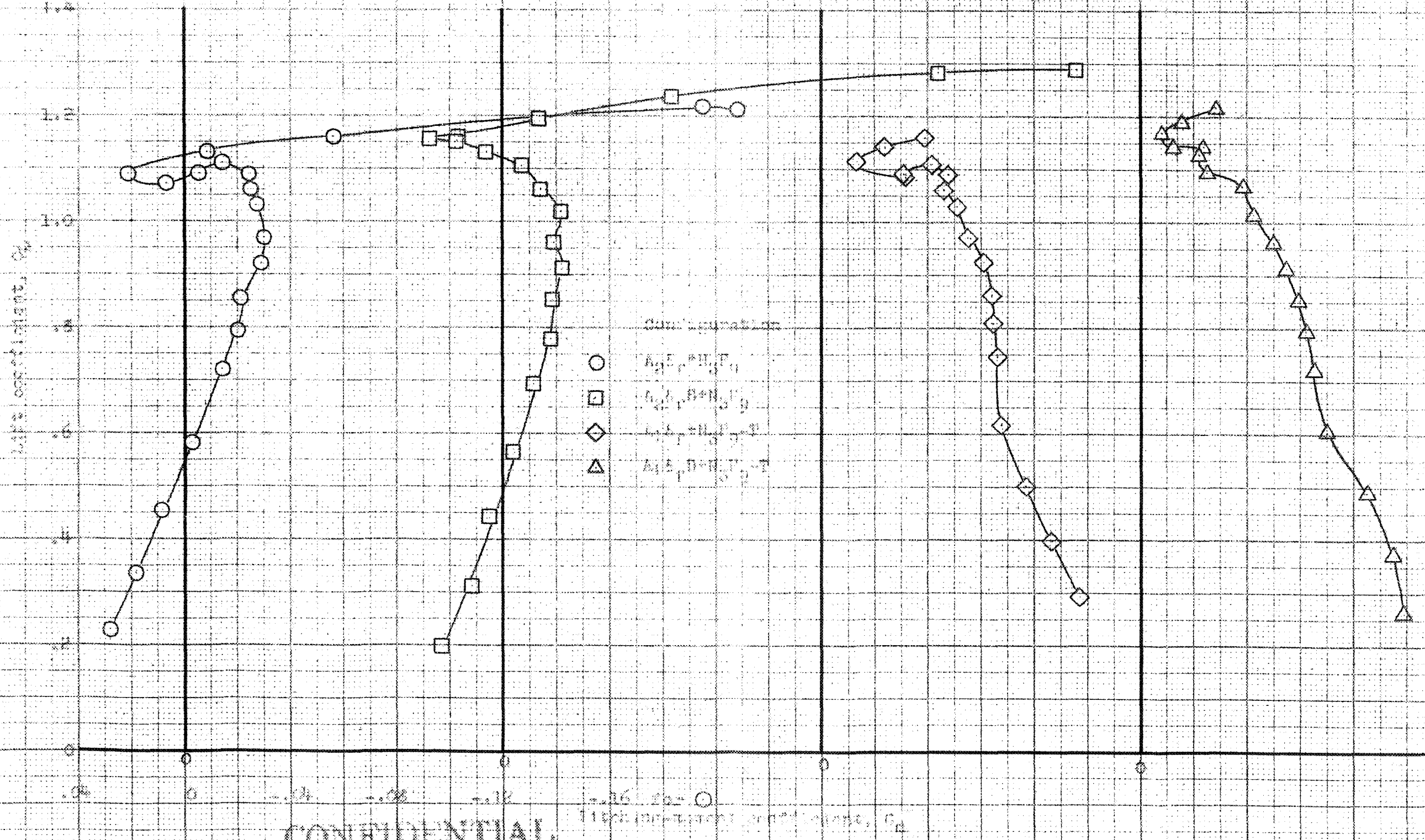
CONFIDENTIAL



(b) Flaps and slats extended, $\beta = 11.6 \times 10^6$.

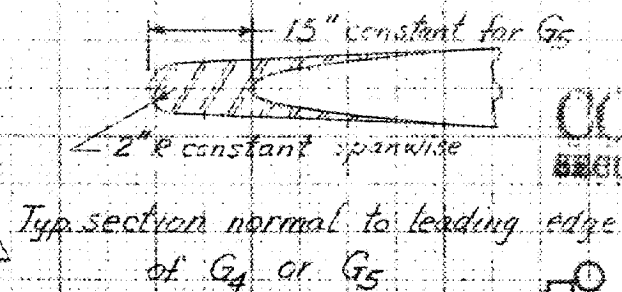
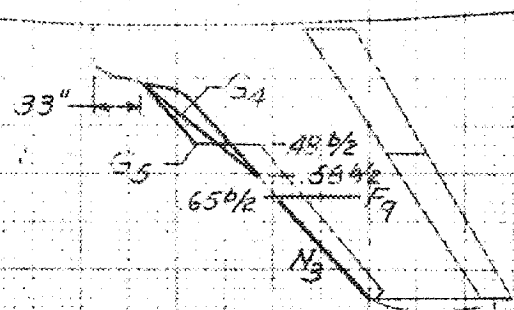
Figure 12c. Continued.

CONFIDENTIAL
SECURITY INFORMATION

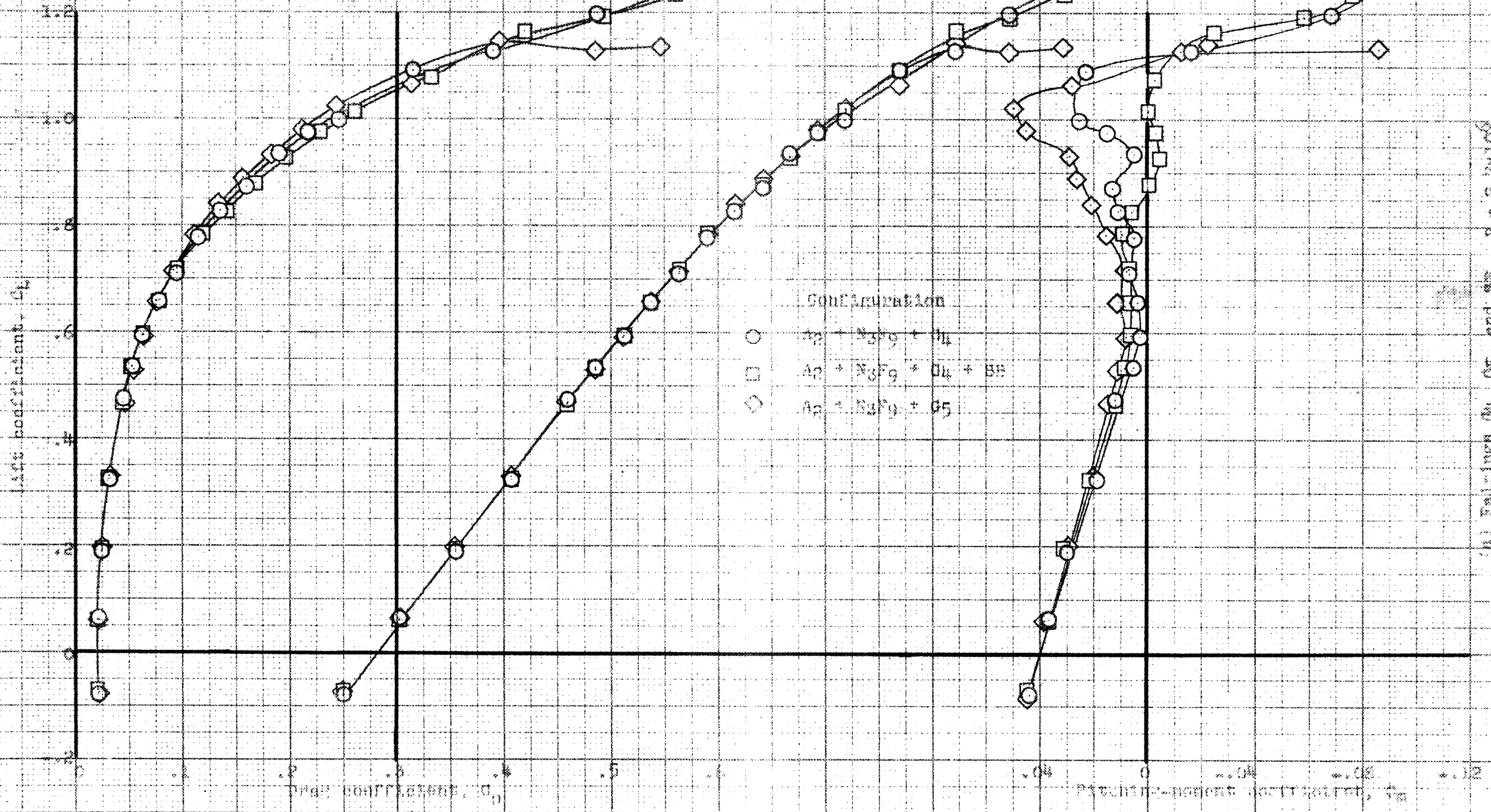
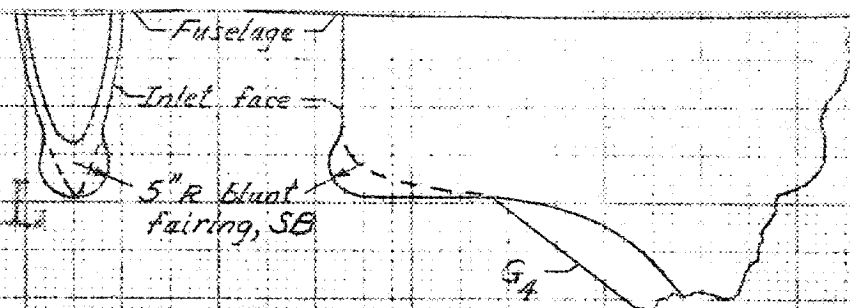


(b) (continued, glass and silt ordered, $\lambda = 11.6 \mu$)
Figure 12 - (continued)

CONFIDENTIAL
SECURITY INFORMATION



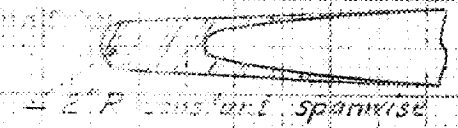
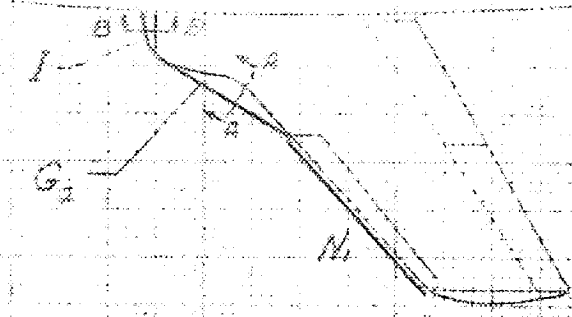
CONFIDENTIAL
SECURITY INFORMATION



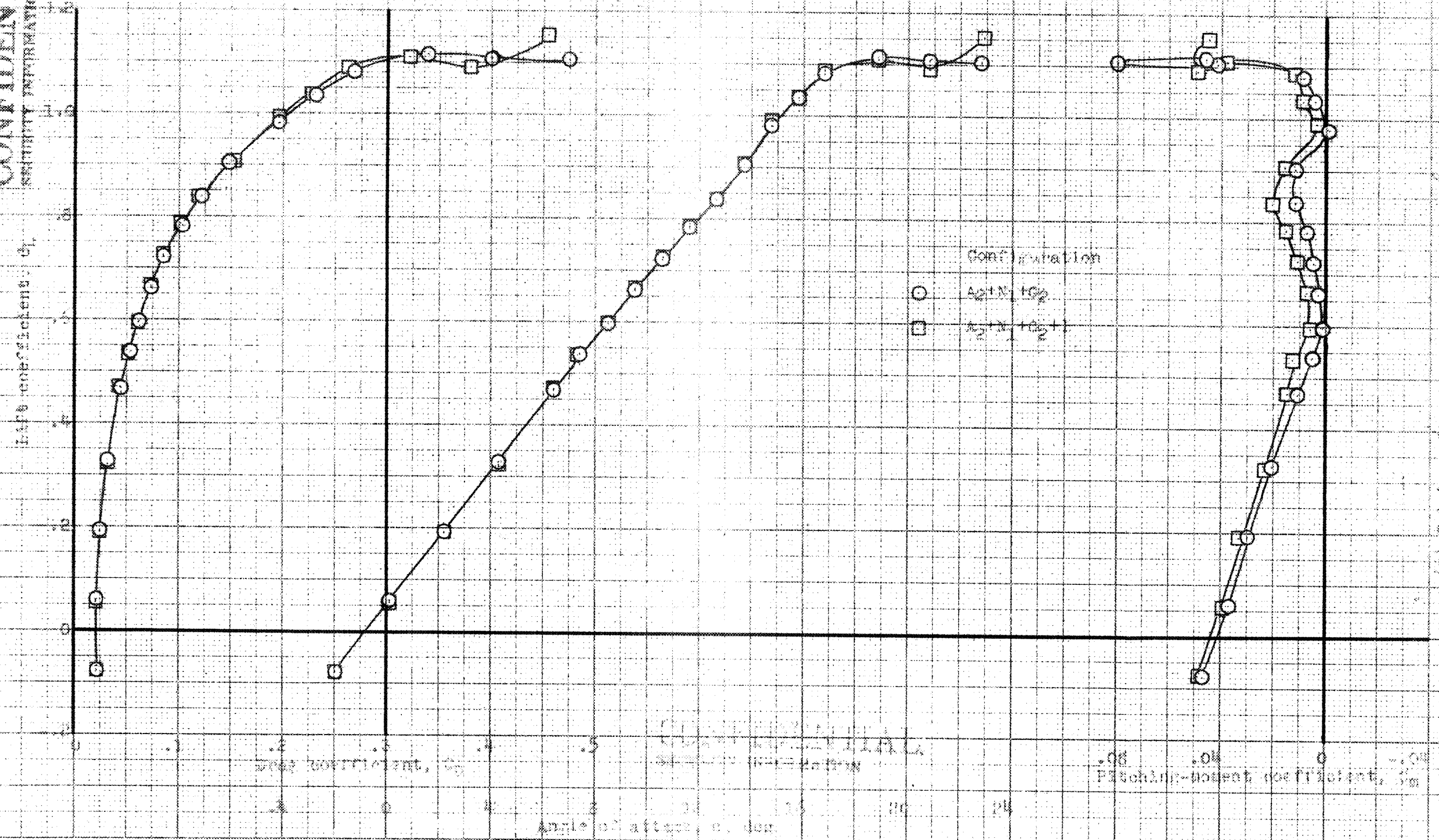
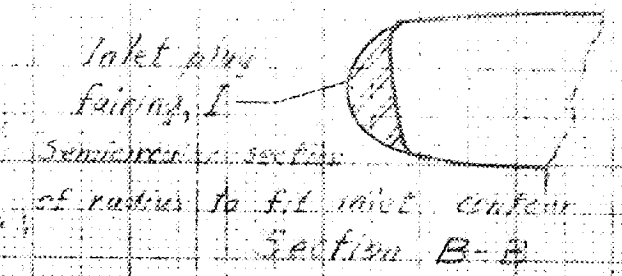
(h) Fairings G_4 , G_5 , and SB , $n = 2.2 \times 10^6$.
Figure 13. - Effects of fairings in the vicinity of the inlet on the characteristics of the airplane.

CONFIDENTIAL
SECURITY INFORMATION

CONFIDENTIAL
SECURITY INFORMATION



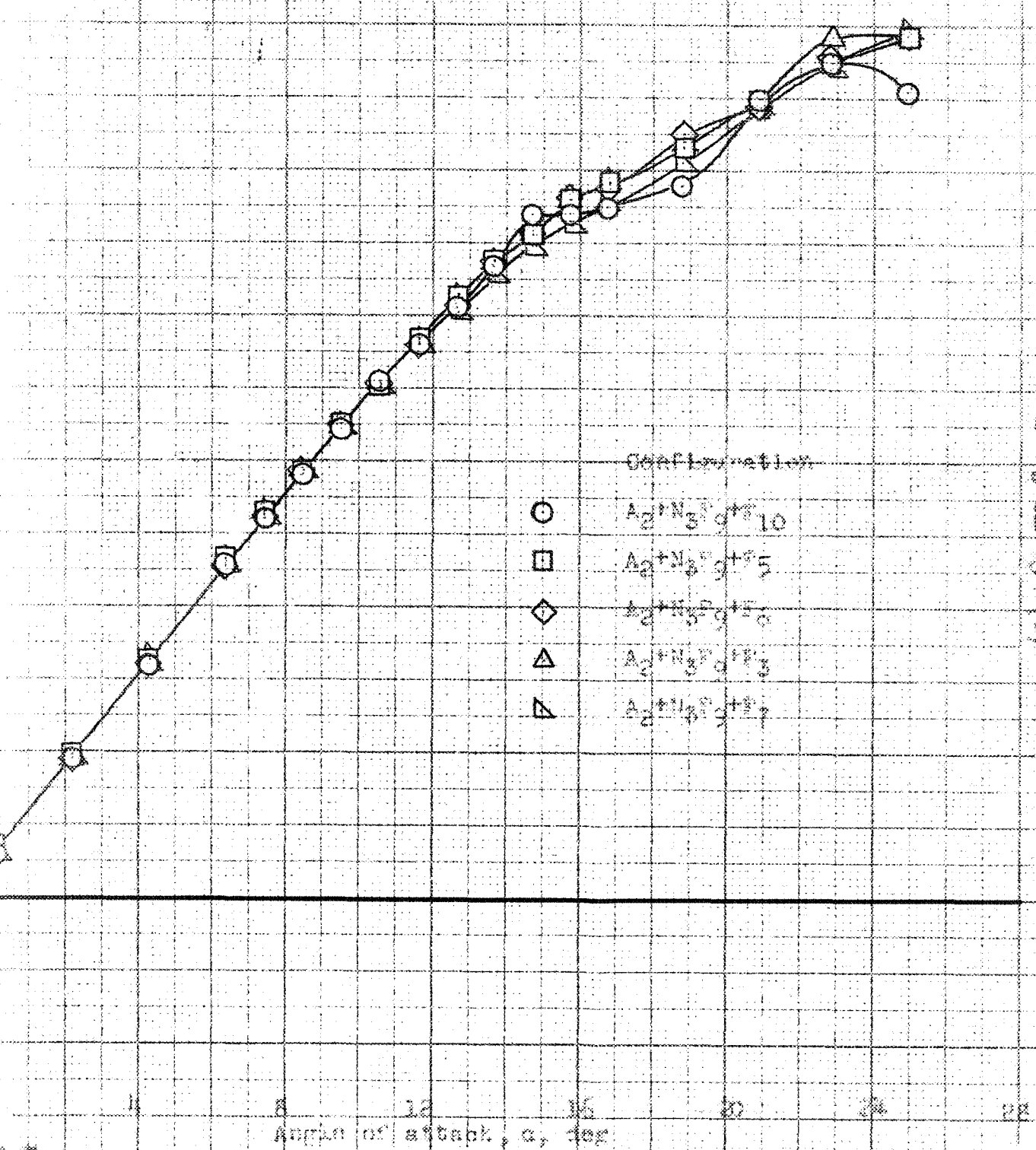
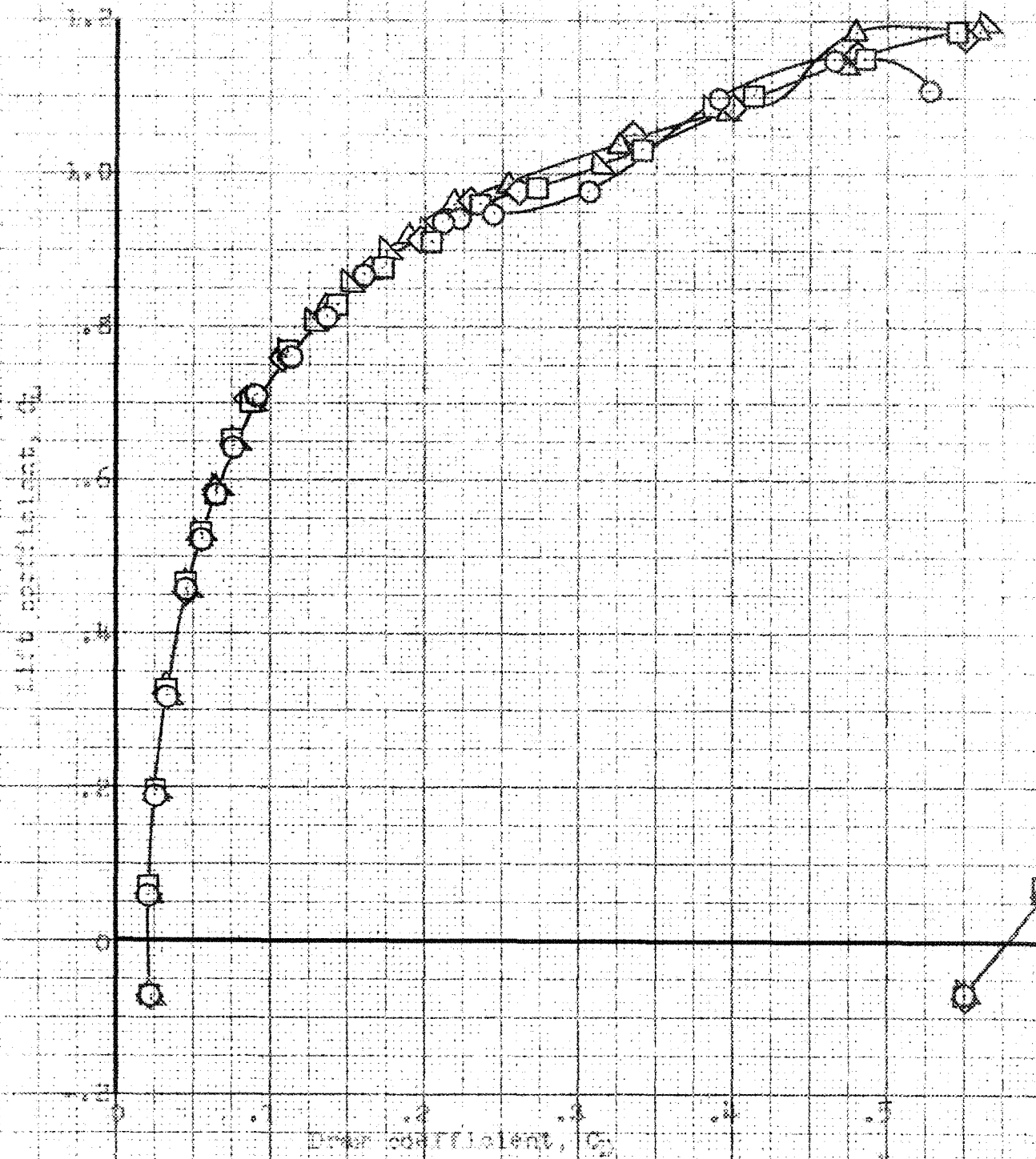
See Fig. A-A



(9) Fairings G_1 , G_2 and L . $Re = 9.2 \times 10^6$.

CONFIDENTIAL
SECURITY INFORMATION

CONFIDENTIAL
SECURITY INFORMATION



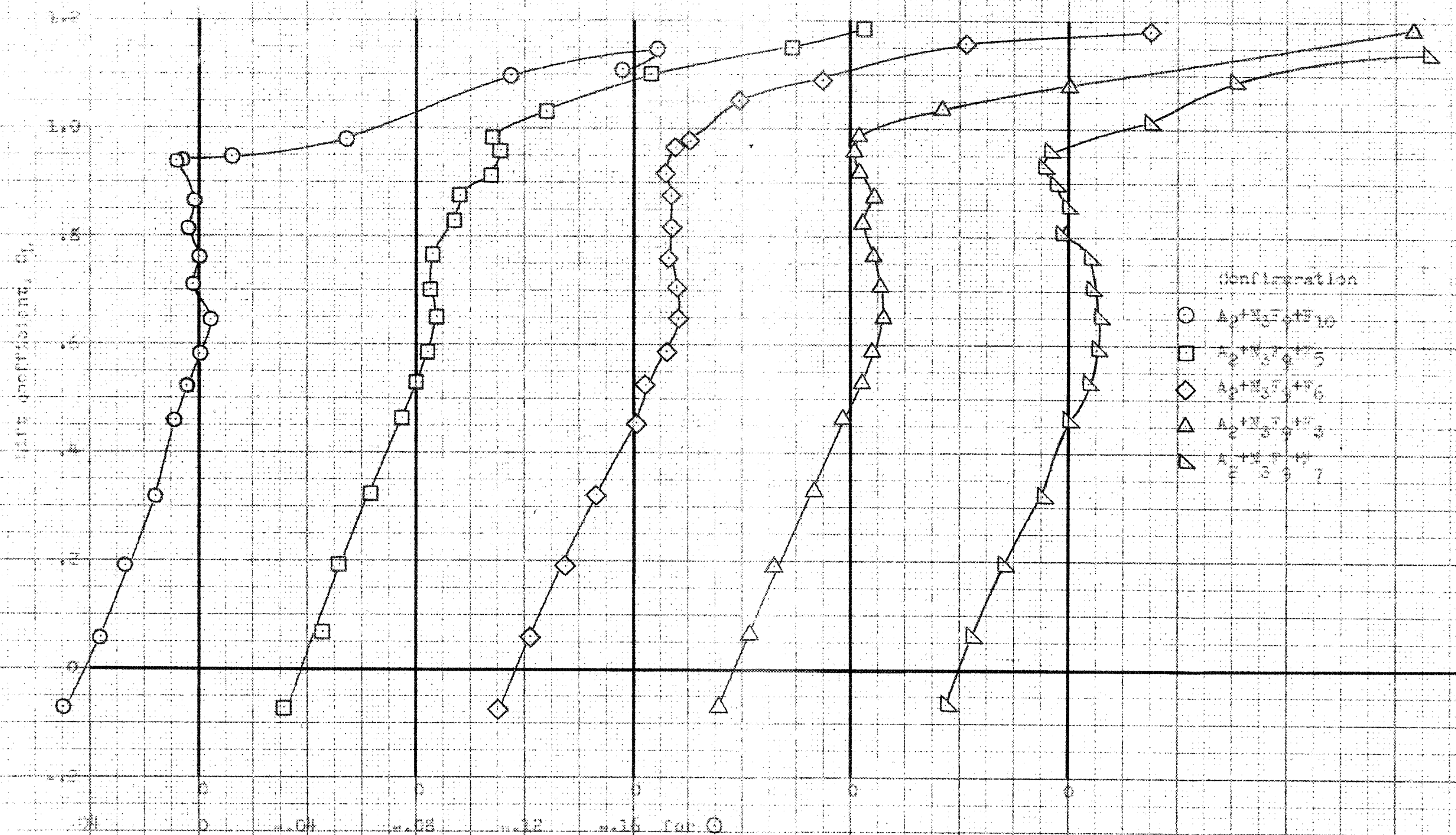
- Configuration
- A_2+N_3+G+10
 - A_2+N_3+G+5
 - ◇ A_2+N_3+G+0
 - △ A_2+N_3+G+5
 - ▽ A_2+N_3+G+5

Figure 15. Effect of various nitrogen losses on the characteristics of the airplane with configuration 1879. $\alpha = 0.5 \times 10^6$.

CONFIDENTIAL
SECURITY INFORMATION

CONFIDENTIAL

CONFIDENTIAL
SECURITY INFORMATION



- Configuration
- $A_0 + B_0 + C_0 + D_0 + E_0 + F_0 + G_0 + H_0 + I_0 + J_0$
 - $A_0 + B_0 + C_0 + D_0 + E_0 + F_0 + G_0 + H_0 + I_0 + J_0$
 - ◇ $A_0 + B_0 + C_0 + D_0 + E_0 + F_0 + G_0 + H_0 + I_0 + J_0$
 - △ $A_0 + B_0 + C_0 + D_0 + E_0 + F_0 + G_0 + H_0 + I_0 + J_0$
 - ▽ $A_0 + B_0 + C_0 + D_0 + E_0 + F_0 + G_0 + H_0 + I_0 + J_0$

(P) C_p vs C_m
Empirical Data - Computed

CONFIDENTIAL
SECURITY INFORMATION

CONFIDENTIAL
SECURITY INFORMATION

CONFIDENTIAL
SECURITY INFORMATION

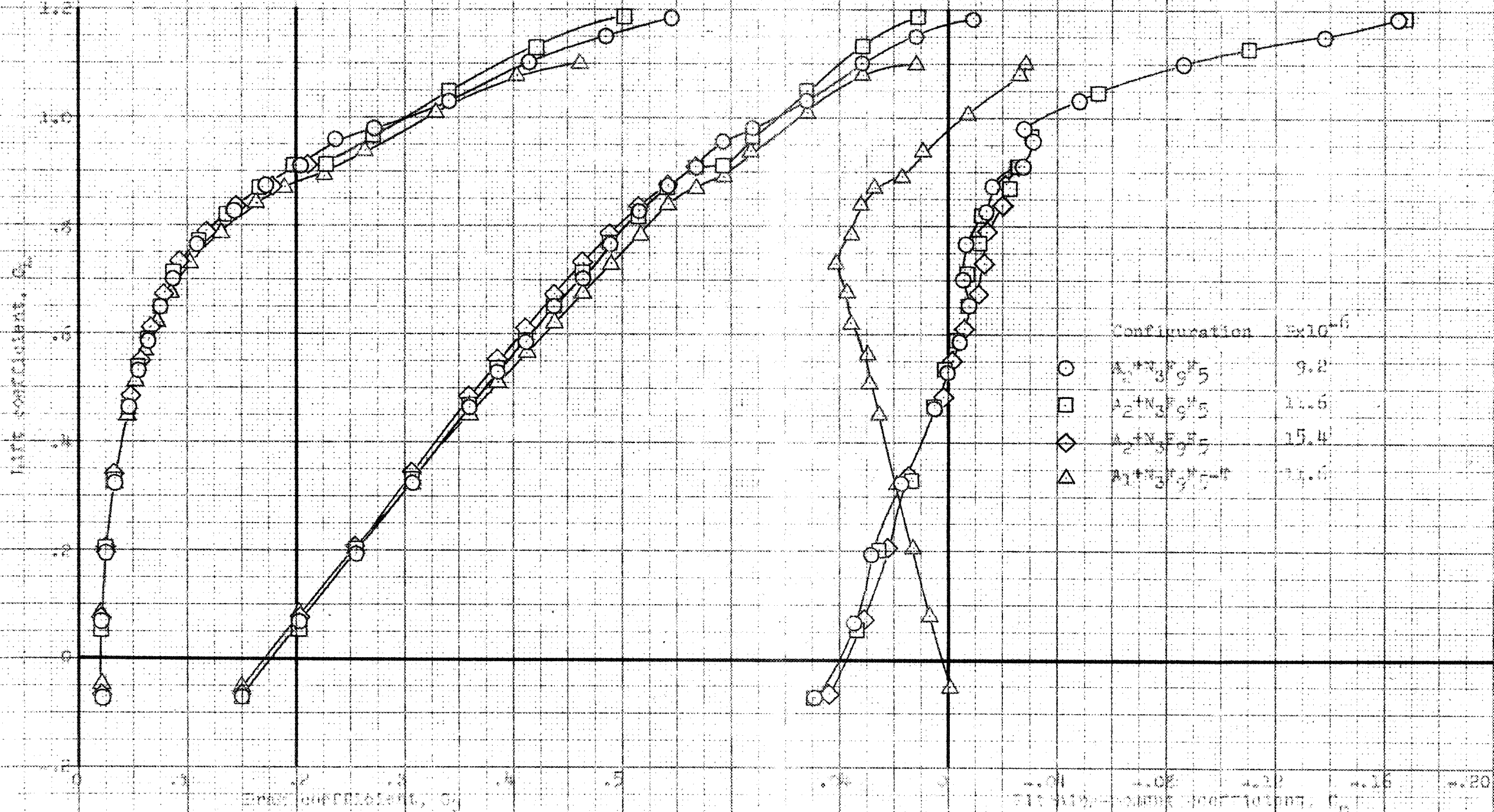
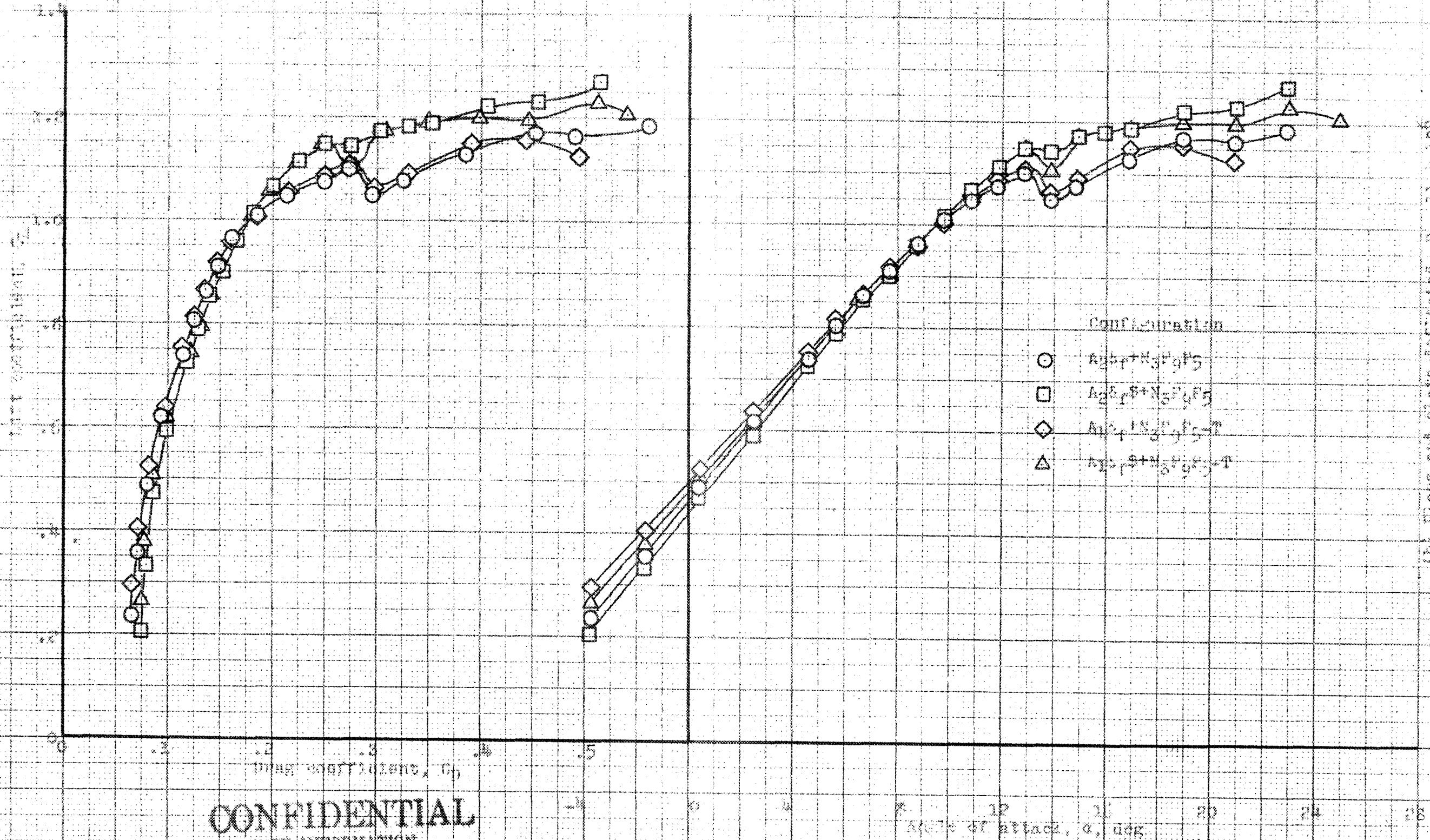


Figure 12. - Effects of $\alpha_{Cl=0.5}$ span modified leading edge and two centers (N87975) on the characteristics of the airplane with and without the horizontal tail.

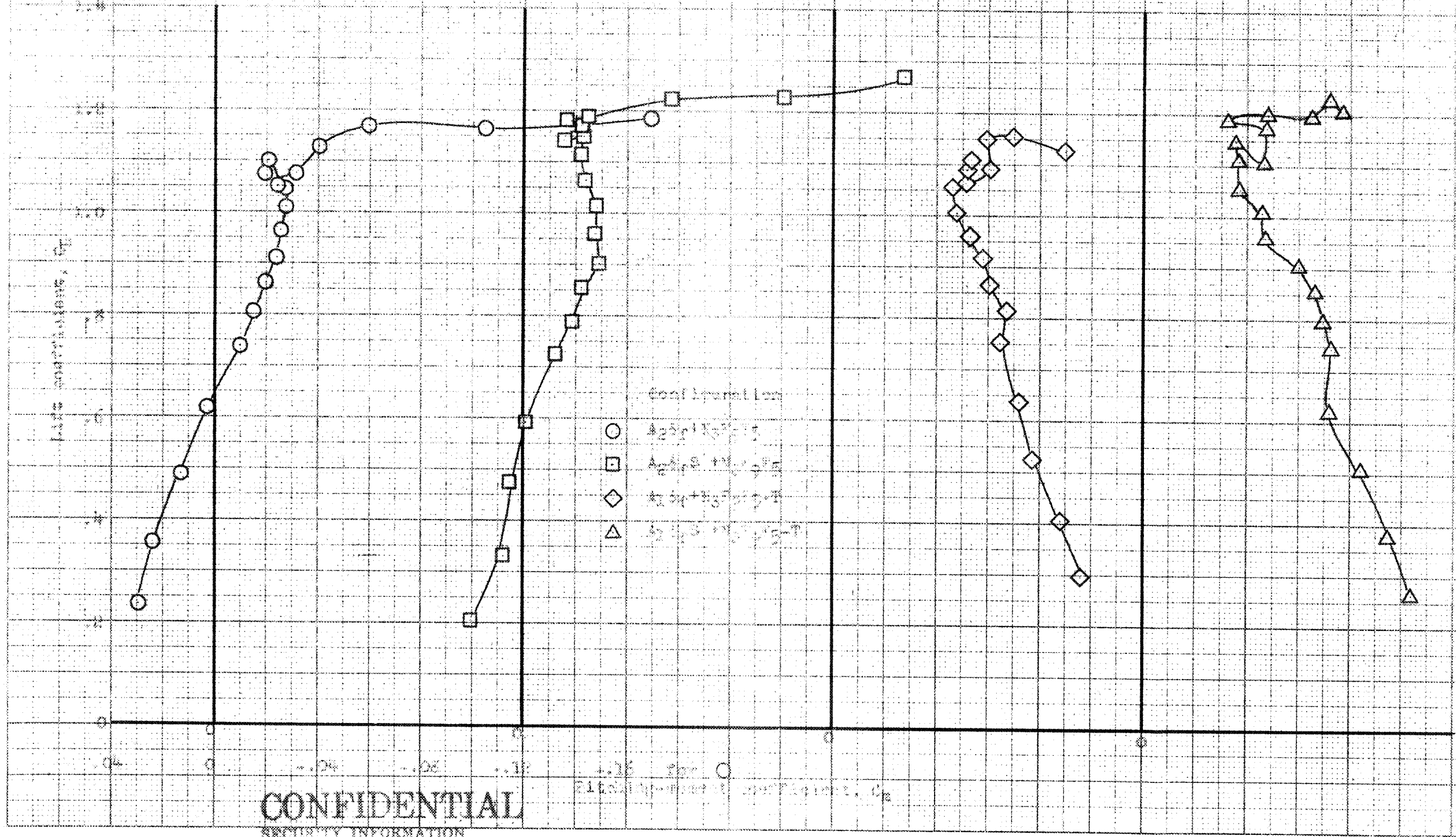
CONFIDENTIAL
SECURITY INFORMATION



- Comparison
- $A_2^2 P_1^2 + N_2^2 P_2^2$
 - $A_2^2 P_1^2 + N_2^2 P_2^2$
 - ◇ $A_2^2 P_1^2 + N_2^2 P_2^2$
 - △ $A_2^2 P_1^2 + N_2^2 P_2^2$

(D) Same as slide Reflected, R = 11, x 10⁶
Figure 15.- continued.

CONFIDENTIAL
SECURITY INFORMATION

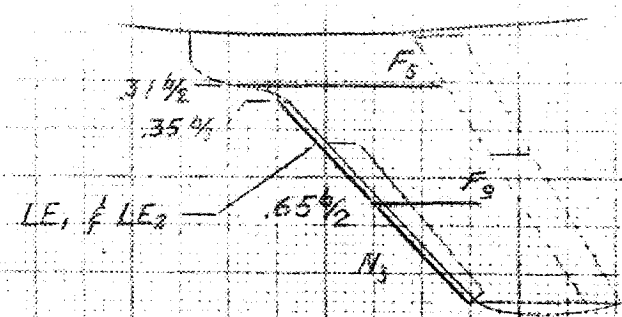


CONFIDENTIAL
SECURITY INFORMATION

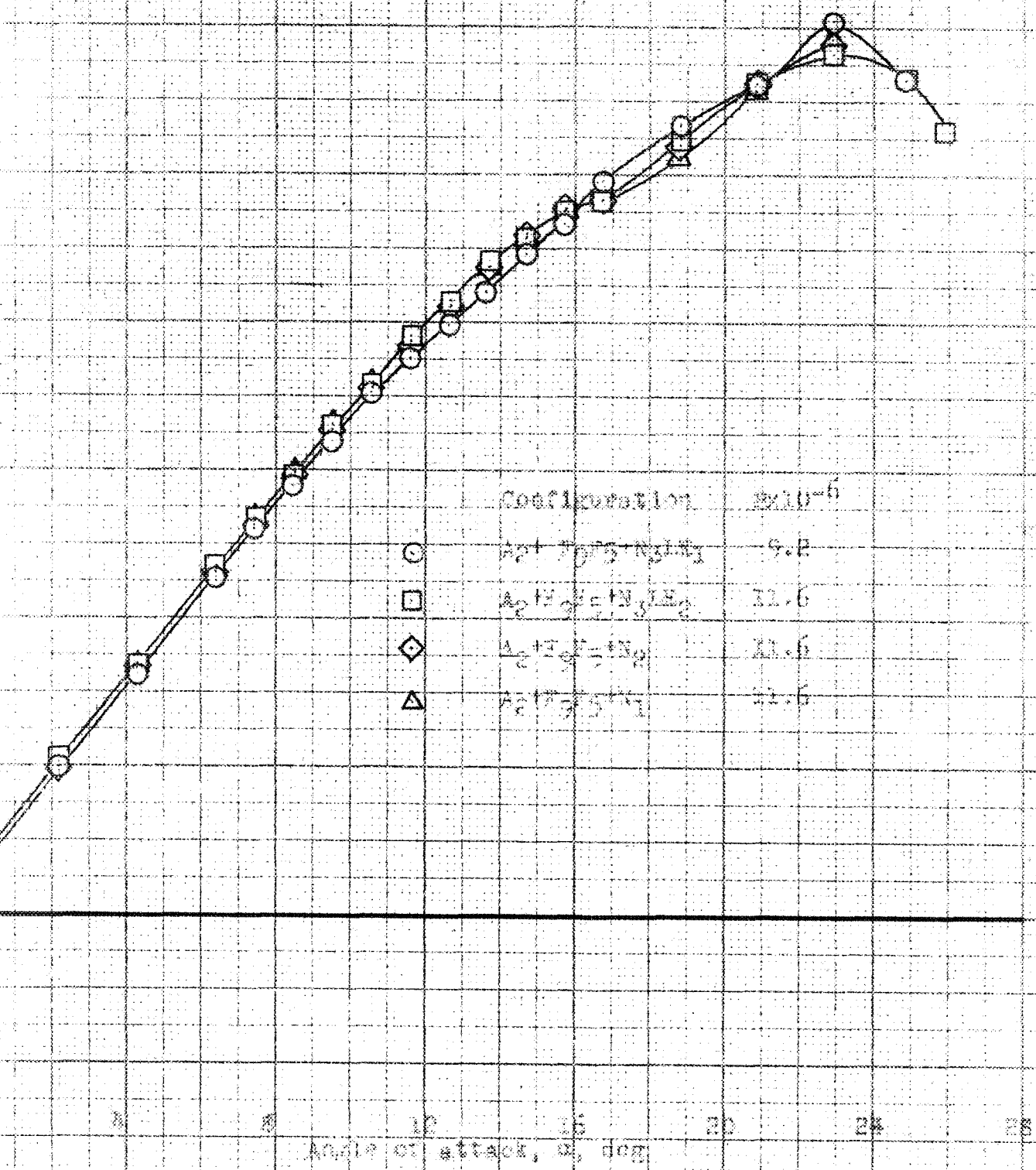
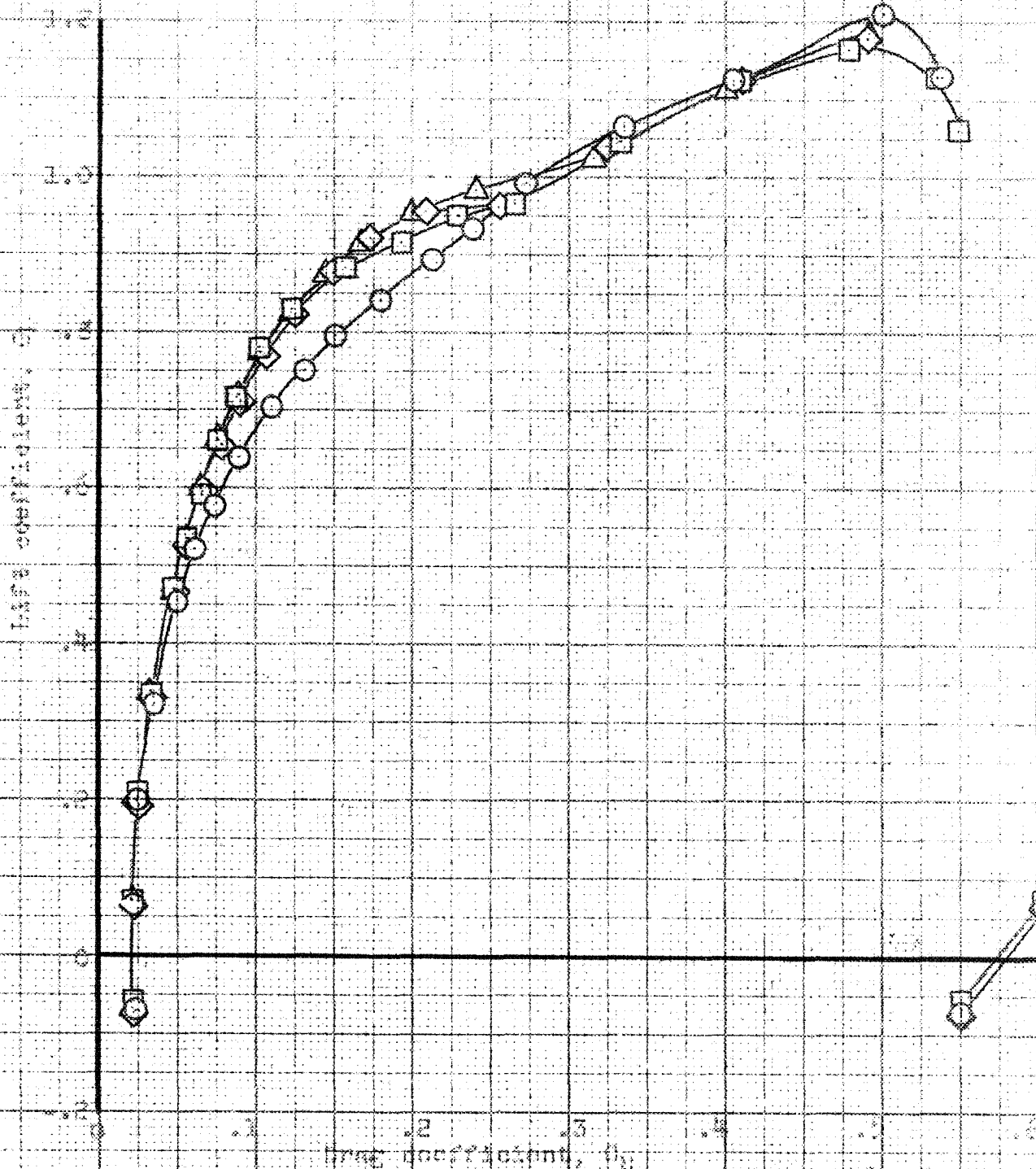
(b) concluded. Flap and plate deflected, $\delta = 11.6 \times 10^{-6}$.
Figure 15. concluded.

Contly. Leading edge radius - %C

	Sta. $35 \frac{b}{2}$	Sta. $60 \frac{b}{2}$
LE ₁ ($\frac{1}{2}$ " rad)	.463	.538
LE ₂ (1" rad)	.926	1.08



CONFIDENTIAL
SECURITY INFORMATION



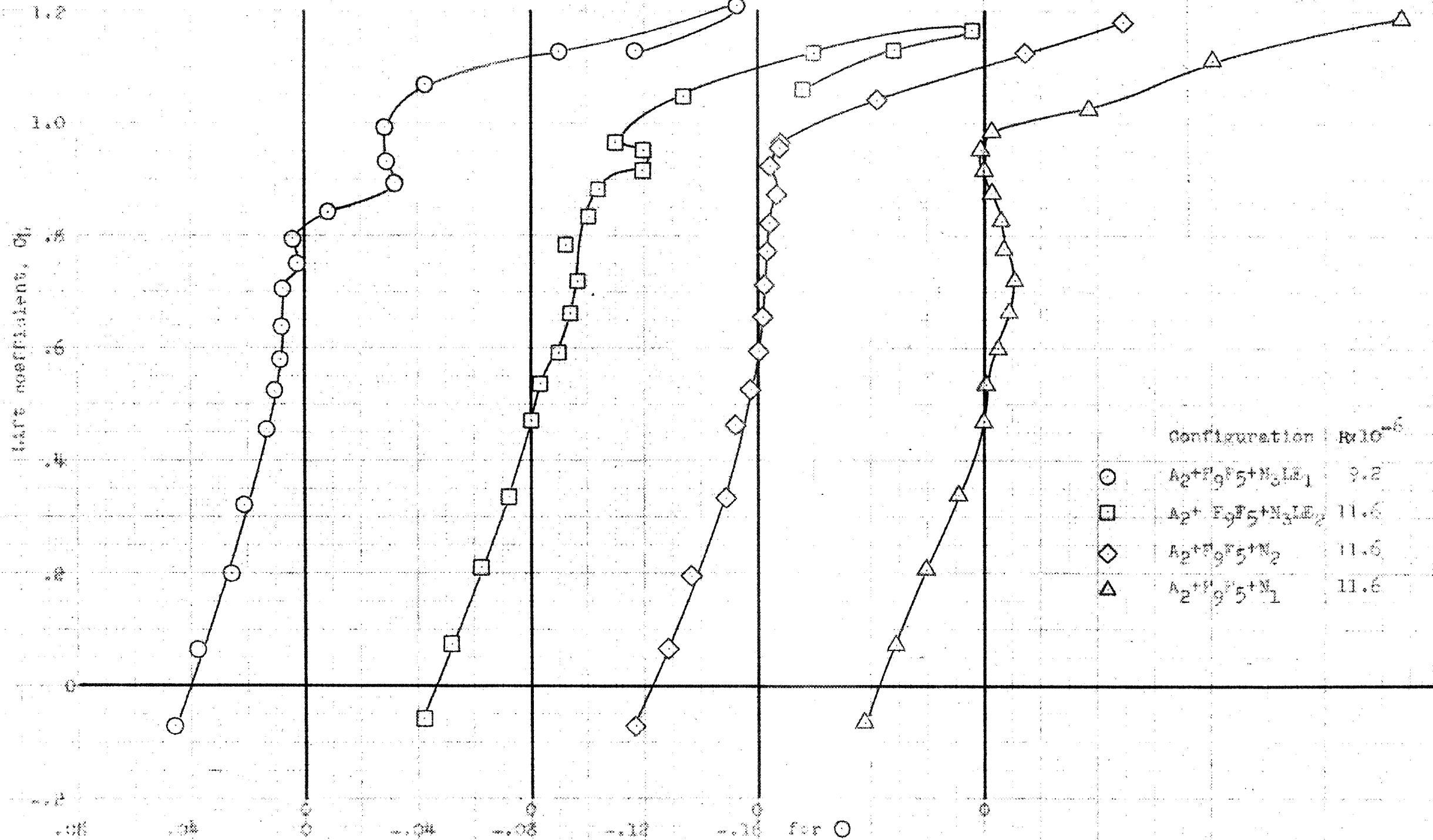
Configuration	$\times 10^{-6}$
$A_1 + F_5 + N_3 + LE_1$	9.2
$A_2 + F_9 + N_3 + LE_2$	11.6
$A_2 + F_5 + N_3$	11.6
$A_1 + F_9 + N_3$	11.6

(a) Cont.

Figure 11. Effects of changes of the leading-edge radius of tapered sections on the characteristics of the airplane with configuration $A_1 F_5 N_3$.

CONFIDENTIAL
SECURITY INFORMATION

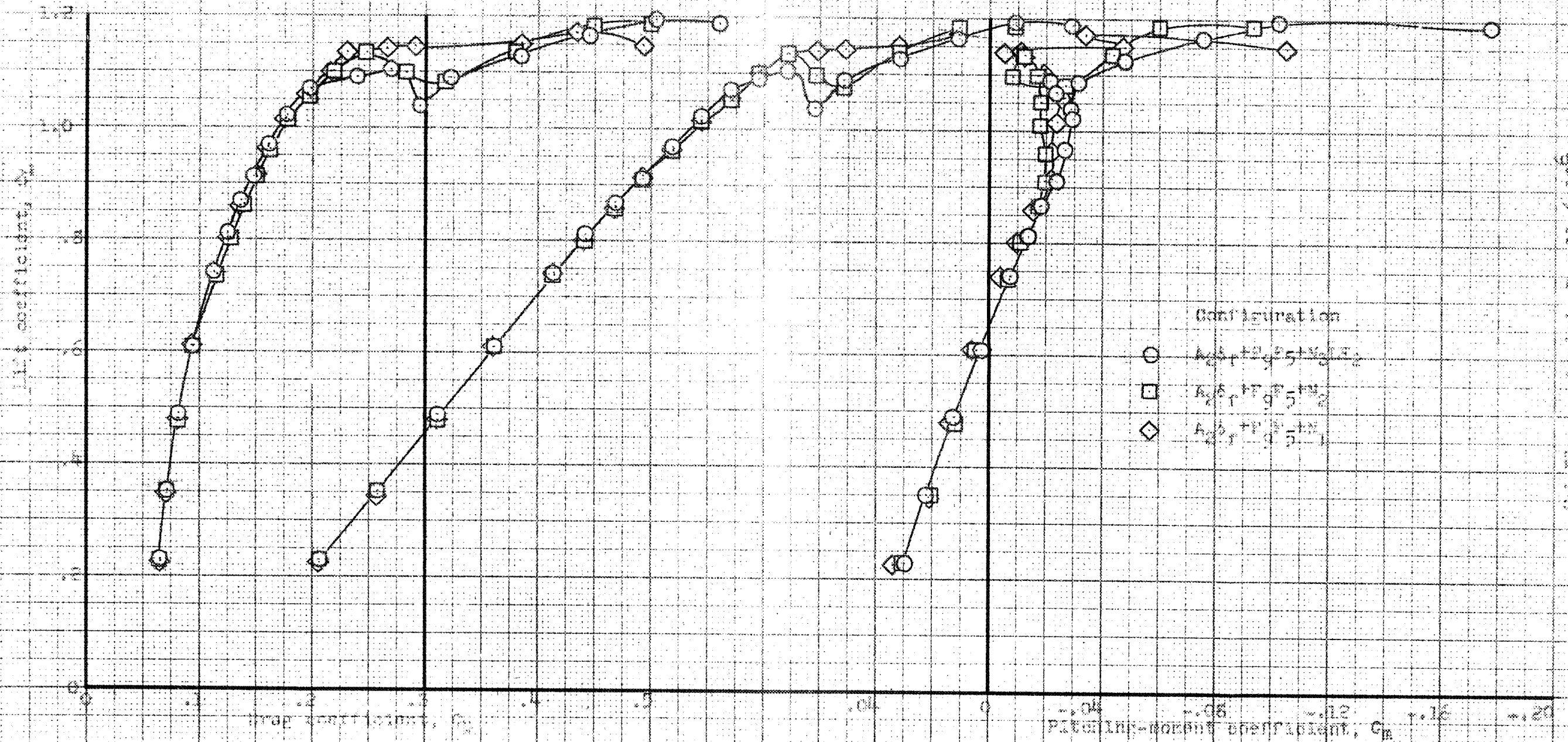
CONFIDENTIAL
SECURITY INFORMATION



(a) Concluded, clean.
Figure 16.- Continued.

CONFIDENTIAL
SECURITY INFORMATION
Pitching-moment coefficient, C_m

CONFIDENTIAL
SECURITY INFORMATION



- Configuration
- $A_2A_1+0.5+1/2A_2$
 - $A_2A_1+0.5+1/2A_2$
 - ◇ $A_2A_1+0.5+1/2A_1$

(b) Fluid extended, $\mu = 11.6 \times 10^{-6}$
Flow is laminar.

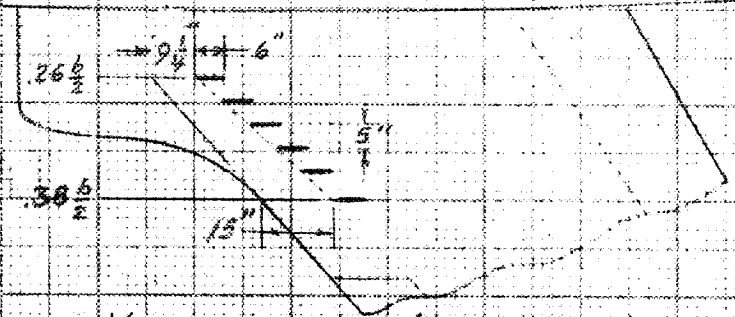
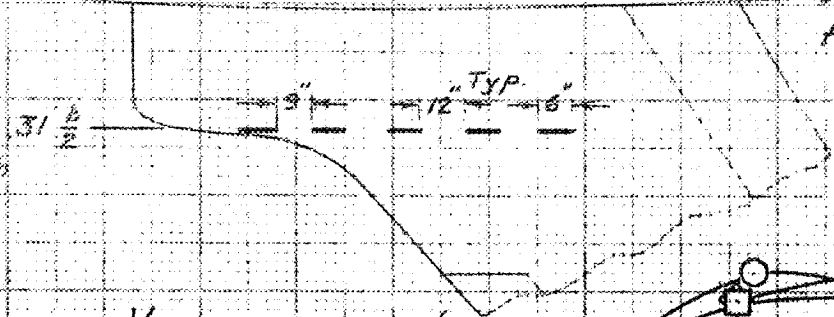
CONFIDENTIAL
SECURITY INFORMATION

CONFIDENTIAL*
SECURITY INFORMATION

Config Gen ht, in
 Va 6
 Vb 4
 Vc 3*

Note: All generators
 0.066" rectangular
 flat metal plates

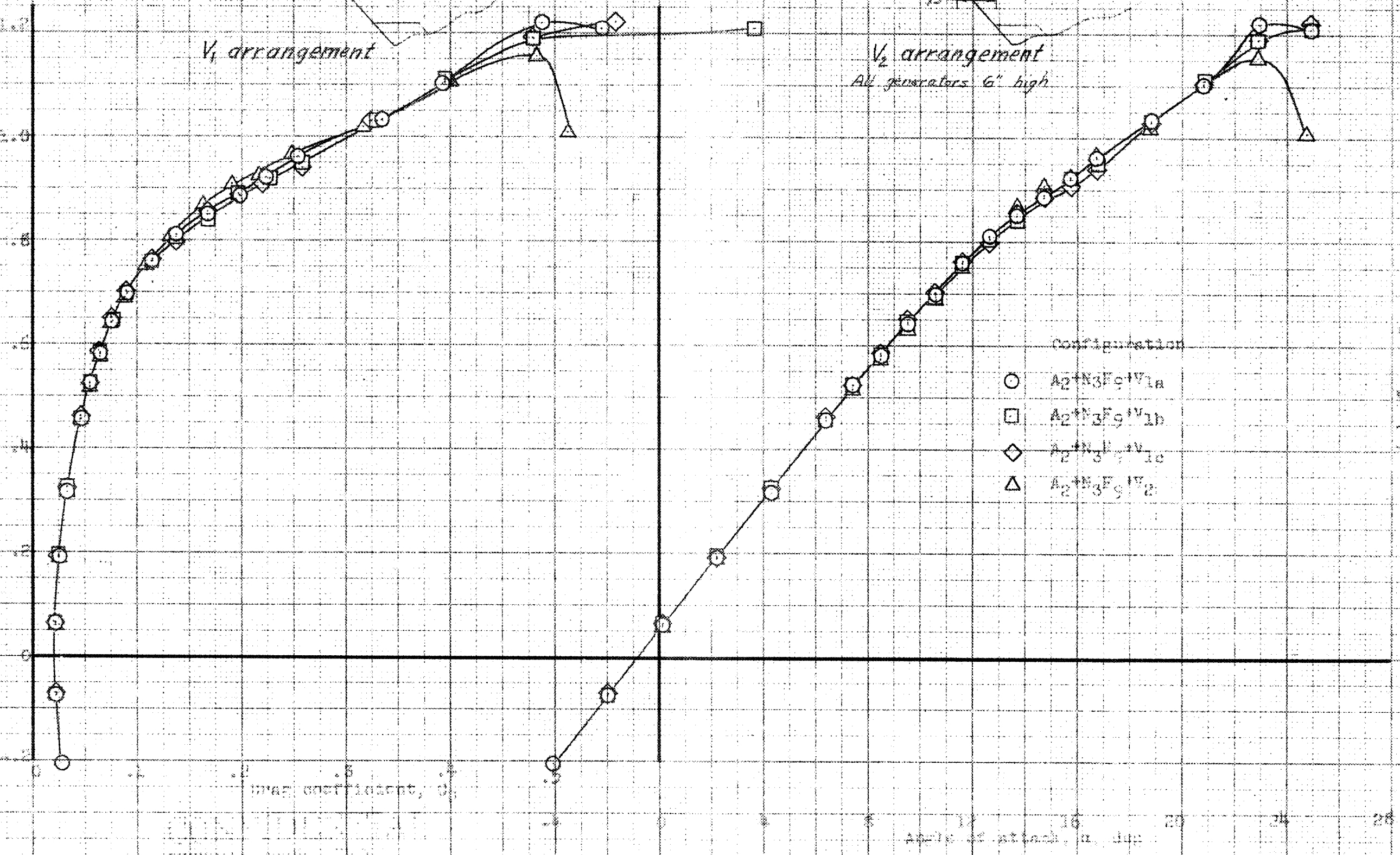
Forward gen. 2" high



V₁ arrangement

V₂ arrangement
 All generators 6" high

Life coefficient, C_L



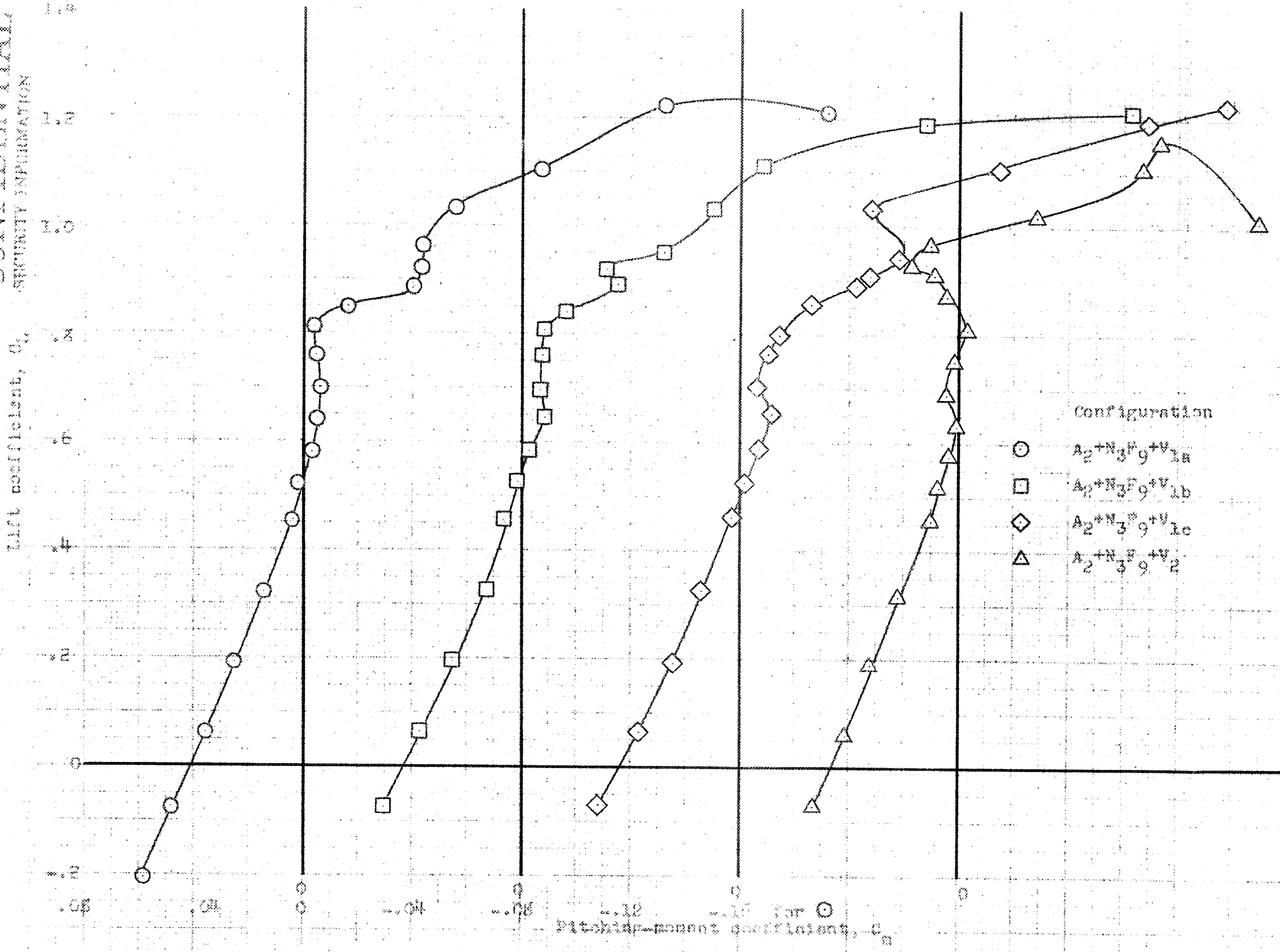
- Configuration
- A₂+N₃F₉+V_{1a}
 - A₂+N₃F₉+V_{1b}
 - ◇ A₂+N₃F₉+V_{1c}
 - △ A₂+N₃F₉+V₂

(a) C_L vs α , α

Figure 17. Effect of various generators on the characteristics of the aircraft with configuration V₁F₉. In a 9.5 deg.

CONFIDENTIAL
SECURITY INFORMATION

CONFIDENTIAL



(b) C_L vs C_M

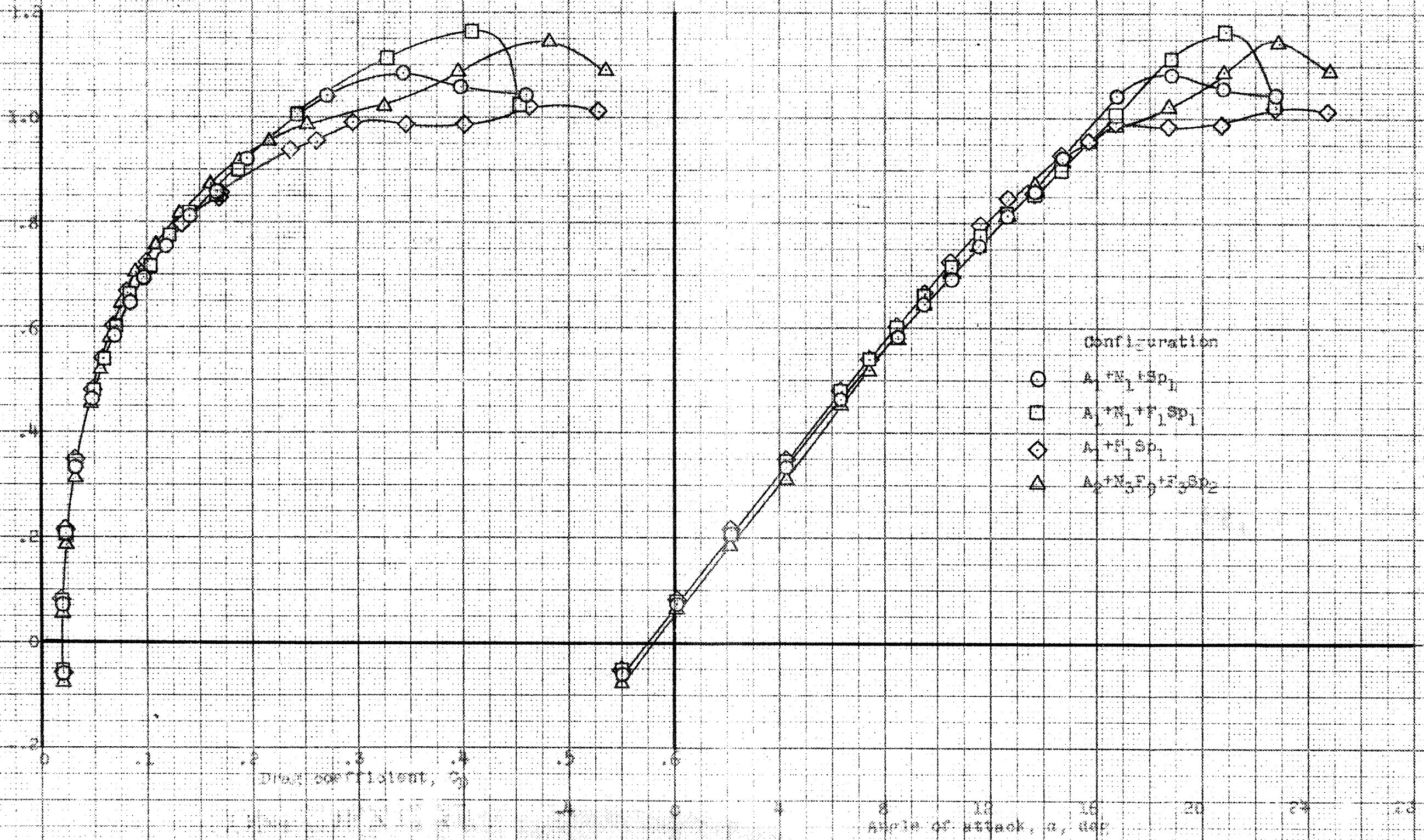
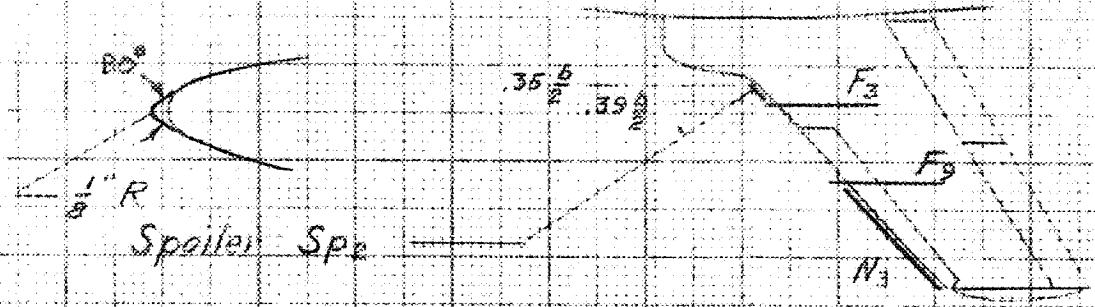
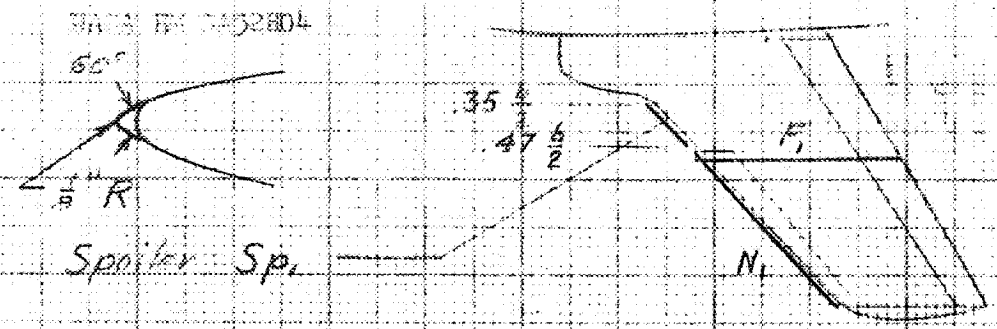
Figure 17. - Concluded.

CONFIDENTIAL

SECURITY INFORMATION

CONFIDENTIAL

Lift coefficient, C_L



- Configuration
- $A_1 + N_1 + Sp_1$
 - $A_1 + N_1 + F_1 + Sp_1$
 - ◇ $A_1 + F_1 + Sp_1$
 - △ $A_2 + N_2 + F_2 + Sp_2$

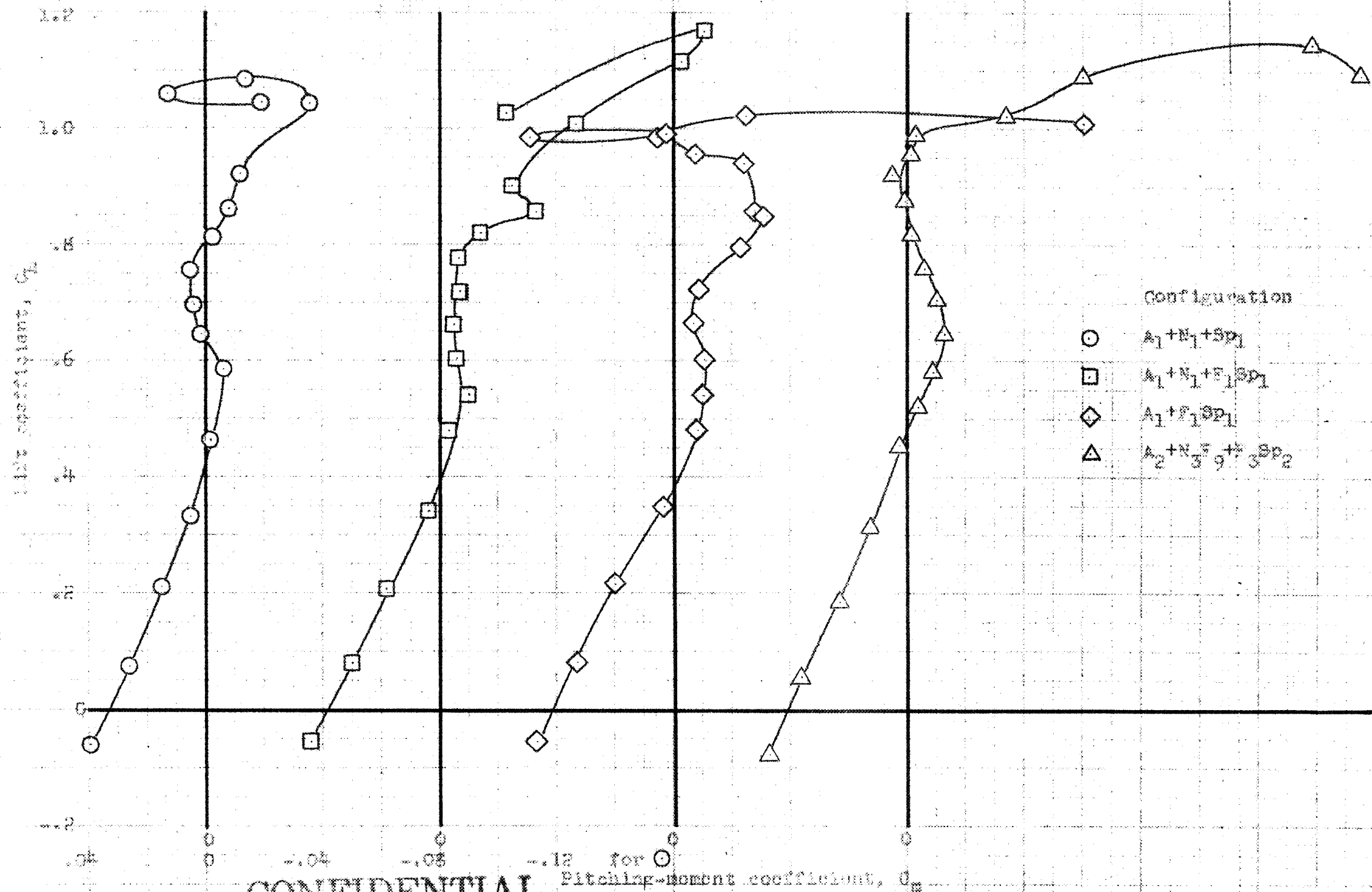
(a) Clean, $M = 9.2 \times 10^6$

Figure 38. Effects of sharp leading-edge rollers of the characteristics of the airfoils.

CONFIDENTIAL

SHUTTLE EXPERIMENT

CONFIDENTIAL
SECURITY INFORMATION

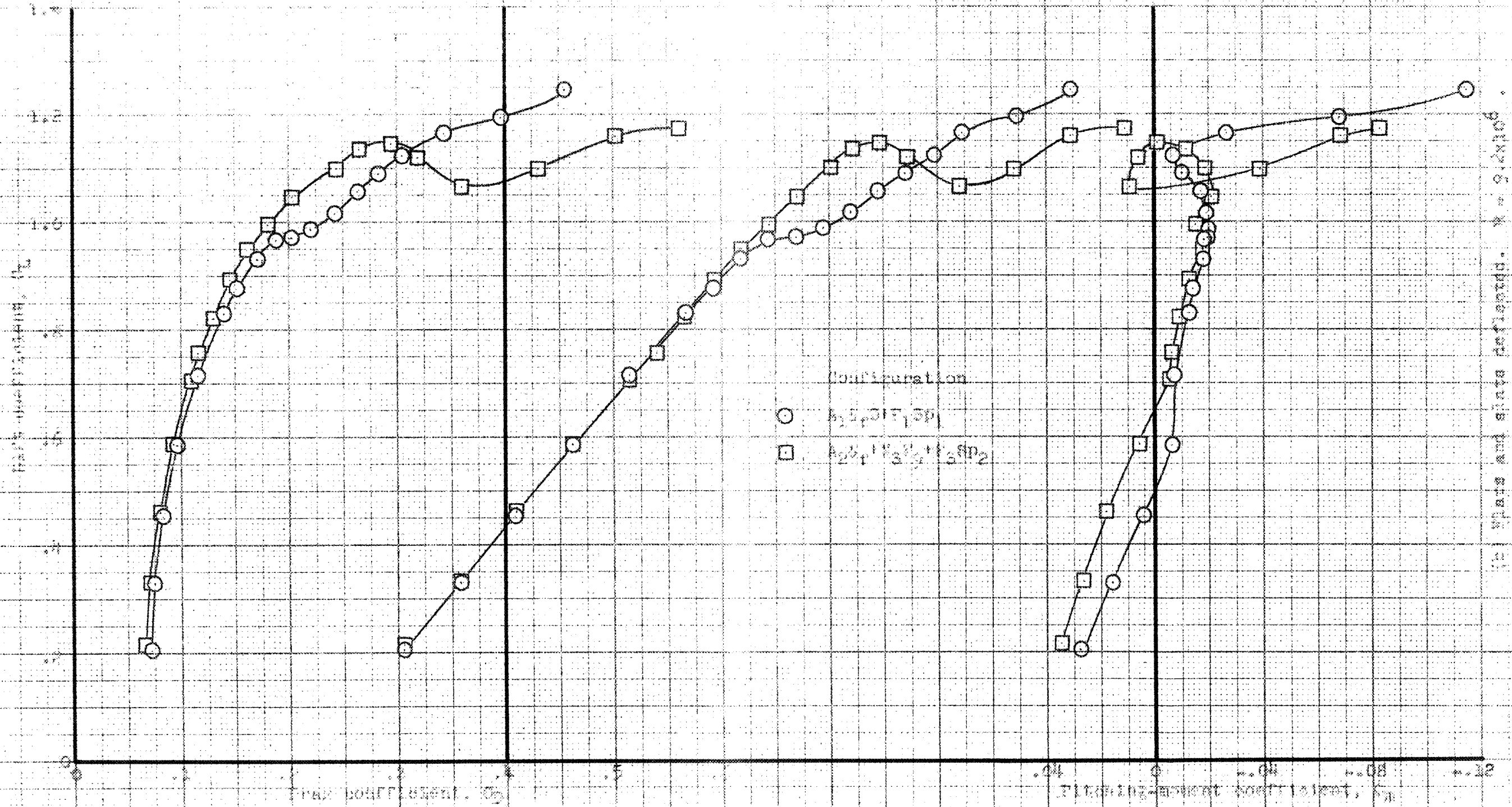


(A) Concluded, clean, $R = 9.2 \times 10^6$.

Figure 18.- Continued.

CONFIDENTIAL
SECURITY INFORMATION

CONFIDENTIAL
SECURITY INFORMATION



Configuration
 ○ $A_1 S_{p1} + F_{1sp1}$
 □ $A_2 S_{p1} + F_{3sp1} + F_{3sp2}$

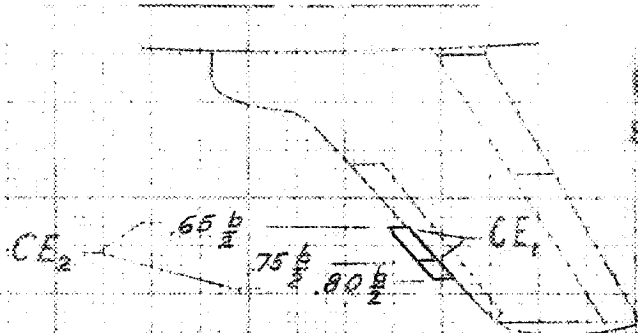
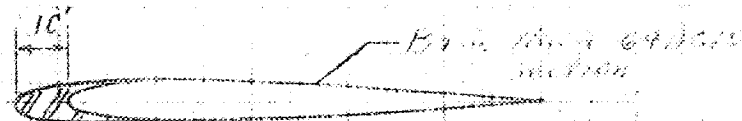
Rate of deflection, %

Pitching-moment coefficient, C_m

CONFIDENTIAL
SECURITY INFORMATION

Rate of deflection, %

Pitching-moment coefficient, C_m



CONFIDENTIAL
SECURITY INFORMATION

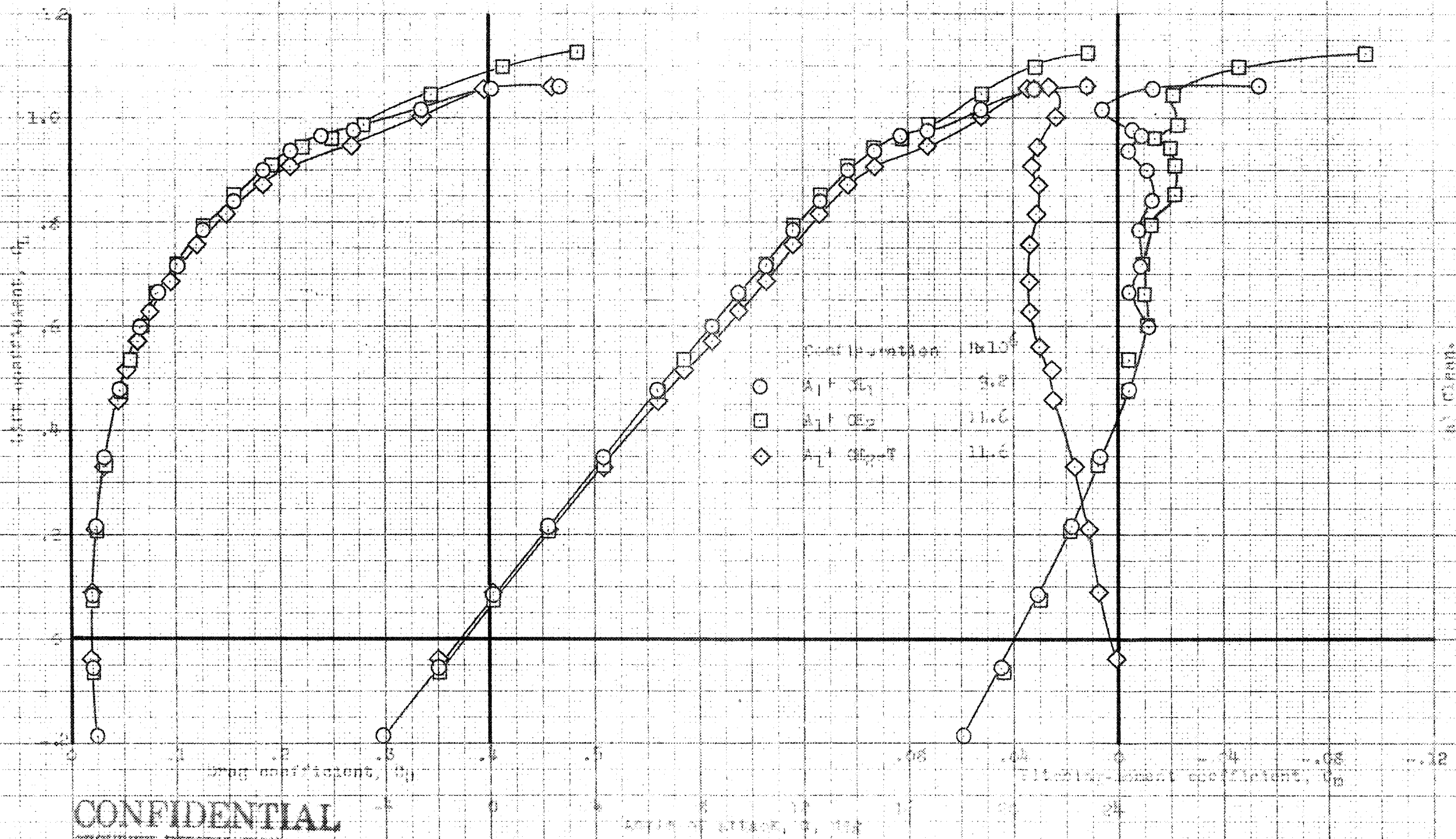
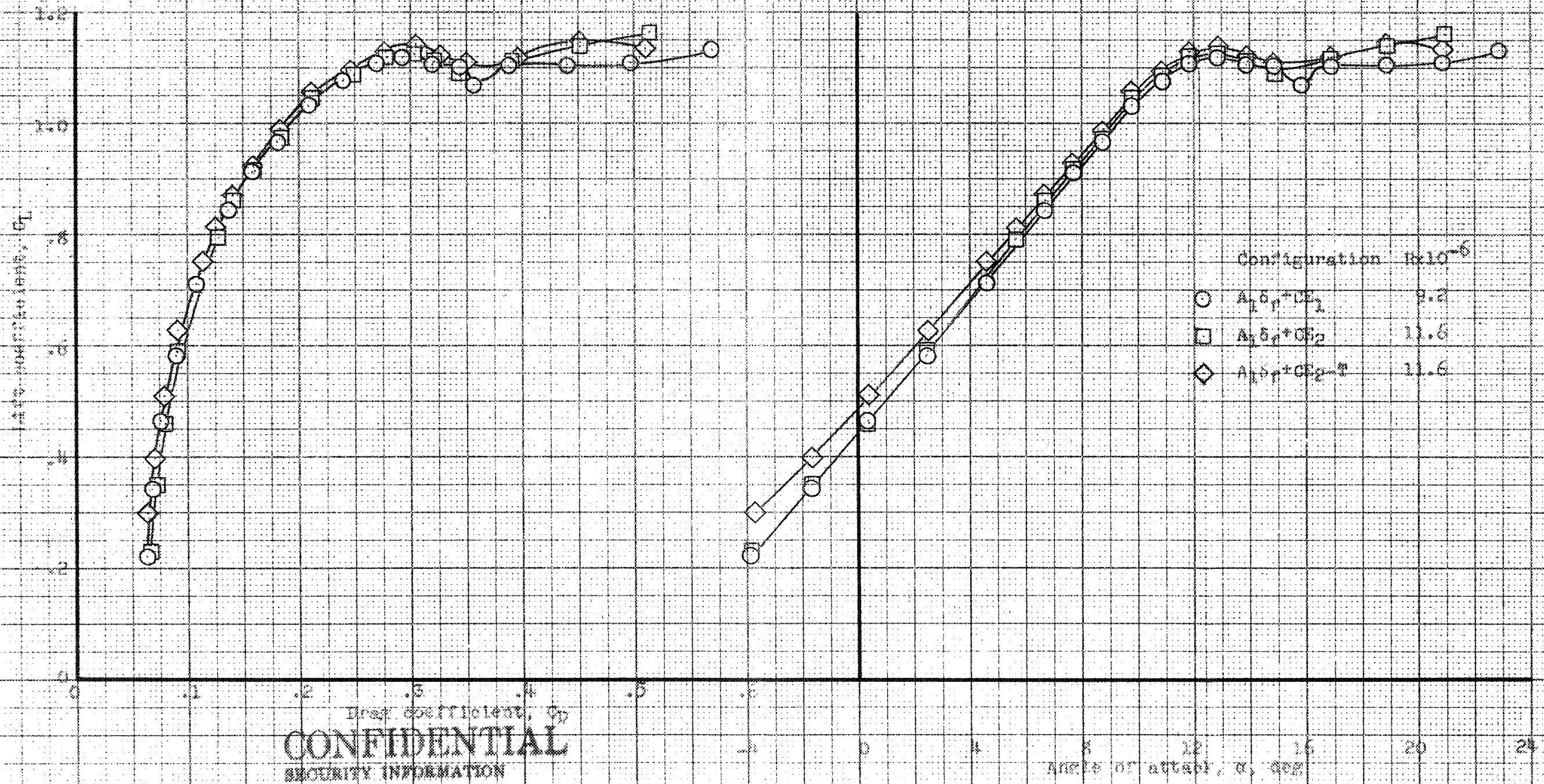


Figure 15. Effect of leading edge extensions on the characteristics of the airfoil with and without the horizontal tail.

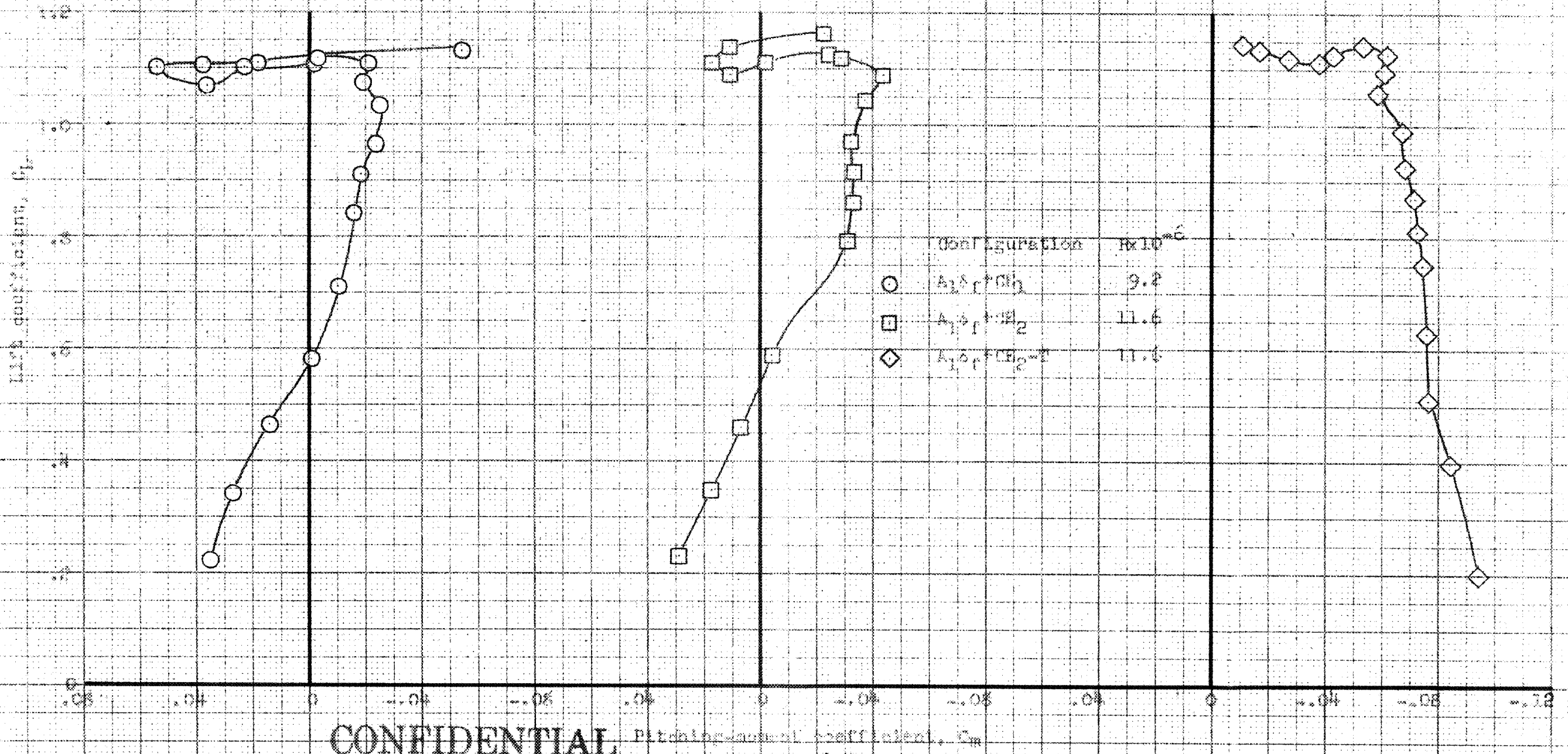
CONFIDENTIAL
SECURITY INFORMATION



Configuration	$R \times 10^{-6}$
○ $A_1 \delta p + CE_1$	9.2
□ $A_2 \delta p + CE_2$	11.6
◇ $A_1 \delta p + CE_{2-3}$	11.6

(b) Flaps retracted.
FIGURE 19. - CONTINUED.

CONFIDENTIAL
SECURITY INFORMATION



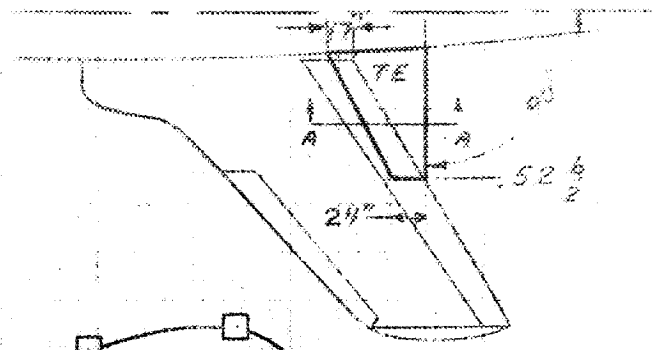
CONFIDENTIAL
SECURITY INFORMATION

(b) concluded, data derived.
Figure 10, continued.

CONFIDENTIAL

SECURITY INFORMATION

DATA BY 5452BD4



Trailing edge extension construction
3/8" plywood with sheet metal trailing edge.

Sect A-A

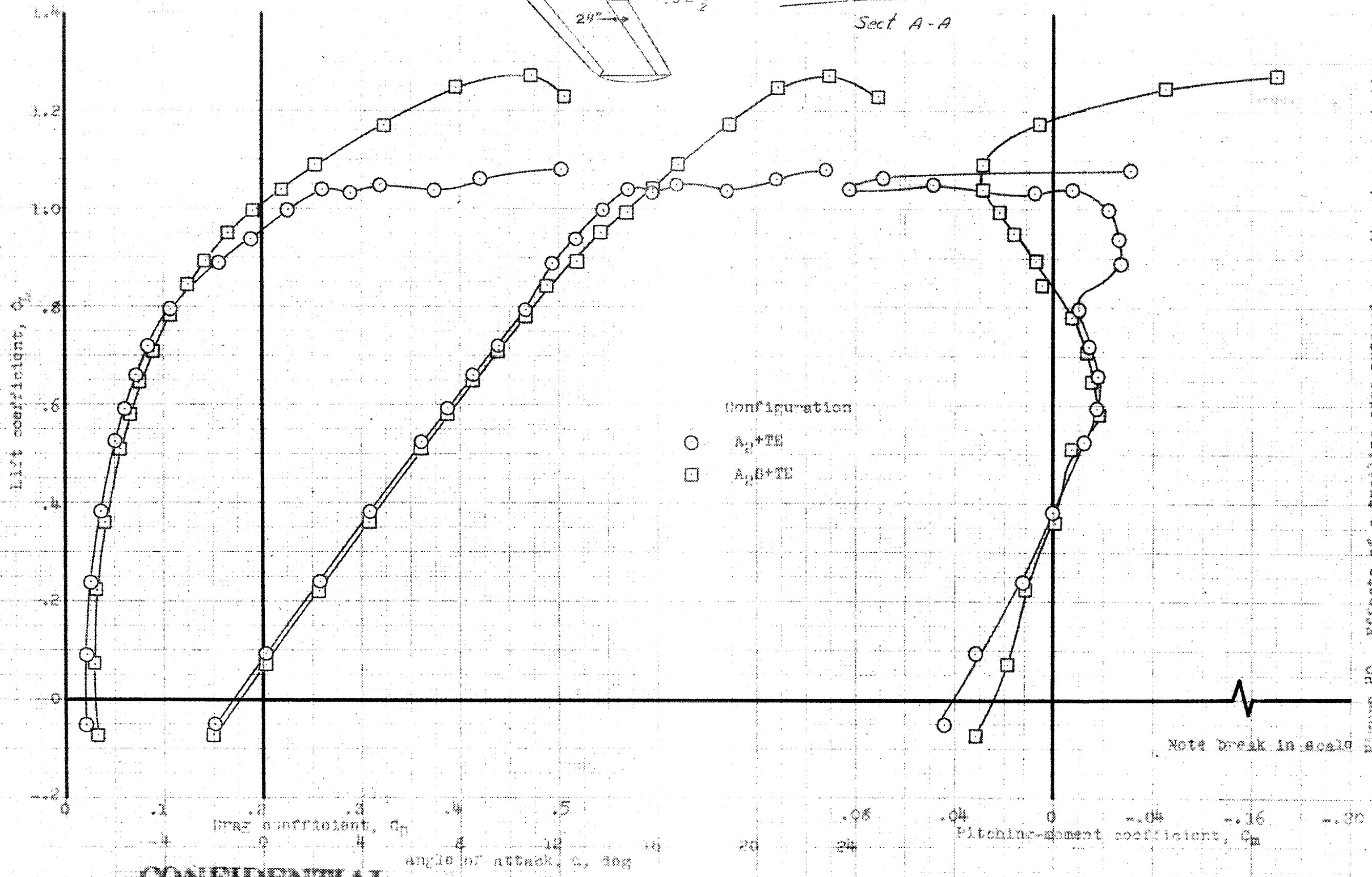
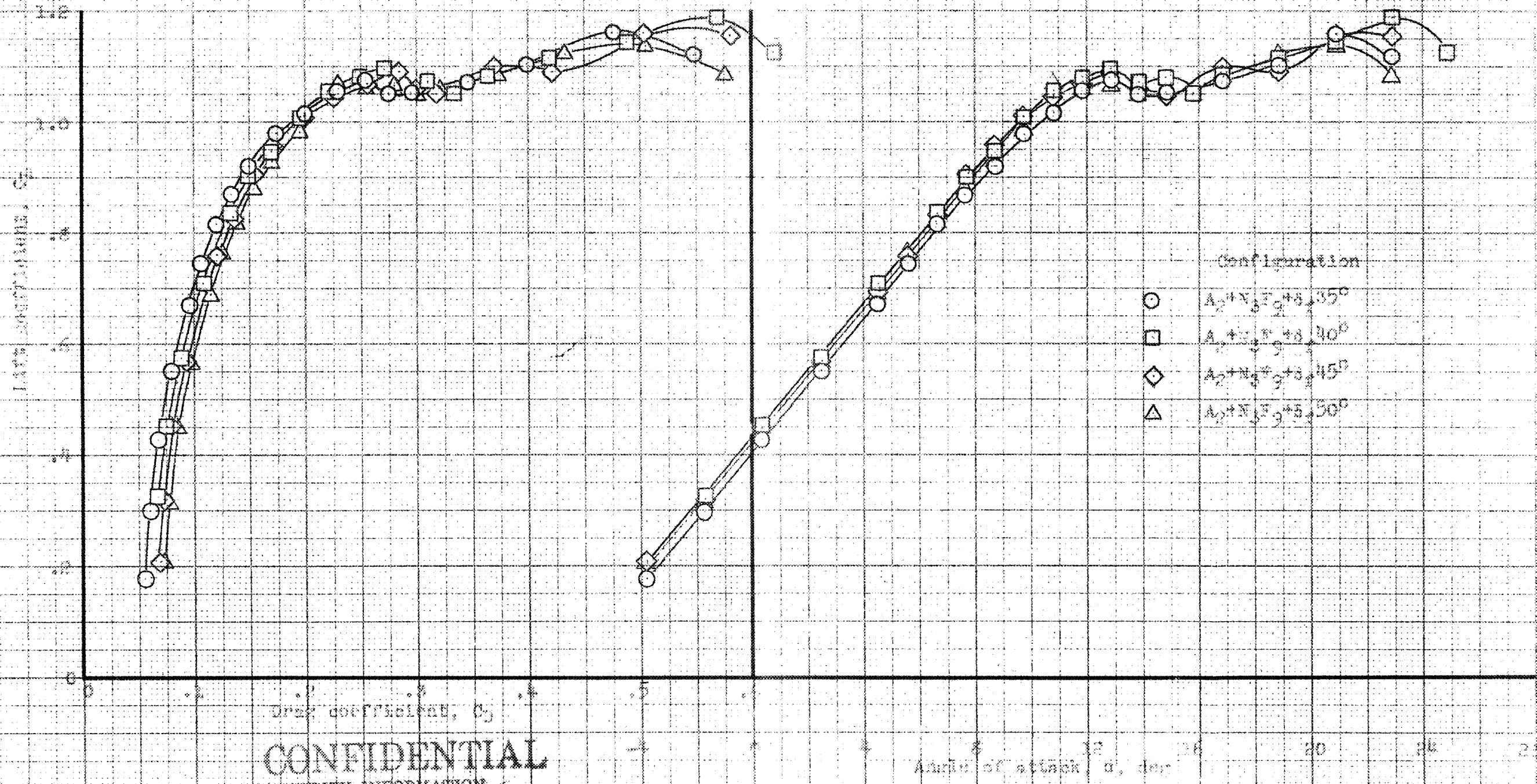


Figure 20.- Effects of a trailing-edge extension on the characteristics of the airplane with and without plate extended. $M = 0.2 \times 10^6$.

CONFIDENTIAL

SECURITY INFORMATION

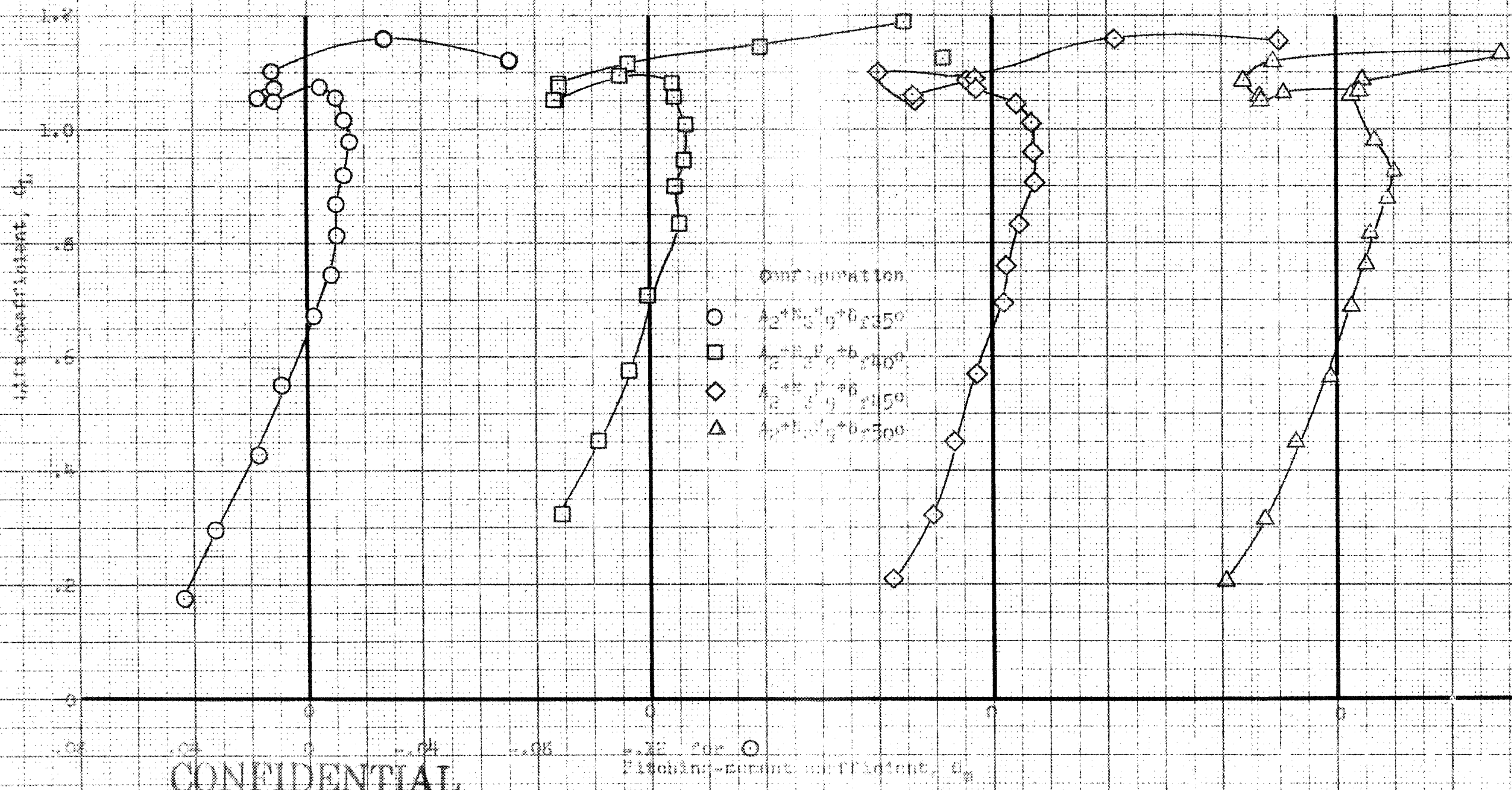
CONFIDENTIAL
SECURITY INFORMATION



CONFIDENTIAL
SECURITY INFORMATION

Figure 2. Lift and drag coefficients vs angle of attack for the configurations $\alpha_0 + 35^\circ$, $\alpha_0 + 40^\circ$, $\alpha_0 + 45^\circ$, and $\alpha_0 + 50^\circ$.

CONFIDENTIAL
SECURITY INFORMATION



(b) q_L vs q_p .
Figure 27. - Concluded.

CONFIDENTIAL
SECURITY INFORMATION

0.02 for ○
Pitching-moment coefficient, q_p

CONFIDENTIAL
SECURITY INFORMATION

REF ID: A52804

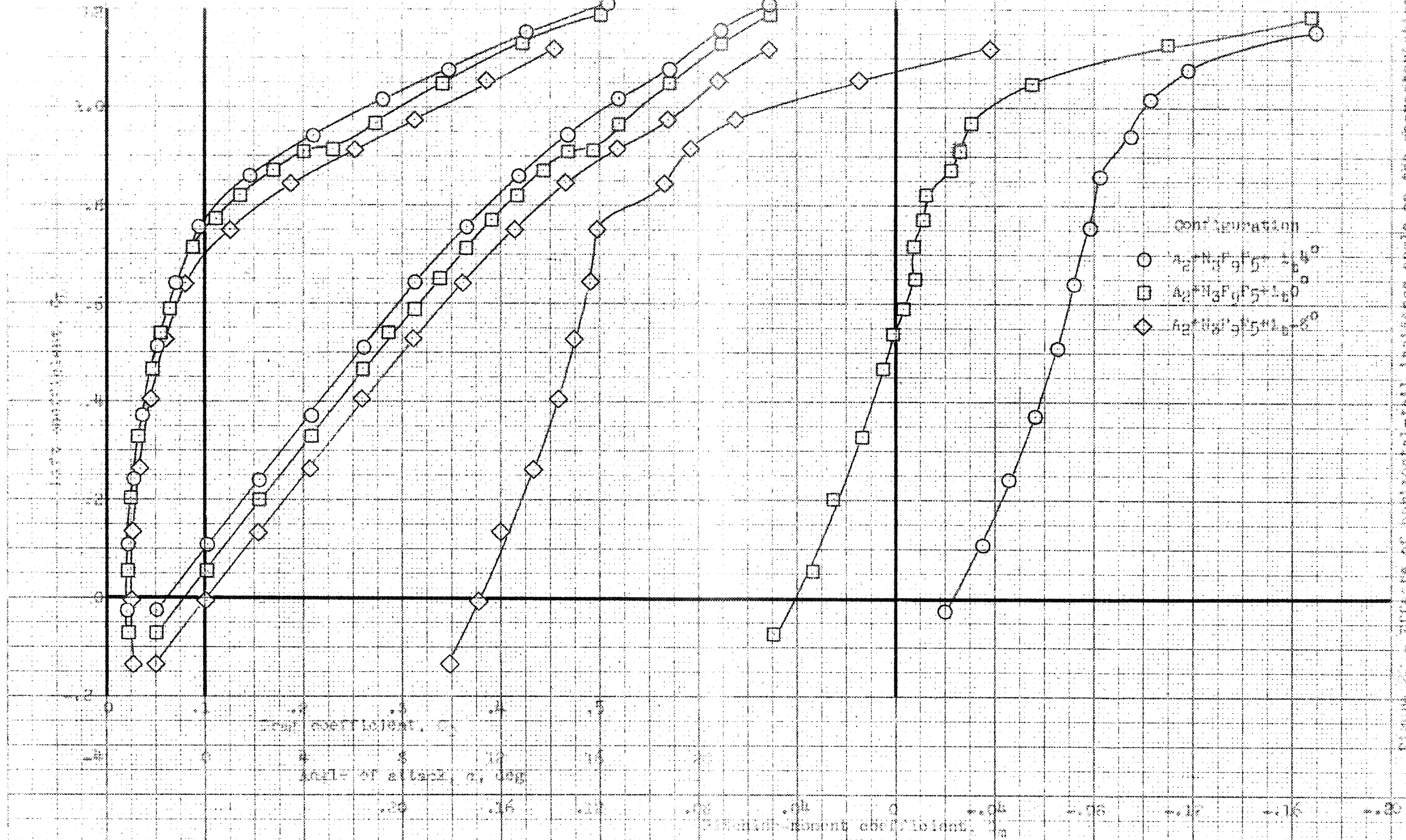


Figure 2. Effect of horizontal-tail incidence angle on the characteristic of the amplifier with configuration N3795.

CONFIDENTIAL
SECURITY INFORMATION

DATA BY TADDELL

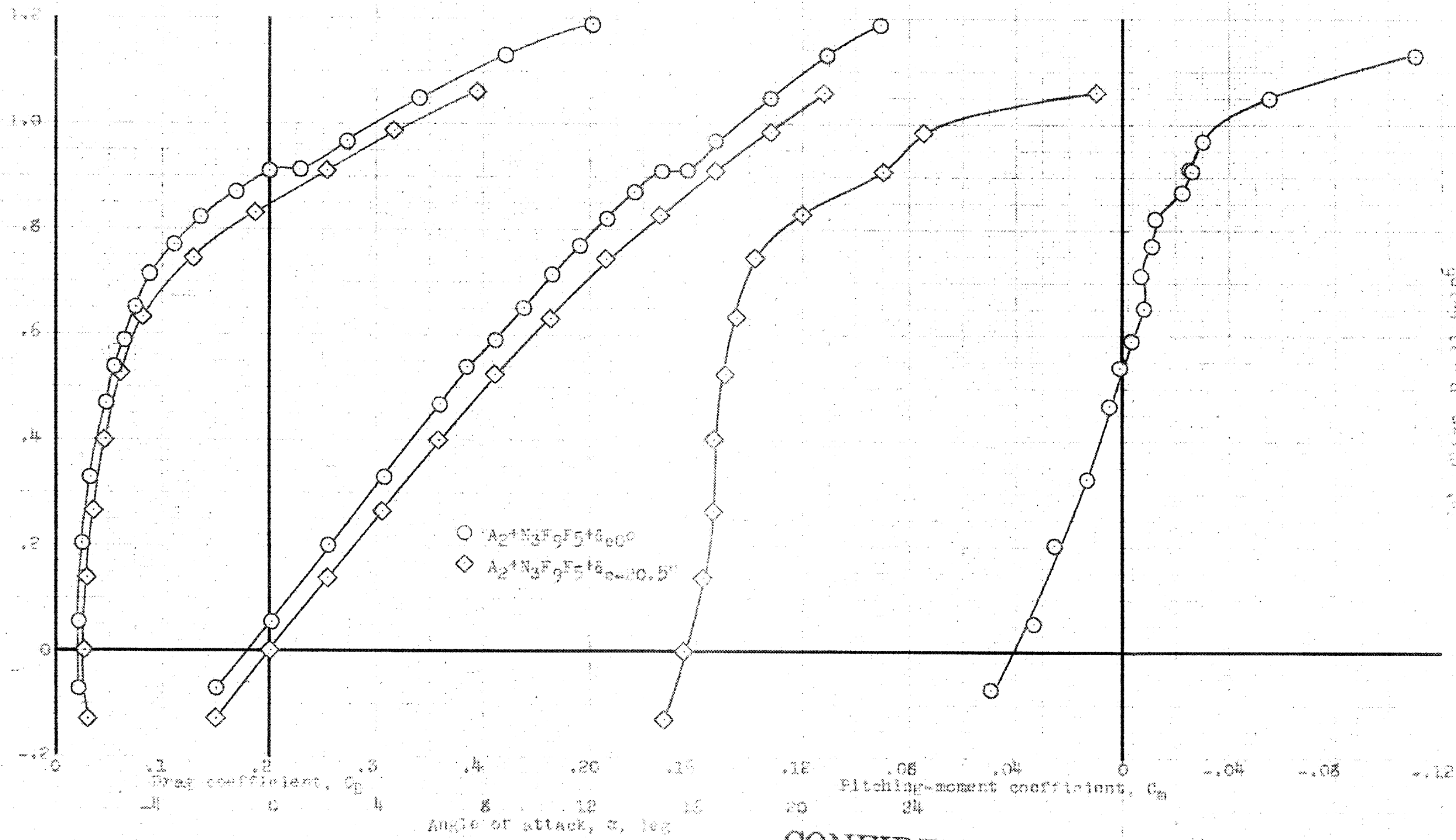
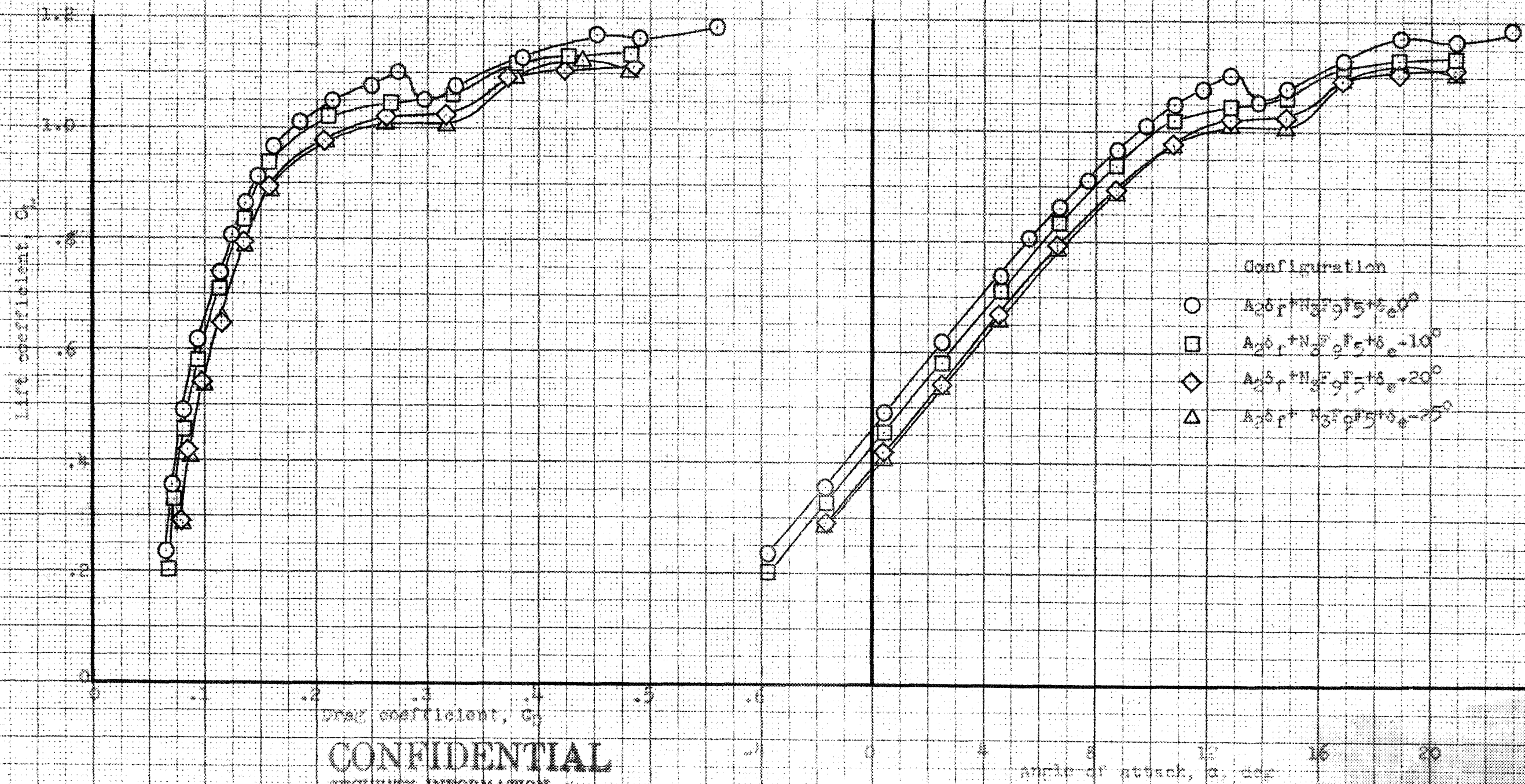


Figure 16.- Effects of elevator deflection angle on the characteristics of the airplane with configuration $N_3F_9F_5$.

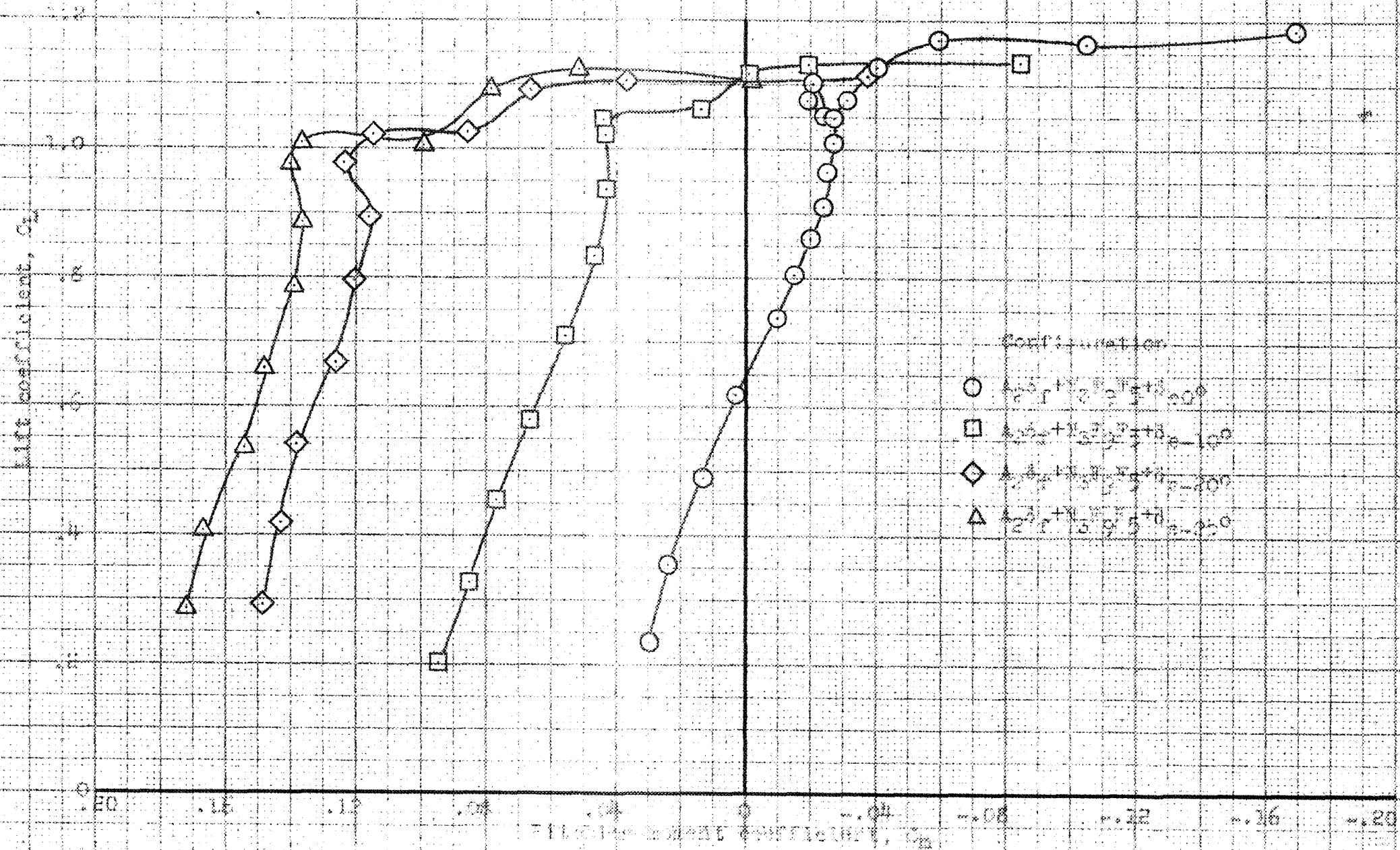
CONFIDENTIAL
SECURITY INFORMATION



CONFIDENTIAL
SECURITY INFORMATION

INFORMATION REFLECTED, N. 21-6X106
Figure 25 - Continues

CONFIDENTIAL
SECURITY INFORMATION



(b) concluded, Flaps deflected. $N = 11,6 \times 10^6$.
Figure 43 - continued.

CONFIDENTIAL
SECURITY INFORMATION

CONFIDENTIAL
SECURITY INFORMATION

WACA RM 5A52HD

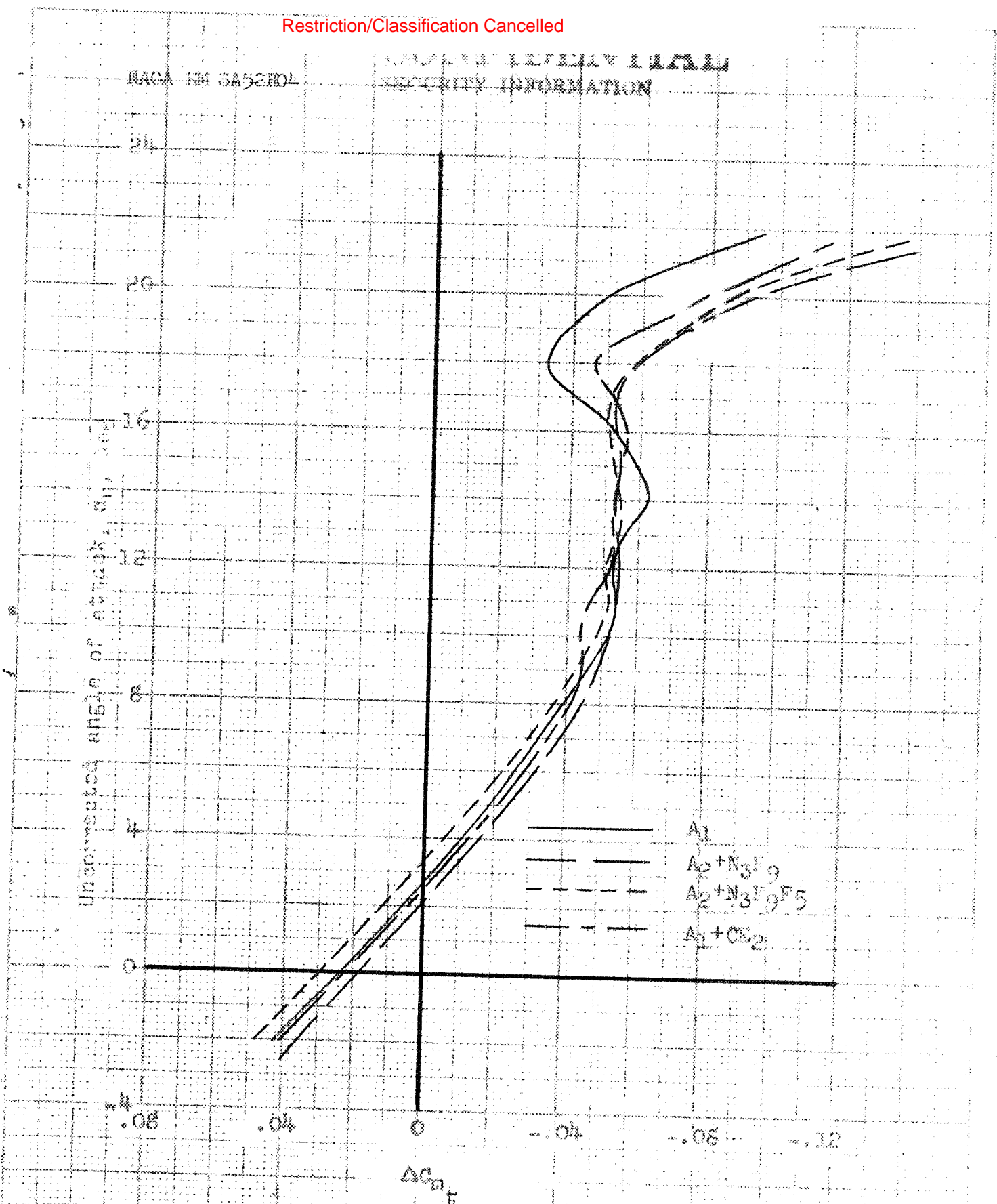


Figure 24.- Comparison of the increments of pitching-moment coefficient contributed by the horizontal tail for the airplane with several of the more promising modifications.

CONFIDENTIAL
SECURITY INFORMATION